CHITOSAN DRUG BINDING BY IONIC INTERACTION: PREPARATION, CHARACTERIZATION AND *IN VITRO* RELEASE STUDY

YAOWALAK BOONSONGRIT

A THESIS SUBMITTED IN PARTIAL FULFILLMENT
OF THE REQUIREMENTS FOR
THE DEGREE OF DOCTOR OF PHILOSOPHY
(PHARMACEUTICS)
FACULTY OF GRADUATE STUDIES
MAHIDOL UNIVERSITY
2006

ISBN 974-04-6845-4

Thesis

Entitled

CHITOSAN DRUG BINDING BY IONIC INTERACTION: PREPARATION, CHARACTERIZATION AND *IN VITRO* RELEASE STUDY

…….....
Ms. Yaowalak Boonsongrit
Candidate

……..
Prof. Ampol Mitrevej, Ph.D.
Major-Advisor

……..
Prof. Bernd W. Mueller, Ph.D.
Co-Advisor

……..
Assoc. Prof. Nuttanan Sinchaipanid, Ph.D.
Co-Advisor

……..
Prof. M.R. Jisnuson Svasti, Ph.D.
Dean
Faculty of Graduate Studies

……..
Prof. Ampol Mitrevej, Ph.D.
Chair
Doctor of Philosophy Programme in Pharmaceutics
Faculty of Pharmacy

Thesis

Entitled

CHITOSAN DRUG BINDING BY IONIC INTERACTION: PREPARATION, CHARACTERIZATION AND *IN VITRO* RELEASE STUDY

was submitted to the Faculty of Graduate Studies, Mahidol University

for the degree of Doctor of Philosophy (Pharmaceutics)

on

January 26, 2006

……..
Ms. Yaowalak Boonsongrit
Candidate

……..
Prof. Ampol Mitrevej, Ph.D.
Chair

……..
Prof. Bernd W. Mueller, Ph.D.
Member

……..
Lect. Kwunchit Oungbho, Ph.D.
Member

……..
Assoc. Prof. Nuttanan Sinchaipanid, Ph.D.
Member

……..
Prof. M.R. Jisnuson Svasti, Ph.D.
Dean
Faculty of Graduate Studies
Mahidol University

……..
Prof. Ampol Mitrevej, Ph.D.
Dean
Faculty of Pharmacy
Mahidol Universy

ACKNOWLEDGEMENTS

I would like to express my sincere gratitude and deep appreciation to my major advisor, Professor Dr. Ampol Mitrevej, for his valuable guidance, supervision, kindness, understanding and encouragement throughout my study.

My profound appreciation thanks to Professor Dr. Bernd W. Mueller, my co-advisor in Germany, for his helpful advice, criticism, consultation and continuous support on my study. His graciousness is also unforgettable.

I am very grateful to Associate Professor Dr. Nuttanan Sinchaipanid, my co-advisor, for her valuable guidance, kindness and encouragement though my Ph.D. research.

My sincere thanks to Dr. Urich Girreser for his assistance and advice in FTIR and ^{1}H-NMR studies.

I would like to acknowledge the Thailand Research Fund (TRF) through the Royal Golden Jubilee (RGJ) Ph.D. program (Grant No. PHD/0169/2542), the German Academic Exchange Service (DAAD) and Pharmatech GmbH, D-Flintbek for financial support during my study in Thailand and at the Department of Pharmaceutics and Biopharmaceutics, Christian-Albrechts-University, Kiel, Germany.

My appreciation is given to all members at the Department of Pharmaceutics and Biopharmaceutics, Christian-Albrechts-University, for their friendship, help, suggestions and encouragement, especially Mr. Steve Minde and Mr. Kai Hueckstaedt.

I would like to thank my colleagues at Faculty of Pharmacy, Mahidol University, in particular Ms. Pimphaka Wanasawas, Ms. Krisanin Chansanroj and Ms. Siracha Tuntikulwattana, for their generous support and companionship.

Finally, I wish to express my infinite gratitude to my parents, grandma and family for their love, patient and encouragement throughout my life.

Yaowalak Boonsongrit

CHITOSAN DRUG BINDING BY IONIC INTERACTION: PREPARATION, CHARACTERIZATION AND *IN VITRO* RELEASE STUDY

YAOWALAK BOONSONGRIT 4336457 PYPT/D

Ph.D. (PHARMACEUTICS)

THESIS ADVISORS: AMPOL MITREVEJ, Ph.D., BERND W. MUELLER, Ph.D., NUTTANAN SINCHAIPANID, Ph.D.

ABSTRACT

Ionic gelation method has been used to prepare drug-chitosan micro/ nanoparticles in order to avoid using organic solvents or high temperature during preparation. Four model drugs, which were used for ionic gelation, (insulin, diclofenac sodium, benzoic acid and salicylic acid) with different pI or pKa were investigated for their physicochemical properties, entrapment efficiency, binding ability and *in vitro* release. The amount of drug entrapped in the formulation affected the zeta potential and the surface charge of the micro/nanoparticles. A high entrapment efficiency of the micro/nanoparticles could be obtained by careful control of formulation pH. The maximum entrapment efficiency did not occur in the highest ionization range of the model drugs. The high burst release of drugs from chitosan micro/nanoparticles was observed regardless of the pH of dissolution media. To confirm the electrostatic interaction between opposite charges of drugs and chitosan, ^{1}H-NMR, FTIR and isothermal titration calorimetry (ITC) were used. No ionic interaction between the carboxyl group of benzoic acid or salicylic acid and the amine group of chitosan could be detected by any means. FTIR spectra and the interaction enthalpy change (ΔH) indicated that there was a weak ionic interaction between insulin and chitosan. However, the interaction enthalpy change obtained is possibly due to the conformational changes and the adsorption phenomena of insulin onto the surface of the particles. An enthalpy change from the titration of diclofenac into chitosan resulted from the protonation of the amine group of diclofenac acid. The ionic interaction between the drug and chitosan is not the main mechanism that causes the formation of high entrapped drug-chitosan particles. Most drugs were entrapped physically in the chitosan network. Although the ionic interaction between the drug and chitosan is too low to control drug release, the combination of this system with site specific carriers can improve the absorption of drugs.

KEY WORDS: CHITOSAN/ IONIC INTERACTION/ MICROPARTICLES/ NANOPARTICLES/ ISOTHERMAL TITRATION CALORIMETRY

181 P. ISBN 974-04-6845-4

การจับระหว่างยากับไคโตแซนโดยอาศัยประจุ : การเตรียม การประเมินคุณสมบัติของตำรับ และการศึกษาการปลดปล่อยยาในหลอดทดลอง (CHITOSAN DRUG BINDING BY IONIC INTERACTION: PREPARATION, CHARACTERIZATION AND *IN VITRO* RELEASE STUDY)

เยาวลักษณ์ บุญทรงฤทธิ 4336457 PYPT/D

ปร.ด. (เภสัชการ)

คณะกรรมการควบคุมวิทยานิพนธ์: อำพล ไมตรีเวช, Ph.D., BERND W. MUELLER, Ph.D., ณัฐนันท์ สินชัยพานิช, Ph.D.

บทคัดย่อ

ในการศึกษานี้เตรียมอนุภาคไคโตแซนขนาดเล็กด้วยวิธีการก่อเจลโดยอาศัยประจุ เพื่อหลีกเลี่ยงการใช้อุณหภูมิสูงและตัวทำละลายอินทรีย์ที่ส่งผลเสียต่อตำรับในระหว่างการเตรียมตำรับ อินซูลิน ไดโครฟีแนค-โซเดียม กรดเบนโซอิก และกรดซาลิไซลิก เป็นตัวแทนที่นำมาศึกษาการเตรียมอนุภาคด้วยการก่อเจลนี้โดยตัวแทนมีความเป็นกรดด่างที่ต่างกัน ได้ศึกษาถึงคุณสมบัติทางกายภาพและเคมี ความสามารถในการกักเก็บยาของอนุภาคขนาดเล็กที่เตรียมได้ ความสามารถในการจับกันระหว่างยากับไคโตแซน และการปลดปล่อยยาในหลอดทดลอง จากการศึกษาพบว่าปริมาณยาที่ถูกกักเก็บในอนุภาคของแต่ละตำรับส่งผลต่อประจุบนผิวของอนุภาค (zeta potential และ surface charge) การควบคุมความเป็นกรดด่างของตำรับอย่างเหมาะสมจะทำให้ได้อนุภาคขนาดเล็กที่มีประสิทธิภาพการกักเก็บยาที่สูง อย่างไรก็ตามตำรับที่มีความเป็นกรดด่างอยู่ในช่วงที่ทำให้ยาในตำรับอยู่ในสภาพที่แตกตัวมีประจุสูงสุดก็ไม่อาจทำให้ประสิทธิภาพการกักเก็บยาสูงสุดได้ จากการศึกษาการปลดปล่อยยาต้นแบบออกจากอนุภาคขนาดเล็ก พบว่ายาถูกปล่อยออกมาอย่างรวดเร็วในสารละลายหลายชนิดโดยไม่ขึ้นกับความเป็นกรดด่างของสารละลาย ในการศึกษานี้ได้มีการประเมินประสิทธิภาพการจับกันด้วยประจุระหว่างยาต้น แบบและไคโตแซนโดยการใช้ FTIR, ^{1}H-NMR และ isothermal titration calorimetry (ITC) พบว่าทั้ง กรดเบนโซอิก และกรดซาลิไซลิกไม่มีการจับกันกับไคโตแซน กราฟจากการศึกษาด้วย FTIR และค่า enthalpy change (ΔH) จากการศึกษาด้วย ITC แสดงว่ามีการจับกันด้วยประจุระหว่างอินซูลิน และไคโตแซน อย่างไรก็ตามการดูดซับของอินซูลินบนผิวของอนุภาครวมทั้งการเกิดการเปลี่ยนแปลงรูปร่างของอินซูลินมีผลต่อค่า enthalpy change (ΔH) ที่วัดได้จากปฏิกิริยาระหว่างอินซูลิน และไคโตแซนนอกจากการจับกันโดยอาศัยประจุ สำหรับค่า enthalpy change (ΔH) ระหว่างไดโครฟีแนคและไคโตแซน เกิดจากการรับโปรตอนของหมู่อะมีนของกรดไดโครฟีแนค จากการศึกษาพบว่าการจับระหว่างยากับไคโตแซนโดยอาศัยประจุไม่ใช่กลไกหลักที่ทำให้ได้อนุภาคที่มีประสิทธิภาพการกักเก็บยาสูง ยาส่วนใหญ่ที่อยู่กับอนุภาคขนาดเล็กของไคโตแซนเป็นการรวมอยู่ของยากับโครงข่ายไคโตแซนทางกายภาพ การใช้การจับระหว่างยากับไคโตแซนด้วยประจุร่วมกับระบบนำส่งยาเฉพาะที่สามารถช่วยเพิ่มการดูดซึมของยาได้ แม้ว่าการจับระหว่างยากับไคโตแซนด้วยประจุจะเป็นระบบที่อ่อนเกินกว่าที่จะใช้ในการควบคุมการปลดปล่อยยา

181 หน้า ISBN 974-04-6845-4

CONTENTS

LIST OF TABLES

LIST OF TABLES (cont.)

LIST OF TABLES (cont.)

LIST OF TABLES (cont.)

LIST OF TABLES (cont.)

LIST OF TABLES (cont.)

LIST OF FIGURES

LIST OF FIGURES (cont.)

LIST OF FIGURES (cont.)

LIST OF FIGURES (cont.)

LIST OF FIGURES (cont.)

LIST OF FIGURES (cont.)

LIST OF FIGURES (cont.)

LIST OF FIGURES (cont.)

LIST OF FIGURES (cont.)

LIST OF ABBREVIATIONS

%	percent
%T	percent transmisstance
µm	micrometer
µM	micromolar
18-Crown-6	crown ether
^{1}H-NMR	proton-neuclear magnetic resonance spectroscopy
$BaCl_2$	barium chloride
BSA	bovine serum albumin
cm	centemeter
COO^-	Carboxyl group
COOH	Carboxylic group
Da	Dalton
ΔH	enthalpy change
DMSO-d_5	dimethyl sulfoxide-d5
DMSO-d_6	dimethyl sulfoxide-d6
et al.	et alii, and others
FTIR	fourier transform infrared spectra
h	hour
HCl	hydrochloric acid
i.e.	id est, that is
IR	infrared spectra
ITC	isothermal titration calorimetry
k	kilogram
Kcal	kilocalorie
KH_2PO_4	potassium dihydrogen phosphate
kJ	kilojoule
kN	kilonewton

LIST OF ABBREVIATIONS (cont.)

M	molar
MEIA	microparticle enzyme immunoassay
mg	milligram
ml	milliliter
μl	microliter
mM	milimolar
mPaS	milipascal per second
mV	milivolt
N	normality
Na_2SO_4	sodium sulfate
NaOH	sodium hydroxide
nm	nanometer
NMR	nuclear magnetic resonance spectroscopy
ºC	degree Celsius
PCD	particle charge detector
R^2	coefficient of determination
rpm	revolutions per minute
TEM	transmission electron microscopy
TPP	tripolyphosphate
TT	tetanus toxoid
UV	ultra violet
w/o	water in oil
w/v	weight by volume
w/w	weight by weight
X_{50}	quantiles of the volumetric distribution
ZO-1	zonaoccudin-1

PUBLICATIONS AND PRESENTATIONS

PUBLICATIONS

Boonsongrit Y, Mitrevej A, Mueller BW. Chitosan drug binding by ionic interaction. Eur J Pharm Biopharm 2005 ; Article in Press.

Boonsongrit Y, Mueller BW, Mitrevej A. Characterization of drug-chitosan interaction by ^{1}H-NMR, FTIR and isothermal titration calorimetry. Submitted to Eur J Pharm Biopharm (2006).

PRESENTATIONS

Boonsongrit Y, Mueller BW, Sinchaipanid N, Mitrevej A. Effect of human insulin on the physicochemical properties of chitosan microparticles. Poster presentation at RGJ-Ph.D. Congress V, April 24-26, 2004, Jomtien Palm Beach Resort, Pattaya, Thailand.

Boonsongrit Y, Sinchaipanid N, Mitrevej A, Mueller BW. Effect of human insulin on the physicochemical properties of chitosan microparticles and in vitro release study. Oral presentation at The Fourth Indochina Conference on Pharmaceutical Sciences, November 10-13, 2005, Ho Chi Min City, Vietnam.

Boonsongrit Y, Mitrevej A, Mueller BW. Characterization and in vitro release studies of chitosan micro/nanoparticles. Poster presentation at 5th World Meeting on Pharmaceutics Biopharmaceutics and Pharmaceutical Technology of International Association for Pharmaceutical Technology, March 27-30, 2006, Geneva, Switzerland.

CHAPTER I
INTRODUCTION

Due to the advances in biotechnology, many bioactive substances such as peptides, proteins and vaccines can be produced. Several attempts have been made to provide the specific delivery systems with low toxicity and high efficacies. Biopolymers seem to be the preference choices for the development of new effective drug carriers. Chitosan is not only a biopolymer which exhibits favorable biological properties, e.g., non-toxicity, biodegradability and biocompatibility but it also provides attractive physicochemical properties. Therefore, chitosan has been applied in various fields, for example, it is used in waste water treatment, agriculture, foods and cosmetics sciences. For pharmaceutical applications, in the early days, chitosan was used as binder (1) and disintegrant in tablet manufacturing (2). Granules and beads from chitosan were developed for oral controlled release purposes (3, 4). Nowadays, chitosan has been widely investigated especially in the development of site specific drug delivery systems such as colon targeting, nasal delivery, gene delivery and vaccine delivery (5-7).

In view of a variety of delivery routes, chitosan based micro/nanoparticles were extensively investigated (8-10). By cross-linking techniques, spray drying method, coacervation method and reverse micellar technique, chitosan particles with different properties can be prepared (8, 9, 11, 12). However, the disadvantages of these techniques include 1) utilization of organic solvents or harmful substances during preparation; 2) the elevated temperature during preparation; 3) the need of specific equipments. Recently, these disadvantages could be overcome by a simple and mild method (13, 14). Due to a number of amino groups on the polymer chains of chitosan which can be protonated and prompt for the chemical reaction (15, 16), chitosan can interact with negatively charged molecules or polymers. Therefore, the chitosan micro/nano particles formulated by ionic interaction between the cationic chitosan and anionic counterions as tripolyphosphates leading to interpolymer

linkages were proposed. It is so-called ionic gelation process to a flocculation into particles. In these particulate gel beads, the cationic chitosan molecules should still have the capability to bind anionic molecules by an ionic reaction. This method of production of drug loaded chitosan micro/nanoparticles has gained much attention because it is a simple method using non-toxic materials and it involves a mixture of aqueous phases at room temperature without using organic solvents (14).

By ionic gelation method, the development of chitosan based micro/ nanoparticles needs to be carefully formulated to achieve the desired quality. The size and the surface charge of the particles are possible to be adjusted by varying the composition in the formulation such as the polymer drug ratio, the concentration of chitosan (17, 18). The model drug is expected to entrap inside and/or adsorb on the surface of particles. As reported by several researchers, the entrapment efficiency veried from 20 to 95 % (18, 19). Such variation could possibly be due to the variety of equipment and preparation condition, especially, the pH of the formulations and the order of mixing (16, 17). The clear methodology is required to confirm the consistency and the reproducibility of the product obtained.

The release characteristics of chitosan micro/nanoparticles prepared by this method seem to be depending mostly on the solubility of drug, the chitosan concentration and the concentration of cross-linking agent. A high burst effect within half an hour and a total release of the drug within a short time of this kind of nanoparticles were also observed (10, 16, 18, 20). The fast release of drug from the particles at pH 7.4 and pH 4 did not depend on the molecular weight of chitosan (18). This behavior shows that the binding properties of chitosans based on an ionic reaction may be poor.

Besides the release study, a simple way to show the binding capacity of drug to chitosan, the binding interaction of oppositely charged molecules was demonstrated by infrared spectra (IR) spectra (15, 20), X-ray photoelectron spectroscopy (17), and viscosimetry (21). The infrared spectroscopy is used very often to indicate the shift of the functional groups involved in the interactions. In addition the NMR spectroscopy and isothermal titration calorimetry (ITC) were used to indicate the interaction between chitosan and several substances (22, 23).

In this study, the general objective was to prepare chitosan micro/nanoparticles by ionic gelation method using high molecular weight chitosan in order to evaluate their functional properties as pharmaceutical carrier and stabilizer in drug formulation technology. According to a chemical point of view, chitosan represents a weak base, the model drugs used to compare the binding ability of chitosan were classified to large molecule model drug (human insulin) and small molecule model drugs with different acidity (diclofenac sodium, benzoic acid and salicylic acid). The strong acid was expected to promote the interaction of chitosan.
The specific aims were:

1. To determine the change in physicochemical properties, entrapment efficacy of chitosan micro/nanoparticles composed of different amount of model drugs.
2. To study the *in vitro* release behavior of chitosan micro/nanoparticles.
3. To evaluate the interaction and binding energy between model drugs and chitosan.

CHAPTER II
LITERATURE REVIEW

1. Chitosan

Chitosan, β(1,4) 2-amino-2-deoxy-D-glucose, is the N-deacetylated derivative of chitin which is the second most abundant natural polymer next to cellulose and can be obtained from crustaceans, insects, fungi etc. The chemical structure of chitin and chitosan is shown in Figure 1. The demineralization with hydrochloric acid and deproteination with aqueous sodium hydroxide are two steps for the isolation of chitin from crustacean shells. The process of deacetylation for chitosan production is achieved by the treatment of chitin with a strong sodium hydroxide solution at an elevated temperature (24, 25). Figure 2 shows the diagram of the production of chitosan. The term chitosan is used to describe a series of chitosan polymers with different molecular weights (50 kDa-2000 kDa), viscosities (1% chitosan in 1% acetic acid, < 2000 mPaS), and degrees of deacetylation (40-98%) (26). It is insoluble at neutral and alkaline pH values but forms salts with inorganic and organice acids such as glutamic acid, hydrochloric acid and acetic acid. However, chitosan salts are soluble in water and its solubility depends on the degree of deacetylation. Chitosan with a low degree of deacetylation (40%) has been found to be soluble up to pH 9, whereas chitosan with a degree of deacetylation of about 85% is soluble only up to pH 6.5 (24). In acidic solutions, chitosan is protonated and has positive charges. It is believed that the polycationic character of chitosan gives the ability for it to interact with polyanionic counterions (17, 27).

Since chitosan exhibits a large molecular weight, a positive charge, film forming ability and gelation characteristics. It is widely used in industry as a flocculant in the clarification of wastewater and a chelating agent for toxic harmful metals. Chitosan is also used in personal care products (hair treatment, skin care, moisturizer, wound healing), food products (wine and juice clarification, protective fruit coating, a weight loss aid, cholesterol lowering agent) in agriculture

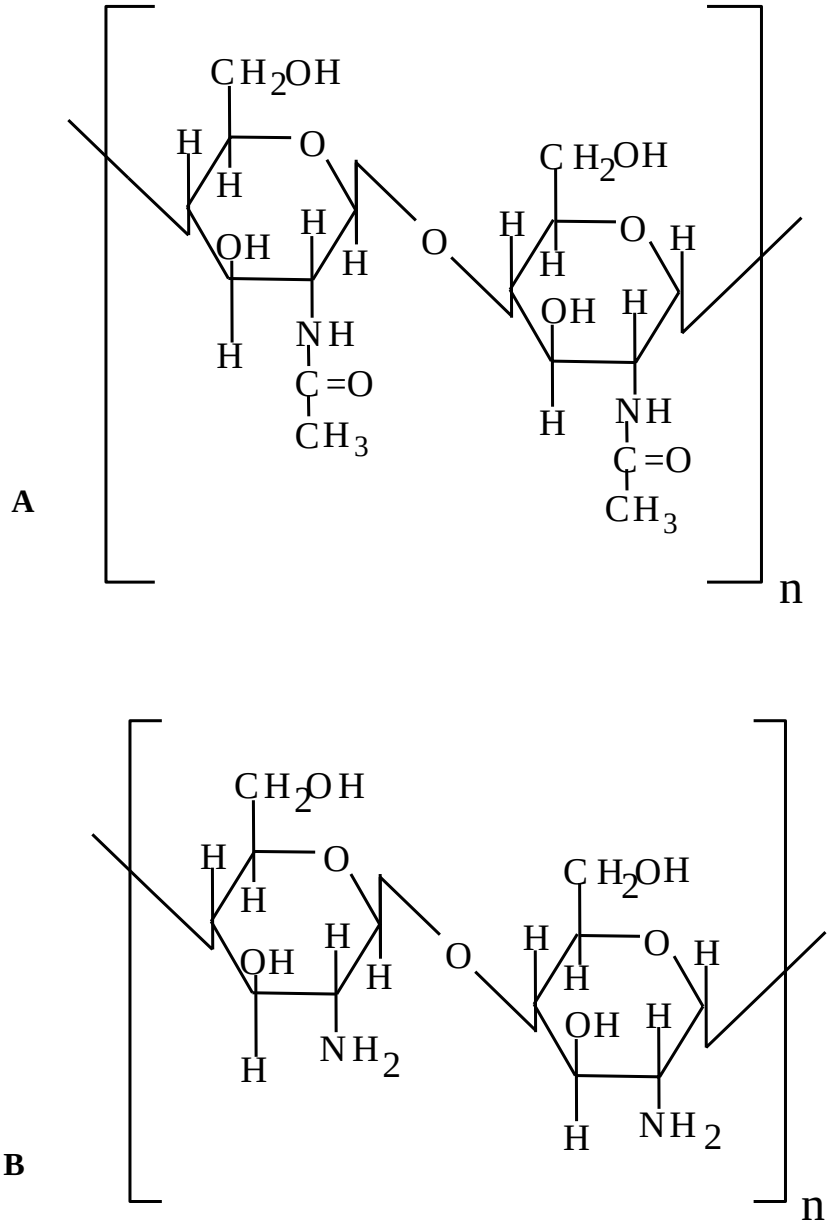

Figure 1. Chemical structure of chitin (A) and chitosan (B)

(seed coating, increasing crop yield, as a controlled release agent for pesticides and herbicides) (28). Moreover, chitosan is a biodegradable and biocompatible polymer that has brought a great attention in pharmaceutical field, especially due to its bioadhesion properties.

1.1. Pharmaceutical uses

Chitosan has been extensively investigated in the pharmaceutical industry (Table 1). Since tablets are still considered as the dosage form of choice for reasons such as low cost of manufacturing and good stability, early studies of chitosan as a diluent, disintegrant and binder have been reported (1, 29).

Nigalaye et al. produced matrix tablets containing chitosan. It was found that using chitosan more than 50% of the tablet weight gave an insoluble non-erosion type matrix tablets (2). In the study of Yao et al. co-compression of small particle size of chitosan (Marine chito, mean particle size: 6 μm) and particles coated with ethylcellulose/HPC prevented the rupture of coating membrane during compression. These tablets showed rapid disintegration into many discrete particles (30). Besides its non-toxic, biodegradable and biocompatible properties, chitosan is a mucoadhesive polymer, an adsorption enhancer and a chelating agent. These properties promoted chitosan as an excipient for novel drug delivery systems.

The mucoadhesion of chitosan is explained by its positive charge which bind strongly with the negatively charged mucosal surface. Furthermore, in an aqueous environment chitosan is able to swell and form a gel-like layer from which a drug can penetrate through surface of polymer and glycoprotein chain of the mucus. There are a number of papers concerning the mucoadhesive properties of chitosan (31-33). It was found that mucoadhesion of chitosan on the intestinal mucosa was able to improve the intestinal absorption of peptide drugs. The degree of adhesion of chitosan-coated particles depends on the amount of chitosan.

For the absorption enhancement property, chitosan has been reported as an absorption enhancer for hydrophilic drugs across the intestinal mucosa. It was demonstrated that the effect of chitosan on the penetration of mannitol in Caco-2 cells was depended on both the degree of deacetylation and the molecular weight of

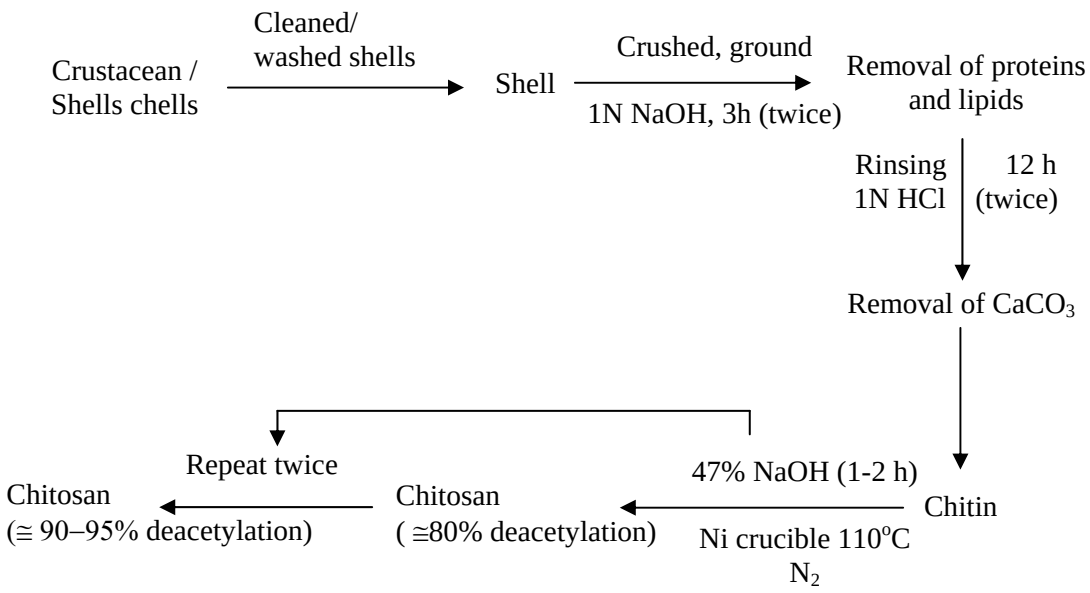

Figure 2. Manufacture of chitosan (adapted from reference no. 24)

polymer (34). Schipper et al. have shown that the absorption enhancing effect of chitosan on epithelial cells was controlled by their positive charges which cause redistribution of cytoskeletal-F actin and the tight junction protein ZO-1 (35). This was further confirmed by Dodane el at. (36).

For the chelating property of chitosan, the amine groups on chitosan serve as a chelation site for the metal ions therefore it has been used as an adsorbent for the removal of heavy metal from waste water stream from mineral operating industries or electronic device manufactures (37). In pharmaceutical field complexing agents are well known to be able to inhibit intestinal peptidase for example carboxypeptidase A and carboxypeptidase B because they can deprive the essential co-factor of enzymes (zinc and calcium, etc) (38). The applicaiton of chitosan to the drug delivery system represents an interesting approach to reduce enzymatic degradation of peptide drugs.

1.2. Biological properties of chitosan

Chitosan, a naturally abundant polymer, is non-toxic and biodegradable polymer with many advantages. Besides the high LD_{50} value of it (> 16 g/kg), the hypocholesterolemic effect, wound healing and antimicrobial effect are outstanding properties and widely investigated (22, 39, 40). Table 2 presents the biological properties and applications of chitosan.

1.2.1. Hypocholesterolemic effect

The belief that chitosan is able to bind fats in the intestine, inhibiting absorption, has brought a great attention to use it as hypocholesterolemic agent. A recent study showed insignificant change of fat absorption in men and women who took chitosan supplements compared with control group (41). Sugano et al. found that after 20 days feeding of 5% cholestyramine or chitosan to rats on a cholesterol containing diet reduced both plasma and liver cholesterol level significantly than control group (42). In the study of Kanuchi and co-workers the mechanism of chitosan to inhibit fat digestion and absorption was proposed, the synergistic effect of ascorbic acid included. In the acid environment, stomachic stage, chitosan was dissolved and mixed well with fat by the strong ability of chitosan for emulsification. In the intestinal stage, rough emulsion of fat with chitosan began to precipitate at pH

Table 1. Pharmaceutical applications of chitosan (adapted from reference no. 26)

Conventional formulation	Novel applications
Direct compression tablets	Bioadhesion
Controlled release matrix tablets	Transmucosal drug transport
Wet granulation	DNA delivery
Gels	Peptide delivery
Films	
Emulsions	
Wetting agent	
Coating agent	
Microparticles	

6.0-6.5 and could not be attacked by intestinal enzyme. Synergistic action of ascorbate was by viscosity reduction in stomach, increase of the oil-holding capacity of chitosan gel and reduction of the leak of entrapped fat in by chitosan in the intestinal tract (40).

1.2.2. Wound healing

Chitin and chitosan based products provide improved healing of surgical wound. The healing process was faster and smooth scars were obtained. The full thickness skin excision on the backs of the rats applied with the water soluble chitosan/heparin complex ointment appeared to be healed better than untreated control groups and those applied with water soluble chitosan (43). In the study of Okamoto et al. by using chitin and chitosan the open wound healing in the dogs was accelerated. The re-epithelialisation was observed clearly in chitin and chitosan treated groups than in control group, although the insignificant different was obtained (44).

Mechanisms of acceleration of wound healing have been investigated by several groups (45, 46). The key factors in rebuilding of physio- logically effective tissues exerted by chitosan were the enhancement of vascularization and a continuous supply of chitooligomers to the wound that stimulate correction deposition and orientation of collagen fibril. The chitooligomers are eliminated by hydrolytic action of lysozyme and N-acetyl-β-D-glucosaminodase (25).

1.2.3. Antimicrobial activity

Great interest in dental caries and infected wounds, chitosan is used as antimicrobial macromolecules with the film forming properties. Zinc is known as disinfectant and bactericide. Comparison to chitosan or zinc alone the chitosan-zinc complexes showed better antimicrobial activities which could be enhanced by increasing the chelate ratios. The hypothesis is the protonated amine groups of chitosan at C-2 interact with anionic constituents on the surface of microorganisms leading to the leakage of intracellular components (47). Liu et, al. reported that the electrostatic force or hydrogen bonding between $–NH_3^+$ and –OH groups of chitosan and –OH groups of β-D-glucopyronoside (nonionic surfactant) caused the chitosan chains extend and disaggregate. Therefore, the antimicrobial activity of chitosan-β-D-

glucopyronoside was higher than that of chitosan and β-D-glucopyronoside separately (48). Several studies revealed the same mechanism of antimicrobial activity (49-51). Jumaa et al. showed, however, that a chitosan in an aqueous solution (1.5%) has no antimicrobial effect (52). An emulsification of the same aqueous phase led surprisingly to formulations which showed antimicrobiological stability. This effect was explained by an increased concentration of the chitosan in the interface and an adsorption and agglomeration of the microorganisms and not by an electrostatical interaction with the excipients.

2. Preparation of chitosan micro/nanoparticles

The broad applications of chitosan–based micro/nanopartilcled could be widely observed over the past decade, include transdermal, parenteral and oral delivery. Several methods are developed in order to obtain high efficacy particles. Concerning the formulation composition (e.g., the thermal and chemical stability of both chitosan and drug) and physicochemical properties of a final product (e.g., particle size) suitable method could be selected.

2.1. Reverse micellar method

The small size nanoparticles with narrow size distribution can be prepared using reverse micelles as a medium (5, 8). The reverse micelles are the systems comprising surfactant dissolved in organic solvent. Chitosan and drug are added at room temperature to the micelles with constant mixing to avoid any turbidity. The mixture is optically transparent. The crosslinking agent such as glutaraldehyde solution is then added and the cross-linking process is continued with constant stirring overnight. By using a rotary evaporator, the organic solvent is removed and the dry mass is obtained. The dry mass is dispersed in water and the surfactant is precipitate out by addition of suitable salt. The precipitate is separated by centrifugation. Next, the supernatant containing drug/chitosan nanoparticles is dialyzed through dialysis bag for 2-3 hour. By lyophilization of the dialyzed solution the dry powder is obtained (Figure 3). These lyophilized nanoparticles can be redispersed easily. An intravenous injections of this nanoparticle suspension in mice showed a longer circulation time in

Table 2. Biomedical properties and applications of chitosan (adapted from reference no.28)

Biological properties	Applications
- Biocompatibility Natural polymer Biodegradability Safety and non-toxicity - Haemostatic - Fungistatic - Anticarcinogen - Anticholesterolimic	- Contact lens (crosslinked to give porous grindable lens material which in non-allergenic) - Wound healing ointment and dressings - Eye bandages - Orthopaedic- temporary bioengineering material - Hypocholesterolemic agent and fat-binding products

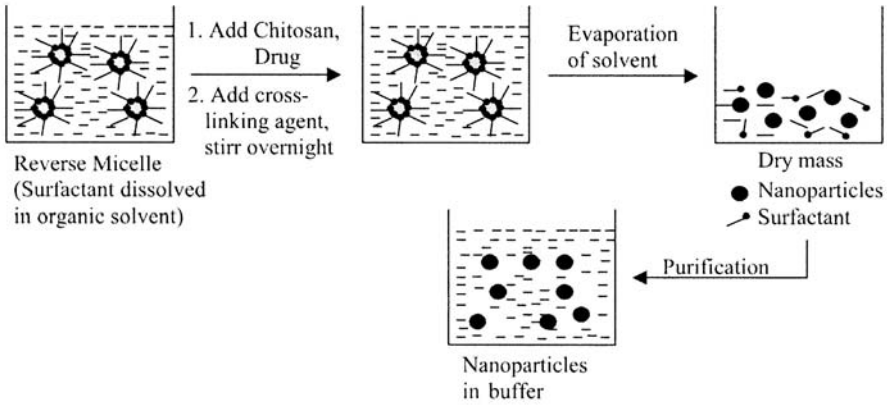

Figure 3. Flowchart of the preparation of chitosan nanoparticles by reverse micellar method (55).

blood circulation system (53).

2.2. Emulsion cross-linking method

Smooth and highly sphere microparticles are obtained by glutaraldehyde crosslinking of chitosan which is emulsified in oil phase. Suitable surfactant is used to stabilize the aqueous droplets. Microsphere are filtered and washed several times with hexane, methanol and finally with water (Figure 4) (9, 54). The incorporation efficiencies of theophylline, aspirin or griseofulvin were more than 80% by the study of Thanoo et al. The drug release was affected by the cross-linked density, particle size and initial drug loading in the microsphere (9). Jameela and co-worker incorporated mitoxantrone in glutaraldehyde cross-linked chitosan microsphere. The particle size was in range of 75-300 μm. The mitoxantrone was released only 25% over 36 days from high cross-linking density microsphere. These microspheres showed insignificant biodegradation over a period of 3 months in the skeletal muscle of the rats.

Via intramuscular injection in rabbit, the long term release up to 5 months of progesterone was achieved from this kind of microsphere without a high burst effect. Cross-linked chitosan microspheres exhibited the potential ability as long term delivery of steroid drugs (10).

2.3. Coacervation method

Based on the property of chitosan that it is insoluble in alkaline pH media, chitosan microparticles are prepared by the precipitation or coacervation of chitoan in alkaline media. By blowing chitosan though a compressed air nozzle or dropping it via syringe equipped with a needle into an alkali solution, for example, NaOH, the perfectly spherical particles are achieved. Then, hardening the particles is done using formaldehyde or glutaraldehyde. Finally, the particles are washed with purified water (Figure 5). In the study of Vasiliu et al, chitosan beads and complexed capsules prepared by simple precipitation and two step coacervation method were compared, respectively. The latter method provided smaller particles with higher stability in the acid media comparing with the particles from the former method (12).

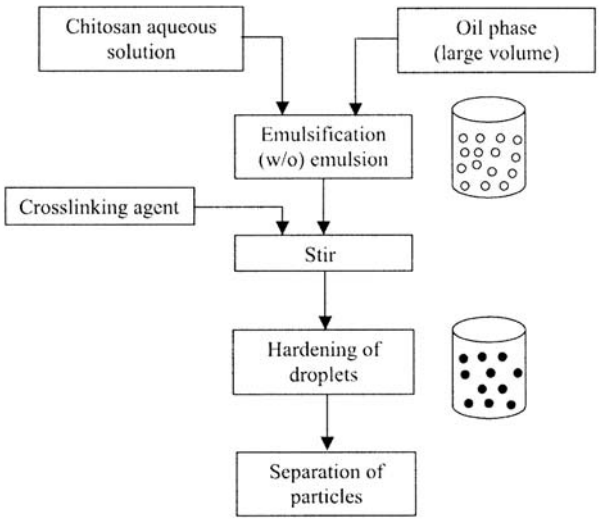

Figure 4. Schematic shows the preparation of chitosan particles by emulsion cross-linking method (55).

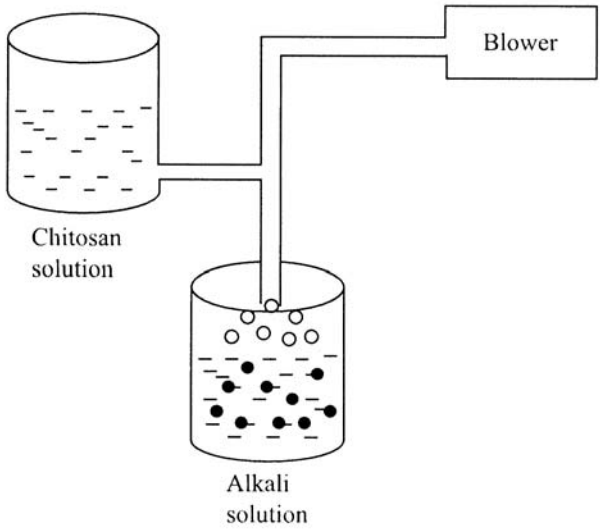

Figure 5. Schematic represents the preparation of chitosan particles by coacervation method (55).

Diltiazem hydrochloride was loaded into casein-chitosan microspheres. These microspheres showed retard release profile. The initial concentration of drug and stirring time were the main parameters affect the properties of microparticles. High concentration of chitosan and high initial drug loading showed a fast drug release profile (56).

2.4. Emulsion-droplet coalescence method

It is the method modified from both precipitation technique and emulsion cross-linked technique. The preparation method is represented in Figure 6. Instead of cross-linking chitosan droplet (w/o), the precipitation by coalescence of chitosan droplets with sodium hydroxide solution is performed. When both emulsions are mixed and high speed stirring, droplets of each emulsion would collide at random and coalesce, thereby precipitating chitosan droplet to give smaller size particles. The deacetylation degree of chitosan affected the size of particles. Decreasing deacetylation degree of chitosan, decrease active amino groups, increasing the particle size (6).

2.5. Spray-drying

Spray-drying is based on drying of atomized droplets in the hot air stream. Cross-linking agent is added to drug-chitosan mixture. These disperision or solution is sprayed in the hot air steam. The size of particles is controlled by the size of spray nozzle, spray rate, atomization pressure, inlet air temperature and amount of cross-linking agent used (Figure 7).

Metoclopramide-chitosan microspheres were prepared by spraying the transparent dispersion of drug in chitosan solution containing various amount of cross-linking agent. Chitosan particles with more than 15% formaldehyde showed good controlled release with small effect by medium pH. For formulation containing 20% of formaldehyde, the release of drug was independent of pH of media. The drug release kinetic is the diffusion control (11). In the resent study of Grenha and co-workers the insulin loaded chitosan nanoparticles were dispersed in aqueous solutionof lactose and mannitol and by spray drying of this suspension dry powders

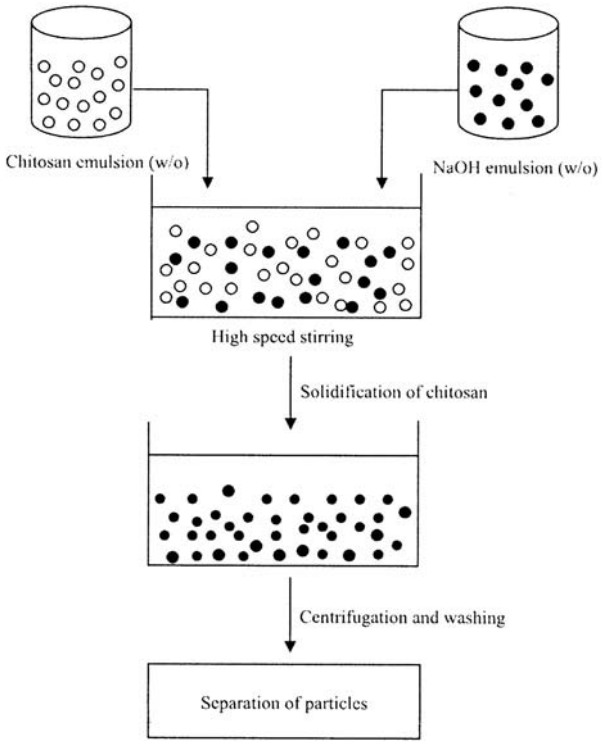

Figure 6. Flow chart of the preparation of chitosan particles by emulsion-droplet coalescence method (55).

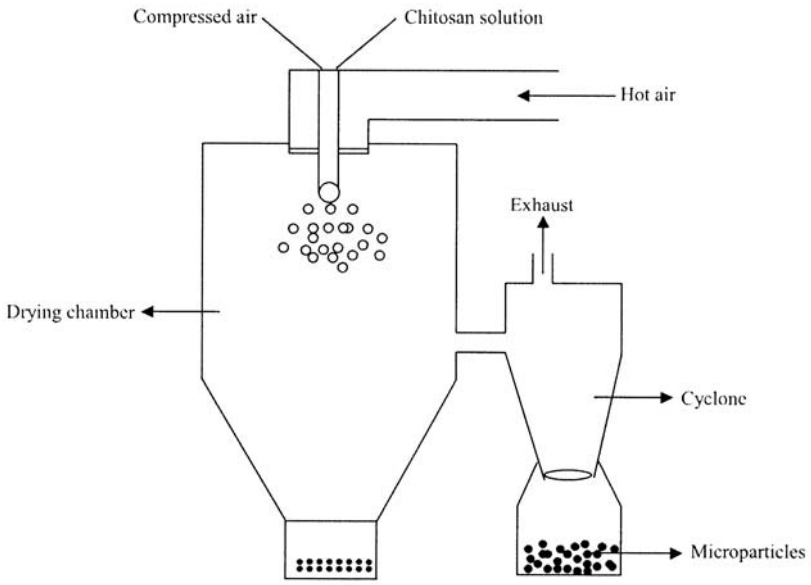

Figure 7. Preparation of chitosan particles by spray drying method (55).

were obtained. The spray dried microspheres are easily reverse to nanoparticles. The microsphere morphology was affected by the content of chitosan nanoparticles. These nanoparticles show a good insulin loading capacity (65-80%), providing the release of 80% insulin within 15 min (57).

2.6. Ionic gelation method

As mentioned above, various methods can be used to prepare micro/nanoparticles. However, using organic solvents or elevated temperature during preparation of these methods can destroy or alter the activity of sensitive drugs such as proteins or peptides. To overcome these limitations, ionic gelation process has been applied. It is a simple method using non-toxic substances and involves a mixture of two aqueous phases at room temperature. It is a reversible interaction of oppositely charged molecules, for example, tripolyphosphate (polyanion) interact with chitosan (cationic polymer) by electrostatic force (16, 58). Figure 8 shows the preparation of chitosan micro/nanoparticles by ionic gelation method.

2.6.1. Effect of molecular weight and deacetylation degree of chitosan

Ko et al. concluded that TPP/chitosan microparticles with a size of 500-710 μm had more spherical shape and smoother surface when increasing molecular weight of chitosan and decreasing pH of TPP solution (59). Bovine serum albumin (BSA) loaded chitosan nanoparticles were prepared from various molecular weight and deacetylation degree of chitosan. Increasing molecular weight of chitosan from 10 to 210 kDa, BSA encapsulation efficiency was enhanced from 7 to 20%. This is possibly due to the fact that the longer chain of chitosan can entrap the greater amount of BSA before adding tripolyphosphate. Increasing deacetylation degree of chitosan from 75 to 92% resulted in slightly improve on the encapsulation efficiency and decelerate the release rate (60). In the study of Shiraishi indomethacin was dispersed in chitosan solution in acetic acid. This suspension was dropped through a glass syringe with a nozzle into tripolyphosphate solution. The beads were washed with distilled water and dried overnice at room temperature. The negative correlation was observed between the molecular weight of chitosan and the release rate constant of indomethacin (61). Vila and co-workers investigated the delivery of vaccine using

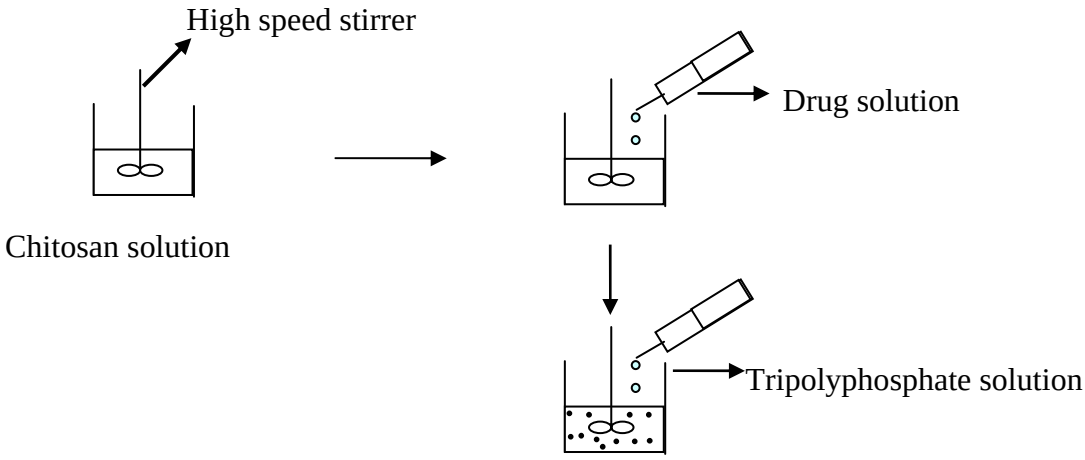

Figure 8. Schematic representation of preparation of chitosan particles by ionic gelation method.

ionic cross-linked chitosan nanoparticles. Tetanus toxoid was loaded into various molecular weights of chitosan nanoparticles. Their physicochemical properties, e.g., size, surface charge and association efficiency were similar, irrespective of the chitosan molecular weight (7).

2.6.2. Effect of drug and chitosan concentration

Two types of Chitosan hydrochloride with different in molecular weight (Seacure 210® Cl and Protasan 110® Cl) were used to produce insulin loaded chitosan nanoparticles. The size and loading capacity were increased when increasing insulin concentration form 0.0 to 1.25 mg/ml, while the zeta potential was decreased. These results indicate the partial neutralization of nanoparticles surface charges due to the association of increasing amount of insulin (18). Aydin and Akbuga have reported that the encapsulation efficiency of salmon calcitonin to chitosan beads with diameter about 0.9 mm was greater than 50% and the drug content of beads was not dependent on the initial drug concentration (62). Contrary to the study of Bodmeier et al, which the sulfadiazine content of chitosan beads increased with increasing payload (14).

The concentrations of chitosan and cross-linking agent are the main factors effect on the particle size of product prepared by ionic gelation method. Nanoparticles can be obtained using the concentration of chitosan and tripolyphosphate between 1 - 3 mg/ml and 0.2-1.0 mg/ml in formulation, respectively (Figure 9) (18, 19).

2.6.3. Drug release from chitosan micro/nanoparticles

The *in vitro* release behavior of chitosan micro/nanoparticles was affected by several factors such as the interactive forces between drug molecules and chitosan, the characteristics of the release medium and the solubility of the drug. The release profiles of tetanus toxoid (TT)-chitosan nanoparticles in 5% v/v thehalose solution show two release phases, a rapid release over the first two hours followed by a slow release for up to 16 days. The first release phase could be attributed to the release of TT molecules that were slightly bind with chitosan molecules and located near the surface of particles, whereas the second phase could be the release of TT molecules which efficiently entrapped to chitosan molecules (7).

Bovine serum albumin-chitosan nanoparticles exhibited different entrapment efficiency from 20-90% depending on the concentration of bovine serum albumin (BSA) and the pH of chitosan solution. The nanoparticles with 20-25% BSA loading released the entrapped BSA with no burst effect at fairly constant rate in water, while the nanoparticles containing 41% BSA released BSA faster as biphasic release profile. The higher the loading the faster BSA released from nanoparticles (17).

Fernandez-Urrusuno et al. prepared insulin loaded chitosan nanoparticles with the loading up to 55% w/w using two types of chitosan hydrochloride, varying in their molecular weight (<50 kDa and 130 kDA). The nanoparticles represented positive surface charge ranging from +54 mV to +25 mV and the particle size in the range of 300-400 nm. Figure 10 shows the *in vitro* release of insulin from nanoparticles when pH 7.4, pH 6.4 phosphate buffer and pH 4 acetate buffer were release media. The very fast release at pH 7.4 and pH 4 were observed and was not affected by the chitosan molecular weight. The slightly slow release at pH 6.4 was possible due to the lower solubility of insulin at this pH (18). The associdated insulin rapidly and completely release from the chitosan-insulin nanoparticles in the media of pH 2 to 7.4 was confirmed by the study of Ma and co-workers (16). Recently, the insulin loaded chitosan nanoparticles by ionic interaction were developed to microspheres by spray drying of the mixture of aerosol excipients and nanoparticles. High burst release profiles of drug were observed within 15 minutes from both spray dried microspheres and nanoparticles (57). The high burst effect already shows that the binding properties of chitosan based on an ionic reaction may be poor and that chitosan as an excipient in micro/nanoparticulate drug delivery are open to doubt.

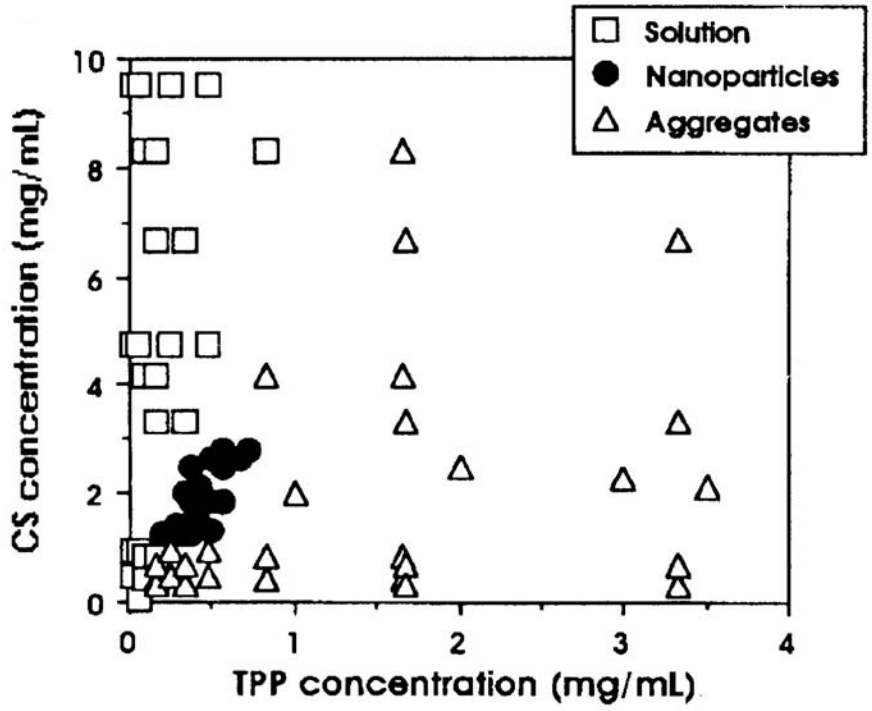

Figure 9. Identification of chitosan nanoparticles domain (19).

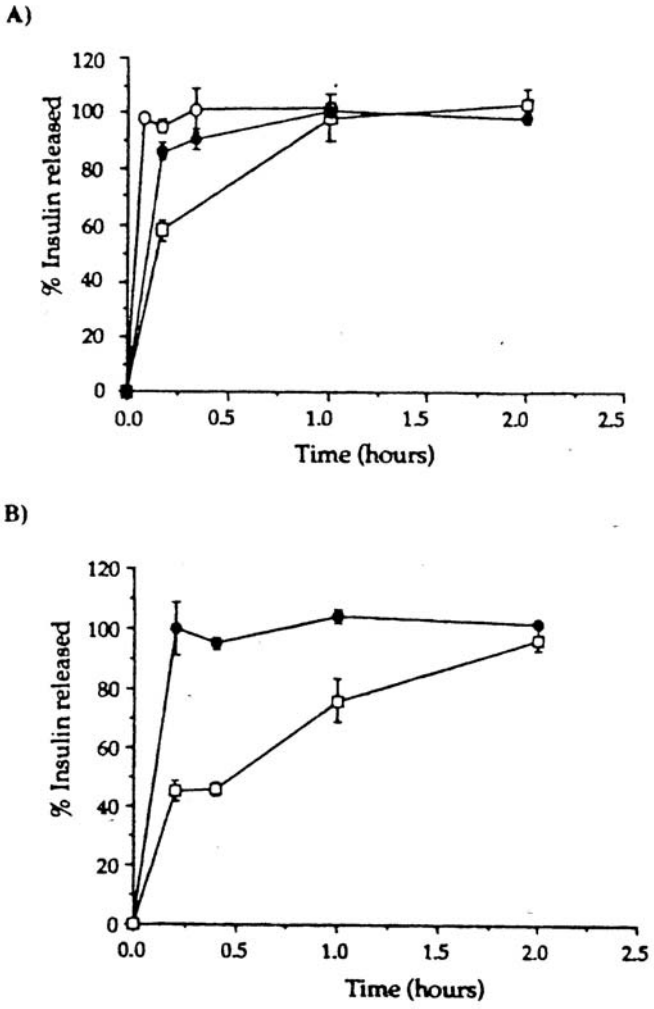

Figure 10. Insulin release profiles from insulin chitosan nanoparticles. A) chitosan (Mw =130 kDa) nanoparticles, at pH 7.4 (○), 6.4 (□) and 4.0 (●). B) chitosan (Mw < 50 kDa) nanoparticles, at pH 6.4 (□) and 4.0 (●) (18).

3. Model drugs

3.1. Human insulin

The most widely investigated protein drug is insulin, a pancreatic hormone. It is secreted by the bata cells in the islets of Langerhans to control the utilization of glucose in all the organs and maintain the glucose concentration at the normoglycemic level. An insufficient production of insulin results in the disease diabetes mellitus. Treatment of this disease involves giving the extra insulin to patient via subcutaneous. Insulin was first isolated in 1921 and the rhombohedral form was first crystallized in 1926. Its amino acid sequence was determined in the late 1950s (63). The importance of zinc and other divalent cations in crystallization was also elucidated. For many years, because of the limited availability of human insulin, most insulin used by diabetics was obtained from the pancreases of slaughter-house animals. Presently, by recombinant DNA technology, a large amount of human insulin can be produced. Human insulin obtained by recombinant DNA technology is sometimes termed biosynthetic human insulin (64).

Insulin is white or almost white crystalline powder. It is slightly soluble in water and soluble in dilute acid (65). Figure 11 shows the primary structure of human insulin. It composes of 51 amino acids distributed in two polypeptide chains, the A and B chain, connected by 2 disulphide bridges. The molecular weight is approximately 6000 Da. The pKa of insulin is 5.3 (16). Insulin can exist as a monomer, dimmer or hexamer. At low concentrations (~ 10^{-6} M) insulin exists as a monomer and forms dimer at higher concentration at neutral pH. At high concentration and in the presence of zinc ions insulin aggregates further to form hexamer (66). The hexamer is stored as granules in the beta cell. This structure is the active conformation of the homone. The hexamer dissociates after insulin is secreted from the beta cell and enters the systemic circulation. The biologically active form of this hormone is the monomer which is the predominate form in the blood circulation (67).

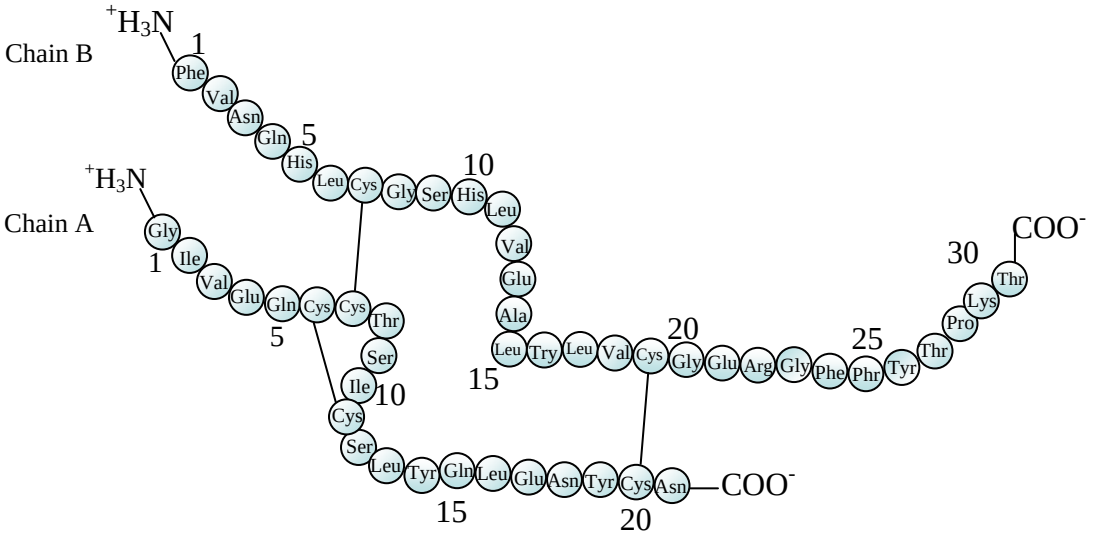

Figure 11. Schematic shows an amino acid sequence (primary structure) of the human insulin. Two disulphide bonds derive from cysteine residues link between A-chain and B-chain (A7-B7 and A20-B19). An intrachain disulphide bond is in A-chain (A6-A11) (adapted from reference no 68).

Several interactions contribute to different structures of protein and insulin. Besides disulphide bonds, there are electrostatic interactions, hydrogen bonds and hydrophobic interactions. These interactions between the amino acid side chains (R groups) change secondary structure of protein to the tertiary structures (68).

Disulphide bonds result from the –SH groups of two cysteine molecules reacting with each other to form a covalent bond. It can involve two cysteine units in the same chain or in different chains as presented in the structure of insulin.

Electrostatic interactions, salt bridges, involve amino acids with charge side chains. The two R groups, one acidic and one basic, interact via ion-ion attractions such as the interaction between COO^- and NH_3^+ of side chains.

Hydrogen bonds can happen between amino acid with polar R groups. The polar R groups are –OH, $-NH_2$, -COOH and $–CONH_2$, for example. The hydrogen bonds can be disrupted by the change in pH and temperature.

Hydrophobic interactions are result from the interaction between nonpolar side chains. Globular protein usually have their nonpolar R groups inward and their polar R groups outward, in aqueous solution therefore the nonpolar R groups interact with each other. Although hydrophobic interactions are weaker than hydrogen bonds or electrostatic interactions, their cumulative effect is greater than the effects of hydrogen bonding because there are so many of them (68). There are several studies about the self association of insulin, polymerization and hydrophobic bonding of insulin in the late 1970s (66, 69).

3.1.1. Degradation of insulin

Chemical instability and physical instability are two pathways for the degradation of proteins, included insulin (Figure 12). Chemical instability can be defined as any process that involves modification of the protein via bond formation or cleavage, yielding a new chemical entity. The physical instability does not involve covalent dodification of the protein. Rather, it refers to changes in the higher order structure (secondary and above). These include denaturation, adsorption to surfaces, aggregation, and precipitation.

Deamidation, a reaction that the side chain amide group in glutaminyl or asparaginyl residues is hydrolyzed to form a free carboxylic acid, is the most common of chemical reactions which cause the degradation of protein (70, 71). As shown in Figure 11 insulin contains six such residues (Gln^{A5}, Gln^{A15}, Asn^{A18}, Asn^{A21}, Asn^{B3} and Gln^{B4}). The three asparagines residues are the most labile sites. In acid solution the rapid deterioration of insulin is due to extensive deamidation at residue Asn^{A21} and in neutral solution deamidation takes place at residue Asn^{B3}. The rate of hydrolysis is independent of the concentration and the species of insulin but vary with the storage temperature and formulation (70). In the stability study of insulin, contrary to the expectation, Pikal and Rigsbee found that the freeze-dried amorphous insulin showed greater stability than crystalline insulin, however, the clarified mechanism for the superior stability of amorphous insulin still need to be evaluated (72). The stability of insulin have been widely investigated for more than three decades (69, 73-75).

3.2. Diclofenac sodium

Diclofenac sodium is a non-steroidal anti-inflammatory drug with pronounced analgesic and antipyretic properties. The chemical structure is represented below. Diclofenac sodium is an odorless, white to off–white crystalline powder with molecular weight of 318.13. The solubility in water and in phosphate buffer is > 9 mg/ml and 6 mg/ml, respectively. The pKa in water is 4.0 (76).

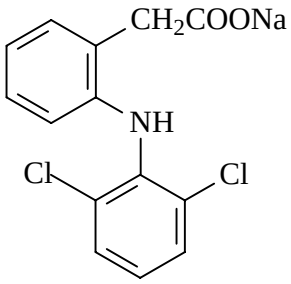

Diclofenac sodium

It was used in several studies as a model drugs for controlled drug release dosage forms (77-79). The drug release behavior of diclofenac sodium loaded

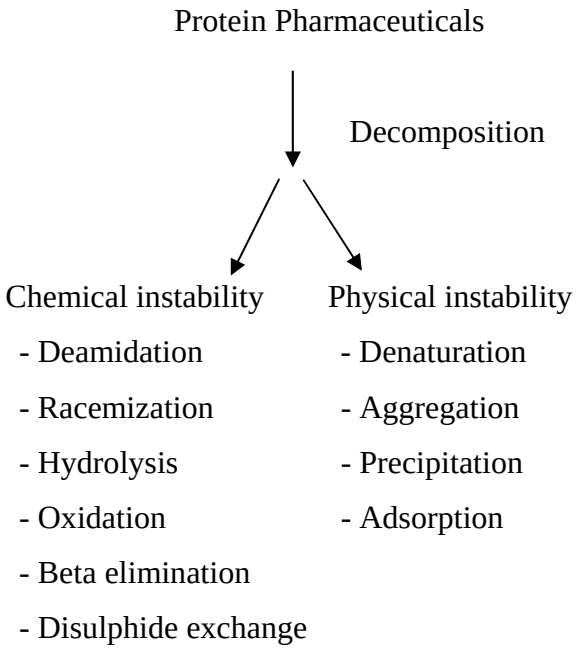

Figure 12. Summary of the physical and chemical instability of protein pharmaceuticals (80).

chitosan beads (diameter ~0.5 mm) and microgranules (diameter of 0.1-0.5 mm) by emulsion cross-linking method were studied. The release of drug depended on pH of the release media. In comparison of the release profiles at pH 2, there was a little drug release at pH 7.4. It could be implied that the release of the drug depended on the swelling of the particles. At pH 7.4 there was very limited swelling of chitosan particles; therefore the drug entrapped in the particles could not be released easily. But at pH 2 the great swelling ability of chitosan particles resulted in the fast release of drug. The release rate of diclofenac sodium from the beads was slower than that of microgranules (81).

3.3. Benzoic acid

Benzoic acid is widely use in cosmetics, foods and pharmaceuticals as an antimicrobial preservative (82). It is white or colorless crystals. The molecular weight is 122.21. The solubility in water (25 ºC) is 3.4 mg/ml. The dissociation constant (pKa) at 25ºC is 4.2 (83). The structural formula of benzoic acid is indicated below.

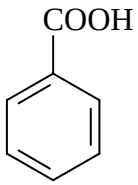

Benzoic acid

Byene and Deasy studied the capacity of commercial porous ceramic particles as sustained drug delivery. Ceramic microparticles with the size in range 850-1000 μm were loaded with benzoic acid. The drug loading was affected by the initial drug concentration and the porosity and bulk density of the ceramic particles. *In vitro* release profiles showed an initial burst release of drug and followed by the sustained release. The release was influenced by the surface pore size distribution of the ceramic and by the electrostatic interactions between microparticle surfaces and the drug (84).

3.4. Salicylic acid

Salicylic acid, a keratolytic agent, occurs as white fine needle crystals (85). The molecular weight is 138.12 and the solubility in water is 2.17 mg/ml (86). The pKa is 2.97. The chemical structure is showed below.

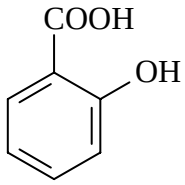

Salicylic acid

Salicylic acid was a model drug for the development of a new method, which utilized a recirculating flow-through system for the dissolution medium and used conductivity measurements to monitor the drug concentration in the system, for characterizing the release of drugs from single agglomerates (87). In the drug release study of glyceryl monooleate/water cubic phase systems (GMO/water system) (88), GMO/water systems were prepared with various water contents by melting Myverol 18-99® at 42ºC and addition then the required amount of water at the same temperature. Salicylic acid was loaded by mixing it in the molten Myverol 18-99® before the addition of water. The release of salicylic acid from a GMO/water cubic phase system was independent of the initial drug loading and initial water content (88).

CHAPTER III
MATERIALS AND METHODS

Materials

1. Chitosan (MW 150kDa, degree of deacetylation 84.5% (Lot number 22741, Fluka chemie AG, Buchs, Switzerland)
2. Pentasodium tripolyphosphate (Lot number 46H105, Sigma Chemical Co., St Louis, USA)
3. Human insulin (HMR 4006, Aventis, Frankfurt, Germany)
4. Diclofenac sodium (Lot number 0207548, Heumann Pharma GmbH, Feucht, Germany)
5. Benzoic acid (Lot number k90808736 836, Merck KGaA, Damstadt, Germany)
6. Salicylic acid (Lot number 200-712-3, Kraemer & Martin GmbH, Sank Augustin, Germany)
7. Glacial acetic acid (Merck KGaA, Damstadt, Germany)
8. Sodium hydroxide (Lot number B239682 251, Merck KGaA, Damstadt, Germany)
9. Monobasic potassium phosphate (Lot A324973 138, Merck KGaA, Damstadt, Germany)
10. Hydrochloric acid (Lot number 0C 123829, Merck KGaA, Damstadt, Germany)
11. Sodium sulphate (Lot number TA955749 117, Merck KGaA, Damstadt, Germany)
12. Methanol (HPLC grade, Mallinckrodt Baker B.V., Deventer, Holland)
13. Acetronitrile (HPLC grade, LGC Promochem GmbH, Wesel,Germany)
14. polyamide membrane (0.2 µm, 0392 11807691001500, Sartorius AG, Goettingen, Germany)

15. Cellulose acetate membrane (0.2 µm, 0202 11107 0101673, Sartorius AG, Goettingen, Germany)
16. PESU member (0.1 µm, Lot number 0904 15458 0451103, Sartorius AG, Goettingen,Germany)
17. Syringes (5ml, Braun Melsungen AG, Melsungen, Germany)
18. Needles (sterican, Gr1; 0.9 × 40 mm, Lot no. 97032146, Braun Melsungen AG, Melsungen, Germany)
19. Hypocholic acid (Merck KGaA, Damstadt, Germany)
20. Bovine serum albumin (Lot number 45H1097, Sigma Chemiecal Co., St Louis, USA)
21. 18-crown-6 (Lot number 05725KB-414, Sigma-Aldrich Chemie GmbH, Steinheim, Germany)
22. Barium chloride dehydrate (Lot number A309910 119, Merck KGaA, Damstadt, Germany)
23. Potassium Bromide (Lot number B149407 227, Merck KGaA, Damstadt, Germany)

Equipments

1. High speed stirrer (Ultraturrax® T 25 B, Ika-Werke GmbH, Staufen, Germany)
2. Centrifuge (Biofuge A, Heraeus Sepatech GmbH, Osterode, Germany)
3. Centrifuge (Biofuge 17 RS, Heraeus Sepatech GmbH, Osterode, Germany)
4. Laser diffractometer (Helos- Partikelgroessanalysator Windox 4, Sympatec GmbH, Clausthal-Zellerfeld, Germany)
5. Zetapotential analyse (Zetaplus®, Brookhaven instruments, Vienna, Austria)
6. Particle charge detector (PCD 03 pH, Muetek Analytic GmbH, Herrsching, Germany)
7. Fourier transform infrared spectroscopy (PerkinElmer 16PC spectrometer, Perkin-Elmer, Boston, USA)
8. Transmission electron microscopy (TEM) (TECNAI G^2, Philip, Czech Republic).
9. High performance liquid chromatography
   - High precision pump (Model 480, Gynkotek, Munich, Germany)
   - HPLC detector (HPLC 430, Kontron instruments, Bletchey, UK)
   - Autosampler (HPLC 465, Kontron instruments, Bletchey, UK)
   - HPLC column (LiChroCart 125-4, LiChrospher 100RP-18(5um), Merck KGaA, Darmstadt, Germany)
10. Shaking water-bath (Julabo SW20C, Julabo Labortechnik GmbH, Seelbach, Germany)
11. ^{1}H-NMR spectrometer (Brucker ARX 300, Brucker, Rheinstetten, Germany)
12. An automated analyzer (IMx System, Abbott laboratories, Illinois, USA)

Methods

1. Preparation of chitosan micro/nanoparticles

1.1. Preparation of chitosan solution

Various concentrations of chitosan solution were prepared by dissolving chitosan in aqueous acetic acid solution (1%). The pH of chitosan solution was adjusted to pH 5 or pH 3.3 with 1N sodium hydroxide solution or glacial acetic acid, respectively.

1.2. Preparation of pentasodium tripolyphosphate solution

The pentasodium tripolyphosphate solution (0.1-1.6% w/v) was prepared by dissolving in purified water.

1.3. Preparation of human insulin solution

To prepare an insulin solution (1-6 mg/ml), insulin powder was dispersed in pH 7.4 phosphate buffer solution. Subsequently, the insulin was dissolved by adding 1 N HCl. An equal amount of 1 N NaOH solution was then added to adjust the pH of the solution to pH 7. Finally, the pH 7.4 phosphate buffer was added to the desired volume (89).

1.4. Preparation of diclofenac sodium solution, benzoic acid and salicylic acid solution

A diclofenac sodium solution (5 mg/ml), benzoic acid solution (0.2-3 mg/ml) and salicylic acid solution (0.2-3 mg/ml) were prepared by dissolving the drugs in purified water.

1.5. Preparation of drug-chitosan micro/nanoparticles

Drug loaded chitosan micro/nanoparticles were prepared by ionic interaction. The chitosan solution (25 ml) was stirred at 11,000 rpm with a high speed stirrer (Ultraturrax®T25B, Ika-Werke, Staufen, Germany) at room temperature (25ºC). The drug solution was dropped into the chitosan solution (0.75 ml/min). The tripolyphosphate solution (10 ml) was gently added to the system to complete micro/nanoparticle formation.

2. Characterization of micro/nanoparticles

2.1. Morphology

The morphological determination was performed by transmission electron microscopy (TEM) (Technai G^2, Philip, Czech Republic). The samples were stained with 2% w/v phosphotungstic acid and placed on copper grids with Formvar films for viewing by TEM.

2.2. Mean particle sizes

Measurements of particle sizes were determined by a laser diffractometer (Helos-Partikelgroessnanalysator Windox4, Sympatec, Clausthal-Zellerfeld, Germany) and photon correlation spectroscopy (Zetaplus®,Brookhaven instruments, Vienna, Austria) was used for detection of submicron particles. The samples were diluted at the ratio of 1:2 to 1:12 with purified water before measurement. With laser diffraction analysis, the suspensions were characterized by X_{50} quantiles of the volumetric distribution.

2.3. Particle charges

The charge of micro/nanoparticles was expressed in terms of zeta potential by laser doppler anemometry (Zetaplus®, Brookhaven instruments, Vienna, Austria) and the particle charge per volume of suspension by particle charge detector (PCD 03 pH, Muetek analytic, Herrsching, Germany). The samples were diluted with purified water. The dilution factor was 1:30 and 1:12, respectively.

The particle charge detector (PCD) provides quantitative determination of the charges of particles by measuring the streaming current. The cylindrical test cell with a fitted displacement piston constituted the centerpiece of the PCD. The oscillating piston forces the sample suspension to flow along the plastic wall of the test cell so that the counter-ions are sheared off and the so-called streaming current is generated. The streaming current is immediately detected and the polyelectrolyte with opposite charge to the sample is titrated to the sample until it reached the point of zero charge (Figure 1). The particle charge is calculated from the titrant consumption. The titrants used to neutralize positive charge and negative charge are polyethylensulfonate

sodium (PES-Na) and poly (diallyldimethylammonium) chloride (PolyDADMAC), respectively.

The formula for calculation of the particle charge is:

$$Q = \frac{V \cdot c}{m} \cdot F$$

Q = particle charge (C/ml); V = titrant consumption (l)

c = titrant concentration (mol/l); m = active substance of sample (ml)

F = Faraday's constant (9.6485×10^4 C/mol)

2.4. ^{1}H-NMR spectroscopy

To prove the existence of ionic interaction between drugs (benzoic acid and salicylic acid) and chitosan, drug solution (0.3% - 0.02% w/v) were mixed with 0.2% w/v chitosan solution, purified water or 0.2% w/v ammonium acetate solution at the ratio 1:2. Then by ^{1}H-NMR spectroscopy the chemical shift was followed. A 0.3% of sodium benzoate and sodium salicylate in above mentioned solutions were also analyzed to show the chemical shift of 100% ionized of benzoic acid and salicylic acid, respectively. The sample measurements were carried out in a Brucker ARX 300 NMR spectrometer (Brucker, Rheinstetten, Germany) at temperature of 300 K and a frequency of 300.13 MHz with water suppression technique. Dimethyl sulfoxide-d_6 with 0.1% tetramethylsilane (TMS) was used as the external standard.

2.5. FTIR spectroscopy

Two of four model drugs were used to prepare micro/nanoparticles for FTIR analysis in order to observe the shift of functional groups. As indicated in Table 3 insulin-chitosan microparticles and benzoic acid-chitosan nanoparticles containing various concentrations of drug, tripolyphosphate or chitosan were prepared according to the preparation method in 1.5. The drug-chitosan micro/nanoparticle suspensions were washed 3 times with purified water to remove non-entrapped drug and chitosan left in the suspending medium. By centrifugation at 10,000 rpm (Biofuge 17 RS, Heraeus Sepatech GmbH, Osterode, Germany) the particles were isolated. Then the micro/nanoparticles were dried by vacuum dryer at 20ºC overnight. The dried drug-

chitosan micro/nanoparticles were studied by FTIR spectrophotometer (Perkin-Elmer 16 PC spectrometer, PerkinElmer, Boston, USA). A 1 mg of drug-chitosan micro/nanoparticles were mixed with 1 g of KBr powder. The mixture was filled in the die and compressed at 9 kN for 2 minutes. The compressed disk was placed in the sample holder. The infrared spectra were detected over 4000-600 cm^{-1} using 8 scans and with resolution equal to 4 cm^{-1}.

3. Evaluation of drug entrapment efficiency

The amount of drug entrapped in the micro/nanoparticles was calculated by two methods. The first method was the calculation of the difference between the total amount of drug used to prepare the micro/nanoparticles and the amount of non-entrapped drug remaining dissolved in the aqueous suspending medium. Micro/nanoparticles were separated from the suspending medium by filtration using 0.2 μm cellulose acetate membrane filters. To avoid the adsorption of insulin on the membrane, the PESU was use for the separation of insulin-chitosan microparticles. The aqueous medium was assayed for drug concentration by HPLC. The drug entrapment efficiency of micro/nanoparticles was calculated as indicated below.

Entrapment efficiency =

$$\frac{(\text{Total amount of drug loading} - \text{free drug in supernatant})}{\text{Total amount of drug loading}} \cdot 100$$

The second method for evaluation of drug entrapped in the micro/nano-particles was an estimation of the drug directly in the micro/nanoparticles. This was used in the release studies to calculate the percentage of the released amount of drug. An accurate volume of micro/nanoparticles suspension was incubated in pH 9.6 alkaline borate buffer at 37ºC and agitated at 100 rpm. At predetermined times, after centrifugation (Biofuge A, Heraeus Sepatech GmbH, Osterode, Germany), the supernatant was assayed for drug concentration by HPLC. The total amount of drug was considered as the entrapped amount.

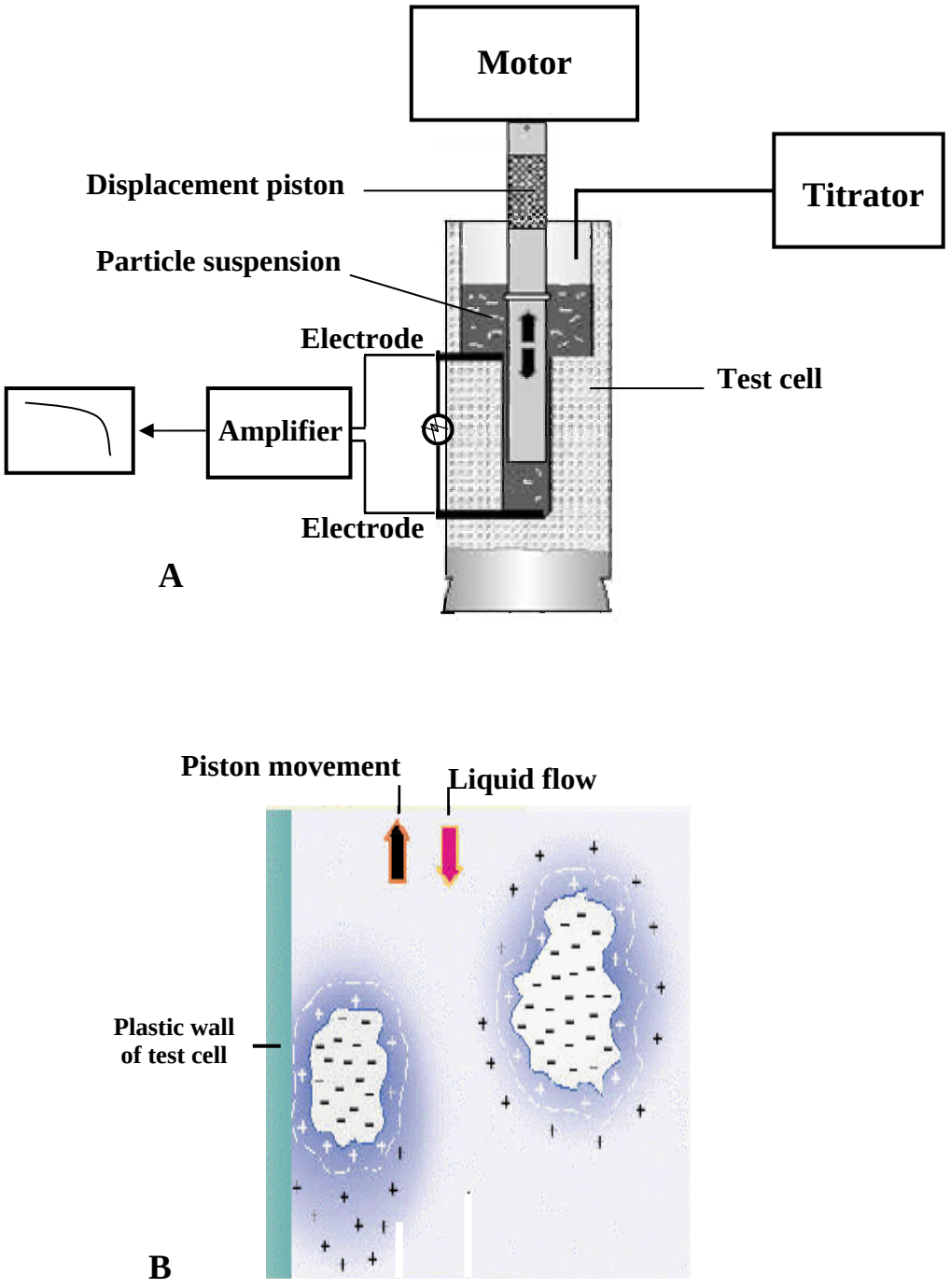

Figure 13. The schematic of particle charge detector (A) and the movement of liquid sample and displacement piston of particle charge detector (B)

Table 3. The formulations of drug-chitosan micro/nanoparticles for FTIR analysis

	Concentration		
	Drug solution (mg/ml)[a]	Chitosan (% w/v)	Tripolyphosphate (% w/v)
Insulin-chitosan microparticles	1	0.2	0.1
	2	0.2	0.1
	3	0.2	0.1
	5	0.2	0.1
	6	0.2	0.1
	5	0.1	0.1
	5	0.2	0.1
	5	0.3	0.1
	5	0.4	0.1
	5	0.5	0.1
	5	0.2	0.1
	5	0.2	0.2
	5	0.2	0.4
	5	0.2	0.8
	5	0.2	1.6
Benzoic acid-chitosan nanoparticles	0.5	0.2	0.3
	1.0	0.2	0.3
	1.5	0.2	0.3
	2.0	0.2	0.3
	2.5	0.2	0.3
	2	0.1	0.3
	2	0.2	0.3
	2	0.3	0.3
	2	0.4	0.3
	2	0.5	0.3
	2	0.2	0.2
	2	0.2	0.4
	2	0.2	0.8
	2	0.2	1.6

[a] The volume of drug solution added into formulation was 6 ml.

4. Analysis of drugs

4.1. High performance liquid chromatography (HPLC)

HPLC was used to assay human insulin, diclofenac, benzoic acid and salicylic acid. HPLC analyses were performed using a high precision pump (Model 480, Gynkotek, Munich, Germany), a UV detector (HPLC430, Kontron instruments, Bletchey, UK), and a reverse phase column (LiChroCart 125-4, LiChrospher 100 RP-18(5 μm), Merck, Darmstadt, Germany) and the column temperature was maintained at 20ºC for analysis of insulin and diclofenac and 40 ºC for analysis of benzoic acid salicylic acid.

For human insulin the mobile phase was composed of 27% v/v acetonitrile and 73% v/v of buffer (0.01 M KH_2PO_4 and 0.1 M Na_2SO_4, adjusted to pH 3 with H_3PO_4). The flow rate was 1 ml/min. A 100 μl of sample was injected and the eluent was monitored for the absorbance of insulin by UV detector at 215 nm.

For analysis of diclofenac samples of 100 μl were eluted with a mobile phase comprising methanol (60% v/v) and 40% buffer (0.01 M of KH_2PO_4 and Na_2HPO_4, adjusted to pH 6.5 with H_3PO_4). The flow rate was 1 ml/min and the detection wavelength was set at 282 nm.

For analysis of salicylic acid and benzoic acid 50% v/v of methanol, 48% v/v of water and 2% v/v of glacial acetic acid were used as a mobile phase. The flow rate was 1.0 ml/min. A 100 μl of sample was injected and the detection wavelength was set at 238 nm.

4.2. Calibration curve of model drugs for HPLC analysis

An accurate weight of drugs were transferred to a volumetric flask and dissolved as described in 1.3-1.4. Appropriate dilutions with mobile phase were made to obtain a series of standard solutions. A portion of each standard solution was injected into the HPLC column. The peak areas of drugs were plotted against the concentrations of model drugs.

4.3. Microparticle enzyme immunoassay (MEIA)

To test the immunological activity of human insulin in formulation compared with human insulin solution MEIA was performed. An automated analyzer (IMx System, Abbott laboratories, Illinois, USA) and IMx insulin reagents were used. Accurate volumes of both washed and unwashed insulin-chitosan microparticles suspension were incubated in pH 9.6 alkaline borate buffer at 37ºC and agitated at 100 rpm. The supernatants were taken at predetermined time intervals after centrifugation. The samples were prepared using a similar method to that described by Mueller and Trenktrog (89). Samples were diluted with 3.5% w/v bovine serum albumin in isotonic phosphate buffer pH 7.4 before analysis.

The IMx insulin assay used is a Microparticle Enzyme Immunoassay (MEIA) for the quantitative measurement of human insulin. The IMx system transfers the test sample and anti-insulin coated microparticles to the incubation well of the reaction cell. During the incubation period, analytes bind to the microparticles, creating an immune complex. The IMx system transfers an aliquot of the immune complex to the reaction cell's inert glass fiber matrix. The immune complex binds irreversibly to the glass fiber matrix. The IMx washes the matrix to remove unbound materials. The IMx system adds then alkaline phosphatase-labeled conjugate to the matrix. The conjugate binds to antibody-antigen complex. The matrix is washed again to remove un bound material. The IMx system adds the fluorogenic substrate, 4-Methylumbelliferyl Phosphate (MUP), to the matrix. The conjugate catalyzes the hydrolysis of MUP to 4-methylumbelliferyl (MU). The MEIA optics measure the rate at which MU, the florescent product, is generated on the glass fiber matrix. The rate at which MU is generated on the matrix is proportional to the concentration of analyte in the test sample.

5. Effect of various concentrations of chitosan and tripolyphosphate on the particle size and zeta potential of chitosan micro/nanoparticles.

The drug-chitosan micro/ nanoparticles were prepared as described in 1.5. A 6 ml of drug solution (insulin, benzoic acid) with constant concentrations was used. The concentrations of chitosan and tripolyphosphate were varied as shown in Table 4.

6. Effect of amount of drugs on physicochemical properties and entrapment efficiency of micro/nanoparticles

To study the effect of the amount of drug on the particle charge, particle size and entrapment efficiency of micro/nanoparticles, various amounts (4 – 140 mg) of drugs were used for preparation of the drug-chitosan micro/nanoparticles according to the method explained in 1.5. Insulin and diclofenac sodium used were in the range of 10 to 140 mg. Benzoic acid was varied from 4 to 24 mg and salicylic acid added in formulation was 4 to 36 mg. The concentrations of chitosan and tripolyphosphate were fixed at 0.2% w/v and 0.1% w/v, respectively.

Table 4. The formulations of drug-chitosan micro/nanoparticles for the study of the effect of concentrations of chitosan and tripolyphosphate on the size and zeta potential of particles

	Amount of drug (mg) [a]	Concentration of	
		Chitosan (% w/v)	Tripolyphosphate (% w/v)
Insulin-chitosan microparticles	30	0.2	0.1
	30	0.2	0.2
	30	0.2	0.4
	30	0.2	0.8
	30	0.2	1.6
	30	0.1	0.1
	30	0.2	0.1
	30	0.3	0.1
	30	0.4	0.1
	30	0.5	0.1
Benzoic acid-chitosan nanoparticles	12	0.2	0.1
	12	0.2	0.2
	12	0.2	0.4
	12	0.2	0.8
	12	0.2	1.6
	12	0.1	0.1
	12	0.2	0.1
	12	0.3	0.1
	12	0.4	0.1
	12	0.5	0.1

[a] The concentration of insulin solution was 5 mg/ml

The concentration of benzoic acid solution was 2 mg/ml

7. *In vitro* drug release studies

Part of the drug-chitosan micro/nanoparticle suspension was washed 3 times with purified water by filtration method to remove non-entrapped drug in the suspending medium. These washed particles were finally suspended in purified water. Both washed and unwashed drug-chitosan micro/nanoparticles of the formulations composed of 6 ml of model drugs were subjected *to in vitro* release studies. A 6 ml of drug solution referred to 30 mg of insulin and diclofenac sodium. And it referred to 12 mg of benzoic acid and salicylic acid in the formulations. The drug-chitosan micro/nanoparticles suspensions (0.1 ml) were placed into centrifuge tubes containing 1.4 ml of dissolution media and incubated at 37ºC under agitation (100 rpm) (Julabo SW20C, Julabo Labortechnik GmbH, Seelbach, Germany). The dissolution media were pH 7.4 phosphate buffer, pH 3 HCl solution (2.3×10^{-3} N) and purified water. After centrifugation of the samples (10,000 rpm, 10 min) at predetermined time intervals, 1 ml samples were withdrawn and replaced by fresh medium. The amount of drug released from the micro/nanoparticles was analyzed using HPLC as described above. All experiments were carried out in triplicate.

8. Isothermal Titration Calorimetry

The heats of drugs or tripolyphosphate binding to chitosan or micro/nanoparticles were measured by calorimetric titration performed using a LKB microcalorimeter, Thermal Activity Monitor (TAM 2277) and computer program of digitam 4.1 for window (Thermometric AB, Sweden). Figure 14 shows the block diagram of titration calorimeter. The titrant containing one of the reactants is introduced from the syringe into the reaction vessel. The resulting temperature change of the reaction is sensed by the temperature sensor and converted to a corresponding voltage in a wheatstone bridge circuit. This voltage is amplified in the amplifying circuit and displayed on the monitor. Assume that the AB is the complex of the interaction between A and B, the heat corrected for all extraneous heat effects due to the reaction can be Q:

$$Q = \Delta H\ (\Delta n) \qquad (1)$$

Where ΔH is the change in enthalpy for the reaction and Δ*n* is the number of moles of AB formed. Δ*n* can be derived if the approximate value of the equilibrium constant (K) is known. For the formation of AB the equilibrium constant can be calculated by the equation below (90).

$$K = [AB]/[A][B] \quad (2)$$

The enthalpy change, ΔH, can be obtained finally. The change in free energy (ΔG) can be determined by the relationship shown below as well as the change in entropy (ΔS).

$$\Delta G = -RT\ln K \quad (3)$$

$$\Delta S = (\Delta H - \Delta G)/T \quad (4)$$

where R is the gas constant (1.987 cal/mole deg)

T is the temperature (°K)

The electrical calibration and standard reaction of 18-crown-6 with $BaCl_2$ were carried out to check the accuracy of the microcalorimeter. Table 2 shows the experiments by ITC. During the calorimetric titration a solution of drugs or tripolyphosphate (titrant) was added to the chitosan solution or micro/nanoparticles suspension (titrand) in the titration cell. In a single experiment 15 injections of 30 µl of titrant were titrated into 2.5 ml of titrand by a motor driven 1000 µl syringe. The solution or suspension in the titration cell was stirred at 80 rpm throughout the experiments and its temperature was controlled at 25 °C. The reference cell of microcalorimeter was filled with 3 ml of purified water. The area under the peak of each injection is proportional to the resulting heat interaction. The blank experiments were performed to obtain the heat of dilution which was subtracted from the heat of interaction to obtain the actual heat of binding. The heat detected from the first injection was recommended to eliminate due to the error during baseline acquisition. All measurements were carried out in duplicate.

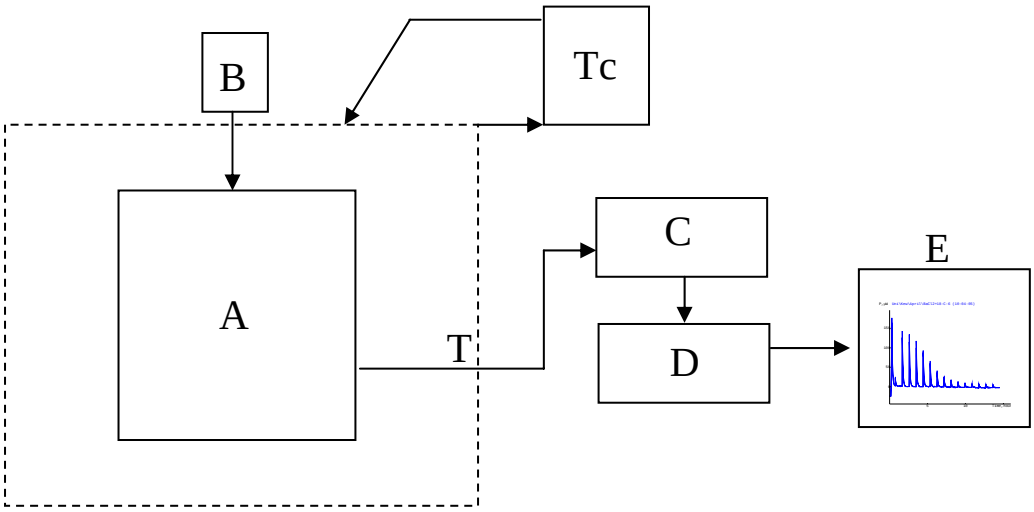

Figure 14. The block diagram of titration calorimeter (90)

A; Reaction cell B; Syringe

C; Temperature measuring circuit D; Amplifier

E; Data output Tc; Temperature controller

T; Temperature sensor

Table 5. The experiments by Isothermal Titration Calorimetry

Experiment no.	Titrant	Titrand
I	Insulin pH 7.2	Chitosan pH 5.0
Blank exp.	Phosphate buffer pH 7.2	Chitosan pH 5.0
II	Diclofenac sodium	Chitosan pH 5.0
Blank exp.	Diclofenac sodium	Dilute acetic acid pH 5.0
III	Benzoic acid pH 3	Chitosan pH 3.3
Blank exp.	Benzoic acid pH 3	Dilute acetic acid pH 3.3
IV	Salicylic acid pH 2.4	Chitosan pH 3.3
Blank exp.	Salicylic acid pH 2.4	Dilute acetic acid pH 3.3
V	Tripolyphosphate	Chitosan pH 5.0
Blank exp.	Tripolyphosphate	Dilute acetic acid pH 5.0
VI	Tripolyphosphate	Chitosan pH 3.3
Blank exp.	Tripolyphosphate	Dilute acetic acid pH 3.3
VII[a]	Tripolyphosphate	Insulin-chitosan microparticles
VIII[a]	Tripolyphosphate	Diclofenac-chitosan microparticles
IX[b]	Tripolyphosphate	Benzoic-chitosan solution
X[b]	Tripolyphosphate	Salicylic-chitosan solution

[a] Titration of tripolyphosphate to dilute acetic acid pH 5.0 was a blank experiment.

[b] Titration of tripolyphosphate to dilute acetic acid pH 3.3 was a blank experiment.

CHAPTER IV
RESULTS AND DISCUSSION

1. Drug-chitosan micro/nanoparticles

In this study chitosan micro/nanoparticles based on ionic interaction between drug and chitosan were prepared and characterized. Because an increased binding to chitosan was expected with decreasing pKa, four model drugs with different pI or pKa were studied (insulin-pI = 5.3, diclofenac sodium-pKa = 4.0, benzoic acid-pKa = 4.2 and salicylic acid-pKa = 3.0). Tripolyphosphate, TPP, (pH 9.1) was used as a crosslinking agent in order to form microparticles or strengthen the microparticle formation.

1.1. Morphology

The insulin-chitosan microparticles and benzoic-chitosan nanoparticles were represented as the typical particles composed of large molecule model drug and small molecule model drug, respectively for morphology examination by TEM. Figure 15A and 15B represent the morphology of insulin-chitosan particles and benzoic acid-chitosan particles, respectively. The almost sphere shape of particles could be observed. The insulin-chitosan particles showed solid and dense structure than that of benzoic acid-chitosan particles. It is possible due to the larger molecule of insulin.

1.2 Effect of various concentrations of chitosan and tripolyphosphate on the particle size and zeta potential of chitosan micro/nanoparticles

From the literature (17), it can be derived that the opposite charge of chitosan and drug cause a spontaneous forming of particles, which are finally improved by adding tripolyphosphate. Furthermore, it is known that increasing chitosan concentrations as well as tripolyphosphate concentrations will lead to and increase in particle diameter and hence to agglomeration of the produced microparticles (19). These were confirmed in the beginning of this study, the large molecule model drug (insulin) and one of the small molecule model drugs were used to prepared drug-

A

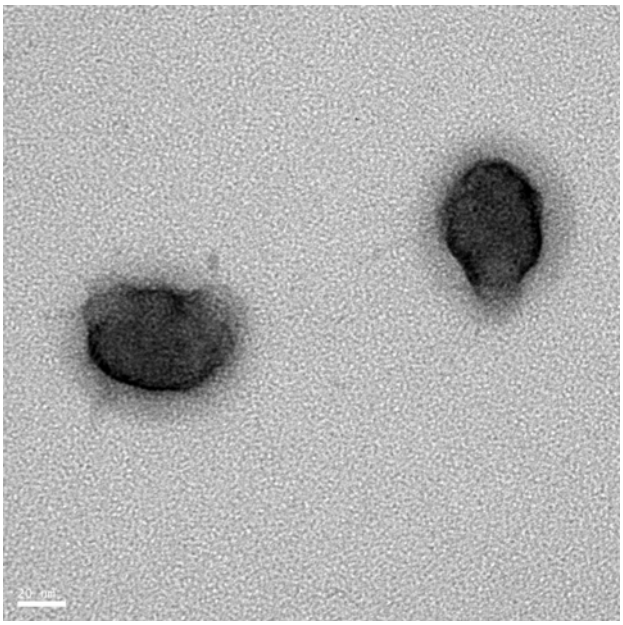

B

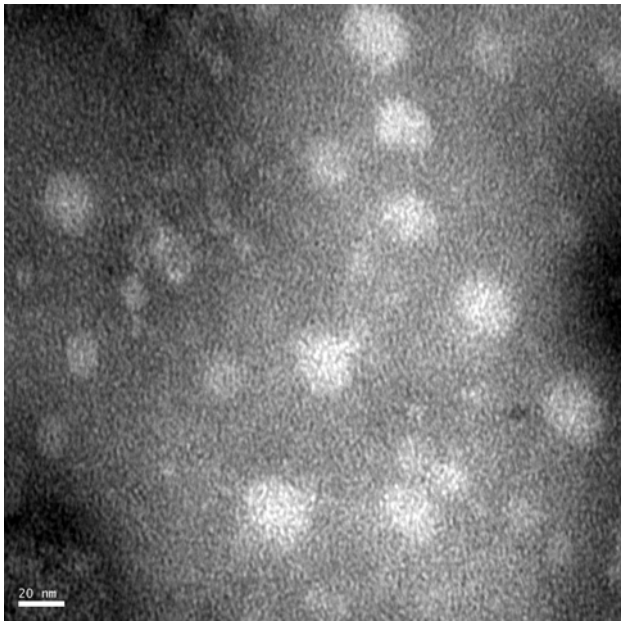

Figure 15. The transmission electron microphotographs of insulin-chitosan microparticles (A) and benzoic acid-chitosan nanoparticles (B)

chitosan micro/nanoparticles. By varying the concentration of tripolyphosphate (TPP) or chitosan in formulation as indicated in Table 4, the change in the particle size were in agreement with literature report (figure 16-19).

As shown in Figure 16 and 17, the concentration of tripolyphosphate showed the greater effect on the increase in size of insulin-chitosan particles than that of benzoic acid-chitosan particles. The 0.1% TPP provided smaller insulin-chitosan particles than the other concentration of tripolyphosphate (Figure 16). To obtain benzoic acid-chitosan particles in submicron range, the suitable concentration of TPP were 0.1% and 0.2% (Figure 17). The higher concentration of TPP led to more negative charged molecules in the system and it resulted in decreasing of zeta potential of particles.

The various concentrations of chitosan, 0.1% to 0.5% w/v in formulations influenced particle size and zeta potential of particles as shown in Figure 18 and 19. The mean particle size was 2.3-3.3 μm for insulin-chitosan particles prepared from 0.2% and 0.3% chitosan solution. Higher chitosan concentration resulted in larger insulin-chitosan particles, such as up to 12 μm for 0.5% chitosan solution (Figure 18). At 0.2% of chitosan solution smallest benzoic acid-chitosan particles in nanometer range were obtained, whereas, the agglomeration of particles was observed at the other concentrations (Figure 19). The zeta potential of particles increased with chitosan because of the addition of positive charged polymer involved in the particle formation. Due to the fact that tripolyphosphate was added only to improve particle formation on a low size level, the tripolyphosphate and chitosan concentration in this study were fixed at 0.1% w/v and 0.2% w/v, respectively.

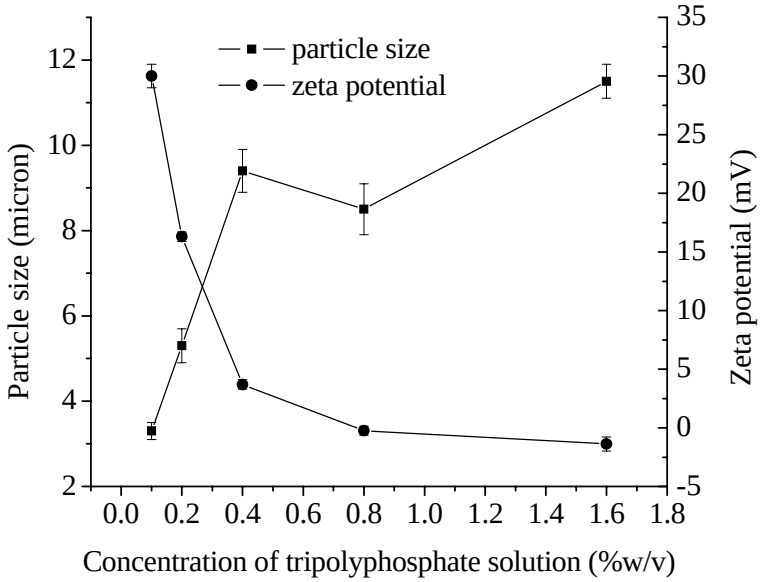

Figure 16. Influence of tripolyphosphate (TPP) concentration on particle size and zeta potential of insulin-chitosan suspension (the concentration of insulin and chitosan in the suspension was 0.07% and 0.12% w/v, respectively).

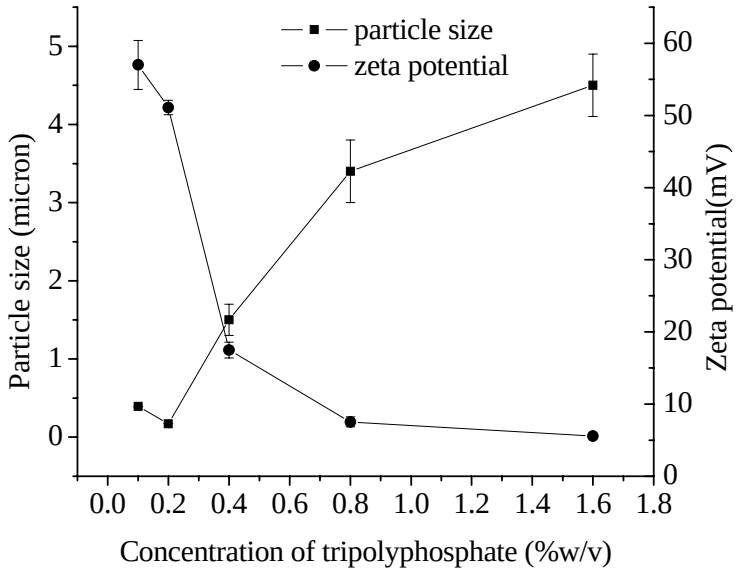

Figure 17. Influence of tripolyphosphate (TPP) concentration on particle size and zeta potential of benzoic acid-chitosan suspension (the concentration of benzoic acid and chitosan in the suspension were 0.03% w/v and 0.12% w/v, respectively).

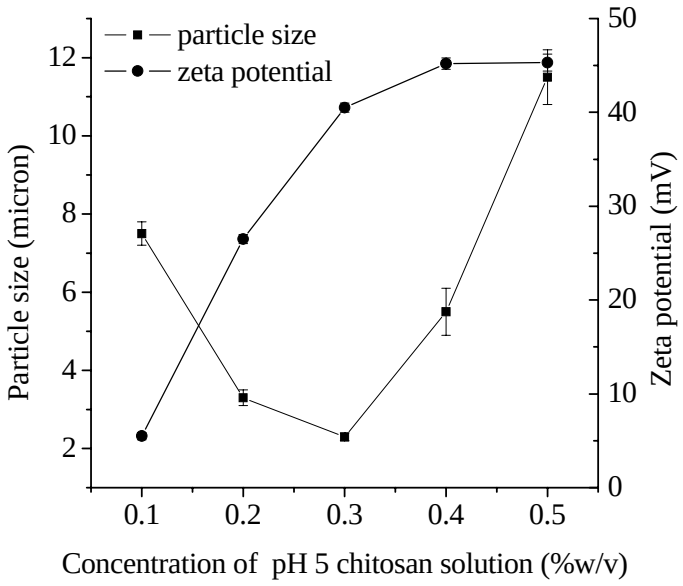

Figure 18. Influence of chitosan concentration on particle size and zeta potential of insulin-chitosan suspension (the concentration of insulin and tripolyphosphate in the suspension was 0.07% w/v and 0.02% w/v, respectively).

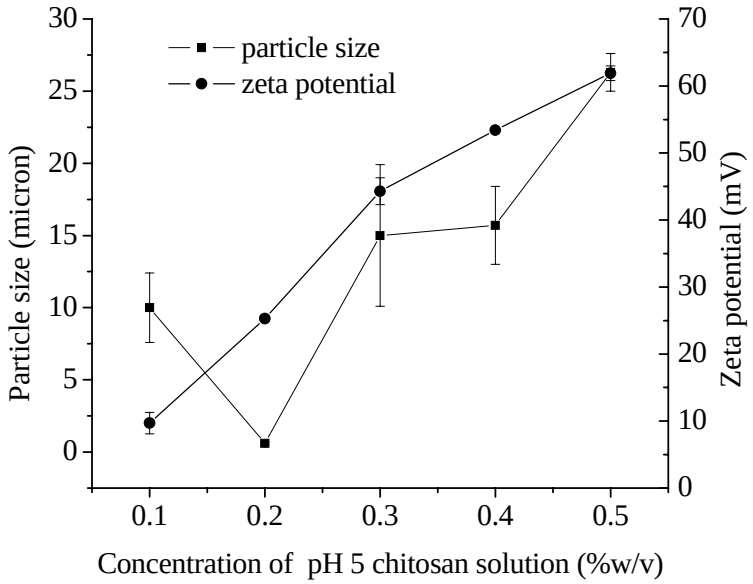

Figure 19. Influence of chitosan concentration on particle size and zeta potential of benzoic-chitosan suspension (the concentration of benzoic acid and tripolyphosphate in the suspension was 0.03 % w/v and 0.02% w/v, respectively).

1.3. Effect of amount of drugs on physicochemical properties of chitosan micro/nanoparticles

1.3.1. Insulin-chitosan microparticles

For production of insulin-chitosan microparticles, a positive charged chitosan solution (pH 5.0) and a negative charged insulin solution (pH 7.2) were used. During production, the pH of the microparticle suspension gradually increased with increasing insulin concentration or addition of tripolyphosphate. The insulin-chitosan microparticles exhibited a particle size (X_{50}) in the range of 1 to 7 µm. After addition of tripolyphosphate solution the particle size was between 2 and 5 µm which means no significant change (Table 6). Increase amounts of insulin had no influence on the size of the microparticles. Figure 20 and 21 illustrate the change in the charge of insulin-chitosan microparticles expressed as zeta potential and particle charge per volume of suspension both before and after adding tripolyphosphate, respectively insulin solution into the system. Particle charge and zeta potential were decreased with increasing insulin concentration which led to constant values at insulin concentrations over 12 ml (1.27 mg/ml of suspension) in the formulations. It seems that the binding of insulin even in higher concentrations could not neutralize the positive charge of the chitosan molecule and even the addition of tripolyphosphate did not resulted in a zero surface charge. This indicated the physical entrapment of insulin to chitosan network.

1.3.2. Diclofenac-chitosan microparticles

The positive charged chitosan molecules in solution (pH 5) and diclofenac sodium solution (pH 7) were mixed. Almost the same development of the pH course and the particle sizes as already seen with the insulin-chitosan microparticles was obtained. The particle size increased from 3-6 µm to 4-9 µm after the addition of tripolyphosphate solution (Table 7). Without trippolyphosphate in formulations, the increase of diclofenac sodium did not change the zeta potential of the particles significantly as shown in Figure 22. But the addition of tripolyphosphate into diclofenac-chitosan suspension resulted in gradually decrease in zeta potential of particles. These indicated that the colloidal chitosan molecule is not influenced by

Table 6. pH and particle size of insulin-chitosan microparticles before and after adding tripolyphosphate (TPP) with increasing insulin concentration

Amount of insulin (mg)	pH of suspension		Particle size (μm)[a]	
	Before adding TPP	After adding TPP	Before adding TPP	After adding TPP
10	5.3	5.4	n	4.6 ± 0.3
20	5.5	5.6	1.6 ± 0.0	3.1 ± 0.1
30	5.7	5.8	1.7 ± 0.0	2.4 ± 0.1
40	5.9	6.2	2.4 ± 0.0	3.7 ± 0.3
50	6.2	6.4	3.5 ± 0.0	4.1.± 0.1
60	6.3	6.5	7.0 ± 0.0	4.7.± 0.1
70	6.5	6.6	3.7 ± 0.0	2.8 ± 0.0
80	6.6	6.7	1.9 ± 0.0	3.7 ± 0.2
90	6.6	6.8	2.5 ± 0.0	4.3 ± 0.1
100	6.6	6.8	2.3 ± 0.0	5.3 ± 0.0
110	6.7	6.9	2.6 ± 0.0	3.0 ± 0.0
120	6.7	6.9	1.6 ± 0.0	2.9 ± 0.0
130	6.8	6.9	2.0 ± 0.0	3.8 ± 0.0
140	6.8	6.9	2.5 ± 0.0	5.2 ± 0.0

[a]Mean ± SD (n = 3)

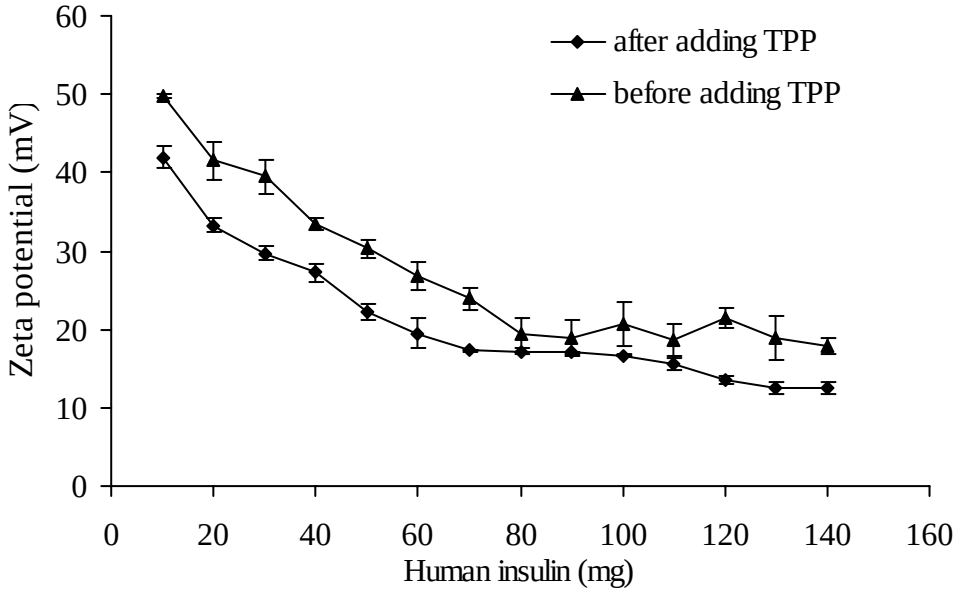

Figure 20. Zeta potential of insulin-chitosan microparticles before and after adding tripolyphosphate with increasing insulin concentration (n = 3)

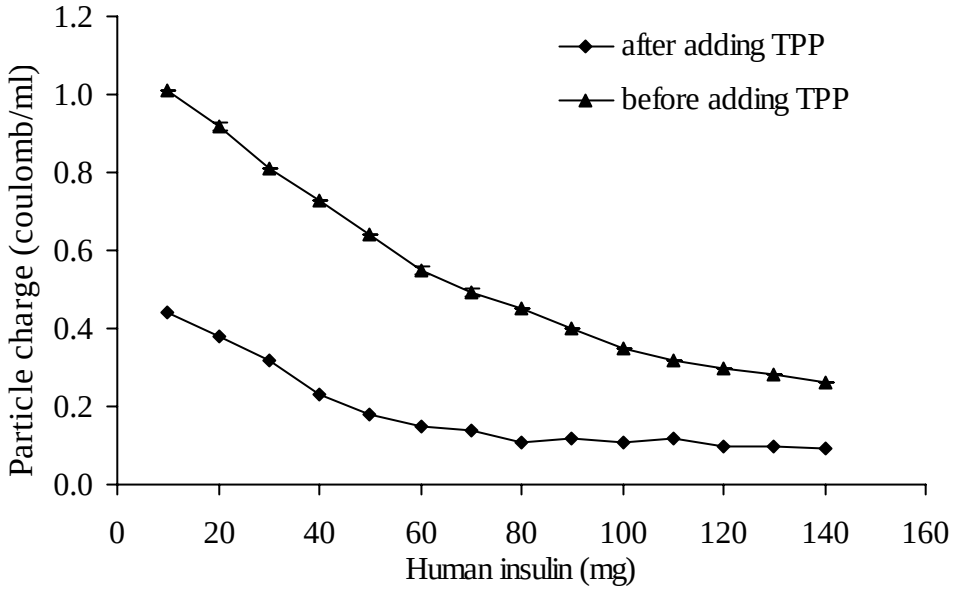

Figure 21. Particle charge of insulin-chitosan microparticles before and after adding tripolyphosphate with increasing insulin concentration (n = 3)

Table 7. pH and particle size of diclofenac-chitosan microparticles before and after adding tripolyphosphate (TPP) with increasing diclofenac concentration

Amount of diclofenac sodium (mg)	pH of suspension		Particle size (μm)[a]	
	Before adding TPP	After adding TPP	Before adding TPP	After adding TPP
10	5.2	5.2	3.6 ± 0.0	4.5 ± 0.1
20	5.2	5.3	4.7 ± 0.0	5.0 ± 0.1
30	5.3	5.3	4.1 ± 0.0	3.5 ± 0.2
40	5.3	5.3	4.2 ± 0.0	3.5 ± 0.1
50	5.3	5.4	3.4 ± 0.1	3.4 ± 0.0
60	5.3	5.4	4.7 ± 0.0	4.1 ± 0.5
70	5.3	5.5	4.3 ± 0.0	4.5 ± 0.2
80	5.4	5.6	2.8 ± 0.3	3.2 ± 0.1
100	5.5	6.0	3.5 ± 0.2	6.7 ± 0.3
120	5.6	6.2	3.6 ± 0.2	8.4 ± 0.3
140	5.9	6.5	5.5 ± 1.2	8.7 ± 0.2

[a]Mean ± SD (n = 3)

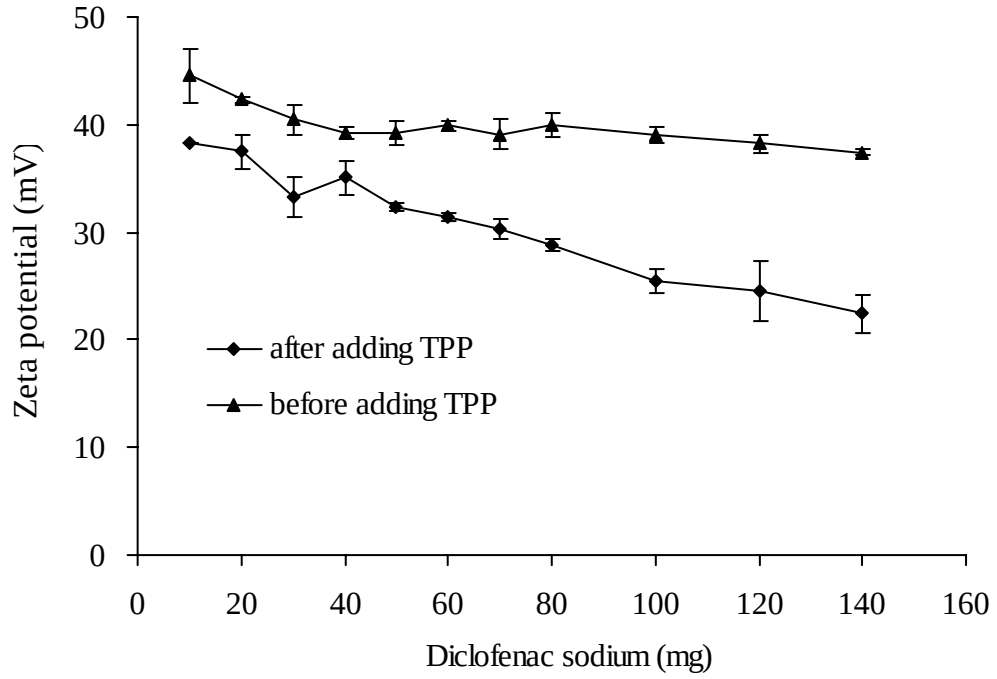

Figure 22. Zeta potential of diclofenac-chitosan microparticles before and after adding tripolyphosphate with increasing diclofenac concentration (n = 3)

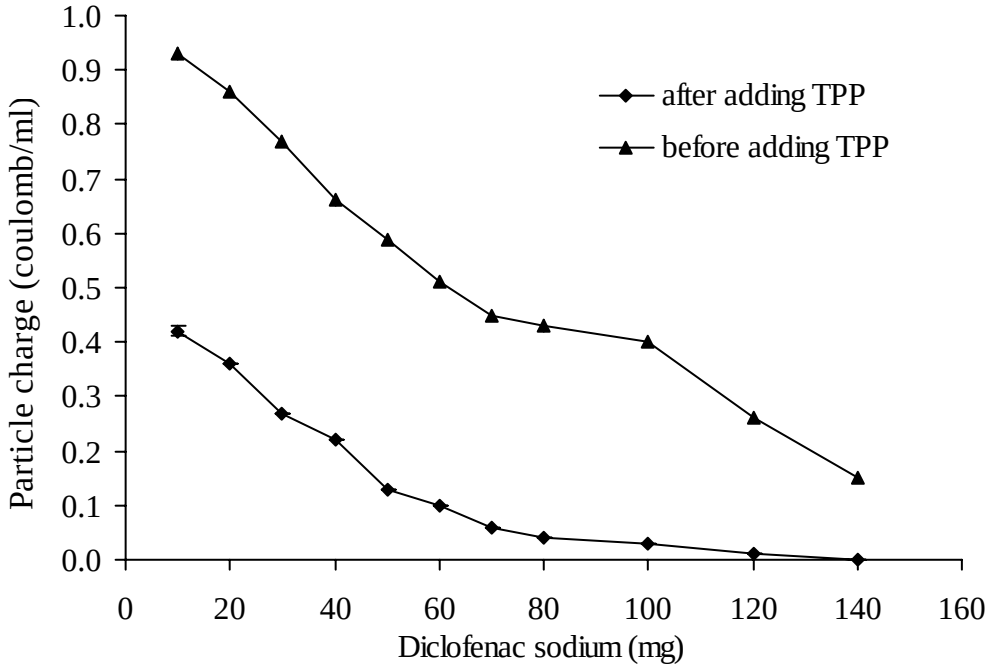

Figure 23. Particle charge of diclofenac-chitosan microparticles before and after adding tripolyphosphate with increasing diclofenac concentration (n = 3)

the addition of weak acid (diclofenac) but tripolyphosphate (cross-linking agent) could reduce the charge of chitosan molecules. However, the particle charge of formed microparticles was strongly influenced by the increase of diclofenac and the addition of tripolyphosphate (Figure 23). The addition of tripolyphosphate could reduce the charged chitosan molecules. It is assumed that diclofenac was physically entrapped to chitosan network and tripolyphosphate could interact with chitosan instead.

1.3.3. Benzoic-acid chitosan nanoparticles

Mixing chitosan solution (pH5) with a benzoic acid solution (pH 5.4) showed no particle formation although a reaction between both components should be expected due to the fact that chitosan exhibits positive charge and more than 90% of benzoic acid were ionized in the formulation pH of 5.2 according to the calculation by Henderson-Hasselbalch equation as indicated below.

$$pH = pKa + \log [A^-]/[HA] \qquad (4)$$

$$5.2 = 4.2 + \log 91/9$$

where $[A^-]$ is the ionized form of drug

[HA] is the unionized form of drug

After adding tripolyphosphate, however, particles were formed in the size of less than 1µm (Table 8). Figure 24 and 25 indicate that there was no marked effect of benzoic acid concentration on zeta potential and particle charge of the chitosan solution after the interaction with tripolyphosphate and thus particle formation. The zeta potential could not be detected in the formulations without tripolyphosphate solution. The slow decrease of the particle charge itself shows that an unexpectedly low interaction between the molecules occurs. This should lead to low entrapment efficiencies if the entrapment is a function of ionic interaction.

1.3.4. Salicylic-chitosan nanoparticles

Salicylic acid is stronger acid (pKa 2.97) compared with diclofenac sodium and benzoic acid. It was promoted to interact with chitosan. The mixture of pH 5 chitosan solution and pH 4.2 salicylic acid solution should resulted in the strong interaction between oppositely charge of them. Similar to benzoic acid-chitosan

Table 8. pH and mean particle size of benzoic acid-chitosan nanoparticles after adding tripolyphosphate (TPP) with increasing benzoic acid concentration

Amount of benzoic acid (mg)	pH of suspension After adding TPP	particle size (nm)[a] After adding TPP
4	5.2	602.8 ± 40.1
8	5.2	531.7 ± 14.9
12	5.2	504.3 ± 21.9
16	5.2	491.7 ± 14.0
20	5.2	456.7 ± 27.8
24	5.2	473.4 ± 21.9

[a]Mean ± SD (n = 3)

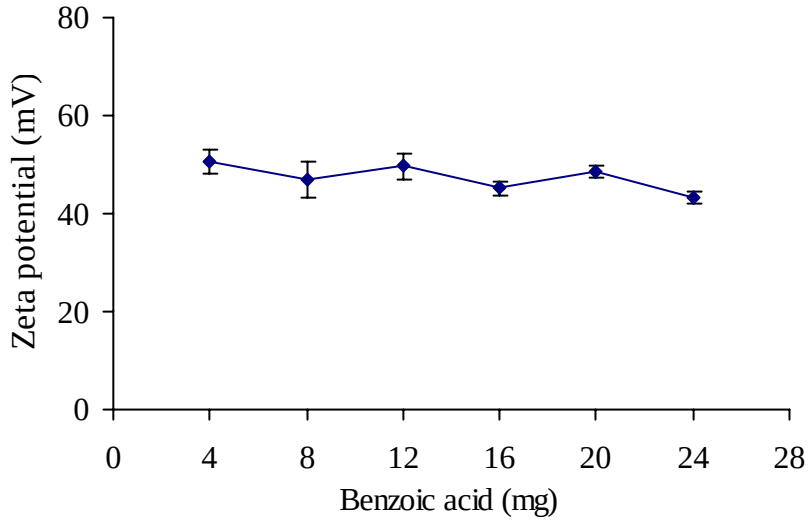

Figure 24. Zeta potential of benzoic acid-chitosan microparticles after adding tripolyphosphate with increasing benzoic acid concentration (n = 3)

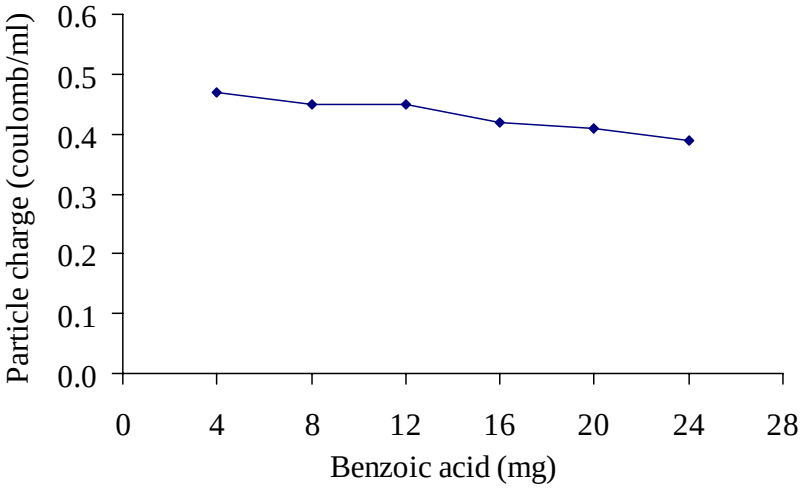

Figure 25. Particle charge of benzoic acid-chitosan nanoparticles after adding tripolyphosphate with increasing benzoic acid concentration (n = 3)

solution, particles with a size in nanometer range were obtained only after the addition of tripolyphosphate (Table 9). Table 9 also shows the pH of salicylic acid-chitosan nanoparticle suspensions which were about 5. The development of zeta potential and particle charge was similar to that of benzoic-chitosan nanoparticles (Figure 26 and 27), although the stronger ionic interaction and dominant change in particle charge were expected. These should also lead to the low entrapment efficiencies of particles. Furthermore, the excellent water solubility of salicylic acid in its dissociated form at pH 5 will hinder a higher entrapment because the lack in ionic interaction leads to a decrease in concentration in the polymeric phase.

1.4. Effect of amount of drug on the entrapment efficiency of chitosan microparticles

All model drugs in this study were dissolved and adjusted to a pH where most of the molecules were negatively charged before adding to a pH 5 chitosan solution (positive charge). The pH of preparations should allow the model drugs molecule to interact with the chitosan polymer if an ionic interaction exists. By measuring zeta potential and particle charge it could be shown that even at higher counter ion concentration the chitosan polymer has a positive charge. Therefore, the negatively charged tripolyphosphate was added in order to complete the microparticle formation.

To evaluate the entrapment efficiency, drug-chitosan micro/nano particle suspensions were freshly prepared and analysed by HPLC. The typical calibration curves of each model drugs were shown in Figures 28-31. The relationship between peak area and drug concentration were linear with good correlation coefficients. The slope and y-intercept were calculated by linear regression analysis.

1.4.1. Insulin-chitosan microparticles

In the case of insulin-chitosan microparticles, the entrapment efficiency increased with increasing drug concentration due to incomplete microparticle formation (Table 10). The addition of tripolyphosphate therefore led to a higher entrapment. Equilibrium was reached at 40 mg insulin referring to 50 mg chitosan. The maximum uptake of insulin was reached at 140 mg (28 ml of insulin solution).

Table 9. pH and particle size of salicylic acid-chitosan microparticles after adding tripolyphosphate (TPP) with increasing salicylic acid concentration

Amount of salicylic acid (mg)	pH of suspension After adding TPP	Particle size (nm)[a] After adding TPP
6	5.2	708.5 ± 35.0
12	5.2	671.4 ± 30.7
18	5.1	699.4 ± 38.1
24	5.1	473.2 ± 20.4
30	5.1	483.7 ± 4.5
36	5.1	476.8 ±15.1

[a]Mean ± SD (n = 3)

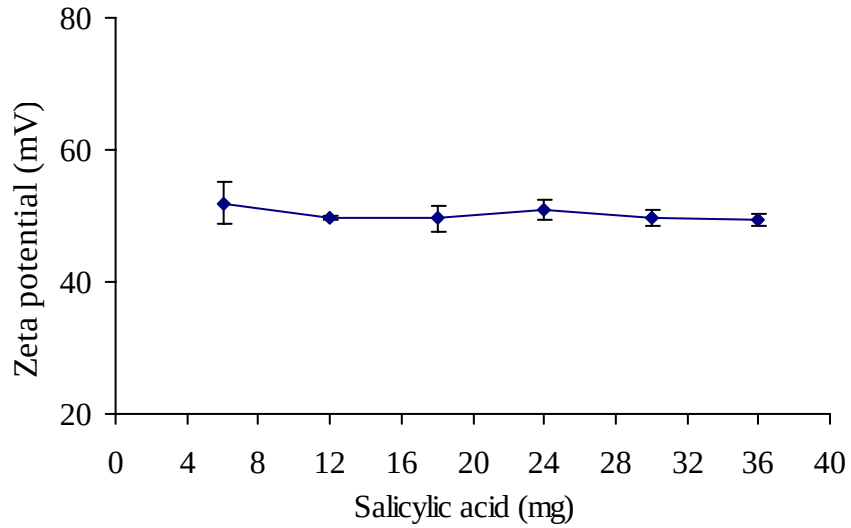

Figure 26. Zeta potential of salicylic acid-chitosan microparticles after adding tripolyphosphate with increasing salicylic acid concentration (n = 3)

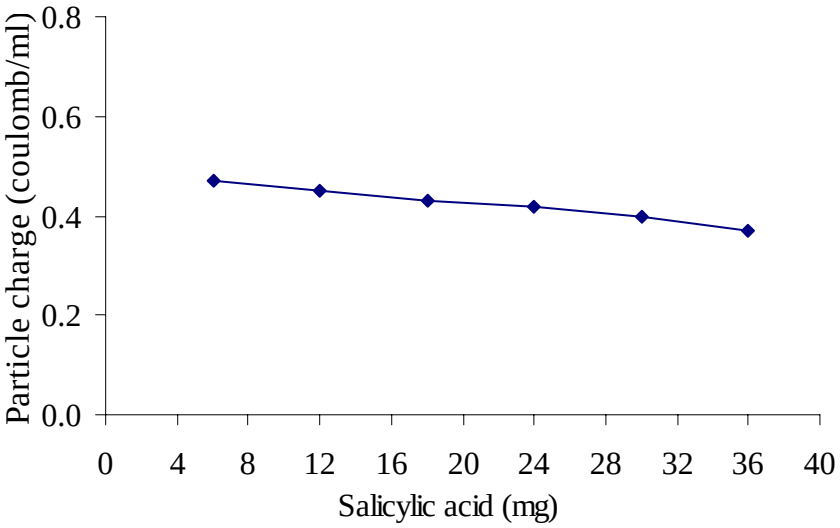

Figure 27. Particle charge of salicylic acid-chitosan microparticles after adding tripolyphosphate with increasing salicylic acid concentration (n = 3).

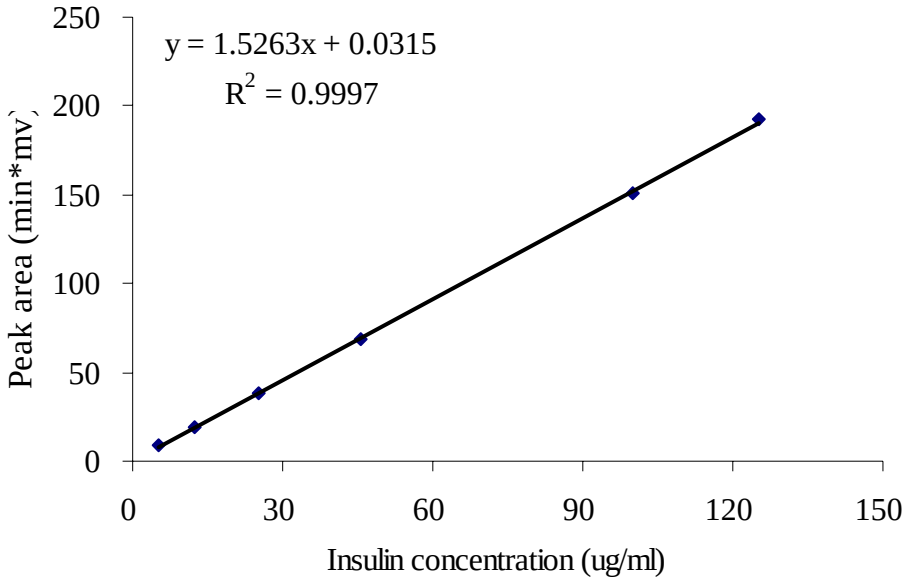

Figure 28. Typical calibration curve of insulin in mobile phase composed of 27% v/v acetonitrile and 73% v/v of buffer (0.01 M KH_2HPO_4 and 0.1 M Na_2SO_4) analyzed by HPLC with UV detection at 215 nm.

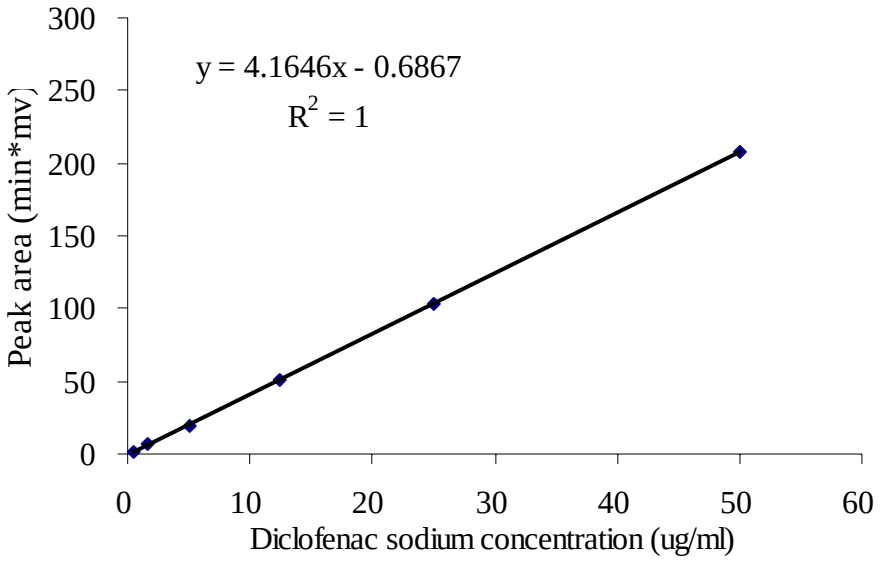

Figure 29. Typical calibration curve of diclofenac sodium in mobile phase composed of 60% v/v methanol and 40% buffer (0.01 M of KH_2PO_4 and Na_2HPO_4) analyzed by HPLC with UV detection at 282 nm.

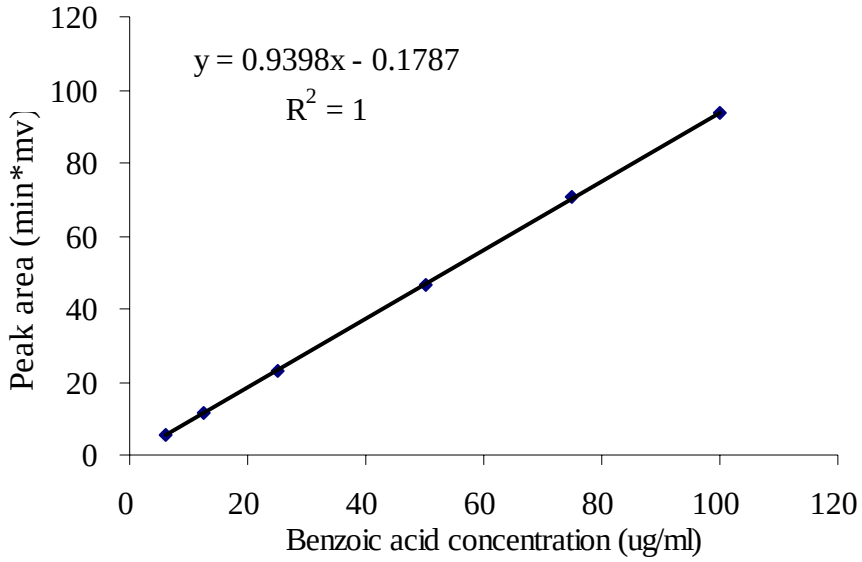

Figure 30. Typical calibration curve of benzoic acid in mobile phase composed of 50% v/v methanol, 48% water and 2% v/v of glacial acetic acid analyzed by HPLC with UV detection at 238 nm.

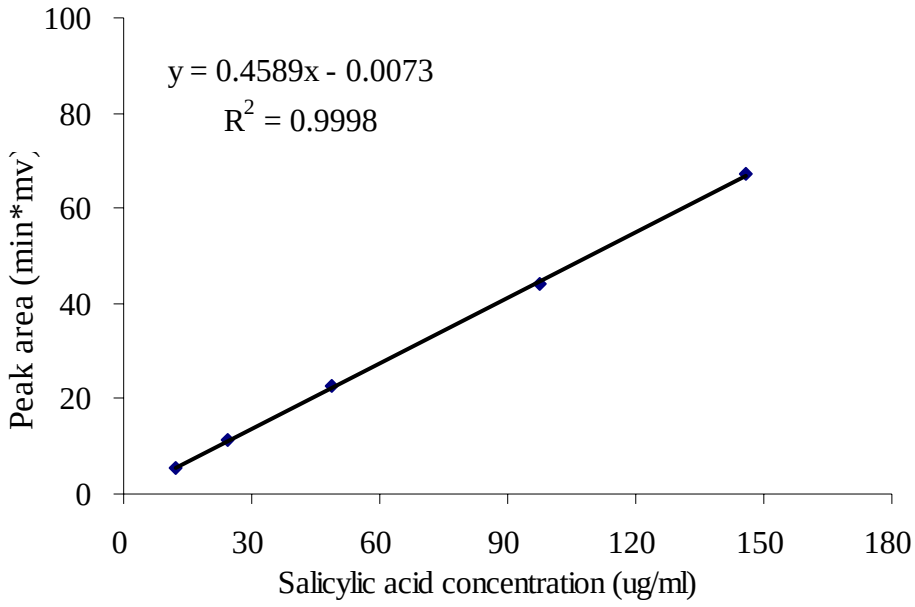

Figure 31. Typical calibration curve of salicylic acid in mobile phase composed of 50% v/v methanol, 48%water and 2% v/v of glacial acetic acid analyzed by HPLC with UV detection at 238 nm.

Table 10. Entrapment efficiency of drug-chitosan particles made of pH 5 chitosan solution

amount of drug (mg)[a]	Entrapment efficiency (% ± SD)[b]			
	insulin-chitosan microparticles		diclofenac-chitosan microparticles	
	before adding TPP	after adding TPP	before adding TPP	after adding TPP
10	0.5 ± 0.4	53.5 ± 2.1	95.0 ± 2.3	98.7 ± 0.1
20	10.4 ± 0.9	79.2 ± 1.1	96.9 ± 1.6	98.3 ± 0.3
30	55.7 ± 9.8	93.9 ± 1.2	99.5 ± 0.4	96.9 ± 1.0
40	91.0 ± 8.4	95.7 ± 1.0	99.0 ± 0.5	97.7 ± 0.3
50	97.1 ± 1.0	96.5 ± 0.1	99.5 ± 0.2	95.3 ± 0.4
60	95.4 ± 0.8	96.8 ± 0.3	99.2 ± 0.2	90.3 ± 0.9
70	98.0 ± 0.3	95.2 ± 0.8	99.3 ± 0.1	84.7 ± 1.1
80	98.7 ± 0.1	94.2 ± 0.3	98.7 ± 0.1	86.5 ± 1.5
90	98.8 ± 0.1	95.2 ± 0.5	-	-
100	98.1 ± 0.2	94.5 ± 0.7	97.6 ± 0.2	78.0 ± 0.4
110	98.3 ± 0.7	94.9 ± 0.9	-	-
120	98.9 ± 0.1	94.5 ± 0.1	92.8 ± 0.9	69.2 ± 1.0
130	98.3 ± 0.4	93.7 ± 0.2	-	-
140	96.9 ± 1.1	91.1 ± 0.8	87.0 ± 0.4	67.7 ± 1.5

[a] insulin or diclofenac sodium
[b] mean ± SD, n = 3

Concerning the influence of pH more than 90% of insulin was entrapped in a pH of 5.8-6.9 (Table 6 and 10). This is contrary to the study of Lim and co-workers in which a dominately high association effiency was observed only at pH 6.1 (16).

1.4.2. Diclofenac-chitosan microparticles

Diclofenac was nearly completely entrapped although the addition of diclofenac did not show much influence on the zeta potential which may indicate that there was no strong ionic interaction with the chitosan polymer. The particle surface charge was, however, continuously decreased. The addition of tripolyphosphate led to zero particle charge and decreasing the entrapment efficiency (Table10). Comparing to the formulations without tripolyphosphate, the decrease in entrapment efficiency in formulations with tripolyphosphate indicated the loss of physical entrapped drug.

1.4.3. Benzoic acid-chitosan nanoparticles

The particles in nano-range were formed only after the addition of tripolyphosphate. The low entrapment efficiency of benzoic acid-chitosan nano-particles was observed. The entrapment efficiencies decreased from 32% to 24% with the increase of benzoic acid from 4 mg to 24 mg in formulations (Table 11). Actually, the low entrapment could be expected by the charge measurement and the small size of drug integrated particles. Nearly no change in zeta potential and particle charge was observed which can be implied to the low interaction between drug and chitosan.

1.4.4. Salicylic acid-chitosan nanoparticles

Only small amount of salicylic acid was entrapped by chitosan nanoparticles. From the Henderson-Hasselbalch equation it can be derived that salicylic acid (pKa =3.0) is in a 99% ionized form if the pH of the system is about two pH units higher than the pKa of the drug. So at pH 5 salicylic acid has a great possibility to bind to chitosan if the ionic interaction really causes entrapment of drug into particles. Only low entrapment efficiencies from 23% to 15% could be reached and this could only be due to physical entrapment (Table 12). Although salicylic acid is a stronger acid than benzoic acid, salicylic acid did not show higher binding capacity to chitosan, a weak base.

Table 11. Entrapment efficiency of benzoic acid-chitosan nanoparticles made of pH 5 chitosan solution after adding tripolyphosphate (TPP) with increasing amount of benzoic acid in formulations

Amount of benzoic acid (mg)	Entrapment efficiency (% ± SD)[a] of Benzoic-chitosan nanoparticles
	After adding TPP
4	32.1 ± 1.6
8	29.1 ± 0.7
12	27.9 ± 1.2
16	25.4 ± 0.2
20	25.8 ± 1.4
24	23.9 ± 1.4

[a] mean ± SD (n = 3)

Table 12. Entrapment efficiency of salicylic acid-chitosan nanoparticles made of pH 5 after adding tripolyphosphate (TPP) with increasing amount of salicylic acid in formulations

Amount of salicylic acid (mg)	Entrapment efficiency (% ± SD)[a] of Salicylic-chitosan nanoparticles
	After adding TPP
6	22.8 ± 1.9
12	19.2 ± 1.8
18	17.4 ± 1.1
24	17.6 ± 0.3
30	16.8 ± 1.5
36	15.1 ± 0.3

[a] mean ± SD (n = 3)

1.4.5. Increase the entrapment efficiency of benzoic acid and salicylic acid-chitosan nanoparticles by changing the formulation pH

In order to get a more pronounced protonization the pH of chitosan solution was decreased to pH 3.3. Table 13 shows the formulation pH and particle size of benzoic acid-chitosan nanoparticles made of pH 3.3 chitosan solution, pH 3.0 benzoic acid solution and pH 9.1 tripolyphosphate solution. The formulation pH was about 3.5. Particle size was 800 nm to 1 μm. It was a little bigger than that of formulation with pH 5. However, comparison to the formulation at pH 5 there was no dominant difference in the charge development of particle (Figure 32 and 33).

The similar development of pH course and physicochemical properties could be seen for salicylic acid-chitosan nanoparticles composed of pH 3.3 chitosan solution, pH 2.4 salicylic acid solution and pH 9.1 tripolyphosphate solution (Table 14 and Figures 34-35).

Surprisingly, the entrapment efficiencies of both benzoic acid and salicylic acid-chitosan nanoparticles increased to maximum values of 79% and 77%, respectively (Table 15). The drug loading of nanoparticles decreased, however, with increasing benzoic acid and salicylic acid concentration which is caused by the restricted dissociation of the drugs.

Compared to formulation pH 5, the improvement of entrapment efficiency of drug-chitosan particles in the formulation pH about 3 without dominant change in zeta potential and particle charge indicated the physical entrapment of benzoic acid and salicylic acid to chitosan.

Using the pH 3.3 chitosan solution in combination with insulin (pH = 3.0), the pH of formulation were about 3.5 and the particle size was in nanometer range (Table 16). Limited entrapment efficiency was observed (Table 17). In comparison with the formulation made of pH 5 chitosan solution, the smaller particle size of insulin-chitosan prepared from pH 3.3 chitosan implied that lesser amount of insulin involved in the particle formation. This was also confirmed by the almost stable zeta potential and particle charge of particles with increasing amount of insulin (Figure 36 and 37). The low entrapment efficiency of particles can be expected by the fact that

Table 13. pH and particle size of benzoic-chitosan nanoparticles made of pH 3.3 chitosan solution after addition of TPP with increasing amount of benzoic acid in formulations

Amount of benzoic acid (mg)	pH of suspension	Particle size (nm)[a]
	After adding TPP	After adding TPP
4	3.6	1160.4 ± 36.2
8	3.6	924.3 ± 5.9
12	3.5	804.5 ± 21.5
16	3.5	799.3 ± 47.9
20	3.5	818.2 ± 63.6
24	3.5	789.1 ± 78.7

[a] mean ± SD (n = 3)

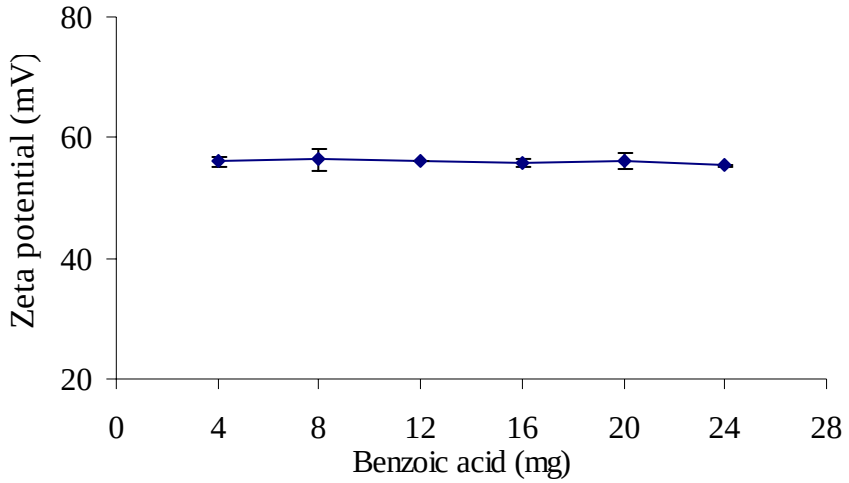

Figure 32. Zeta potential of benzoic acid-chitosan nanoparticles made of pH 3.3 chitosan solution after adding tripolyphosphate with increasing benzoic acid concentration (n = 3)

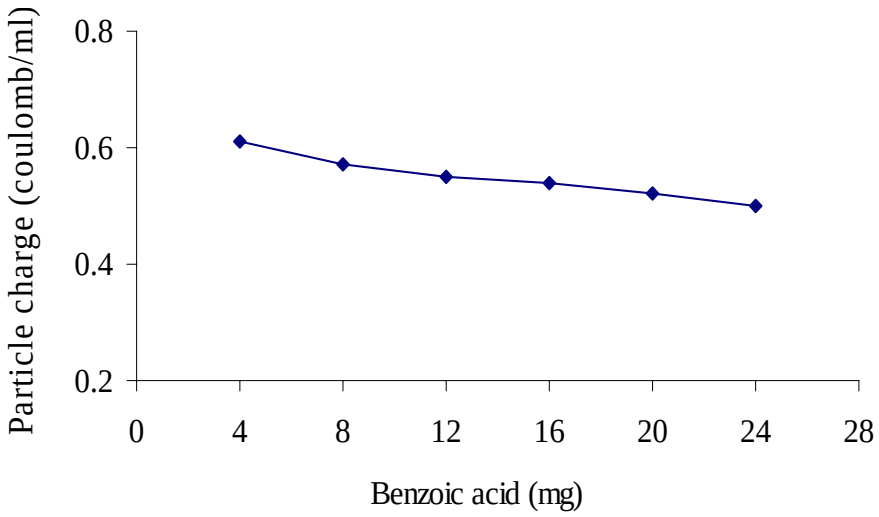

Figure 33. Particle charge of benzoic acid-chitosan nanoparticles made of pH 3.3 chitosan solution after adding tripolyphosphate with increasing benzoic acid concentration (n = 3)

Table 14. pH and particle size of salicylic-chitosan nanoparticles made of pH 3.3 chitosan solution after addition of TPP with increasing amount of salicylic acid

Amount of salicylic acid (mg)	pH of suspension	Particle size (nm)[a]
	After adding TPP	After adding TPP
4	3.6	1104.4 ± 39.9
8	3.4	1031.8 ± 140.5
12	3.4	994.5 ± 51.7
16	3.4	839.1 ± 25.0
20	3.3	780.6 ± 53.2
24	3.3	753.2 ± 4.8

[a] mean ± SD (n = 3)

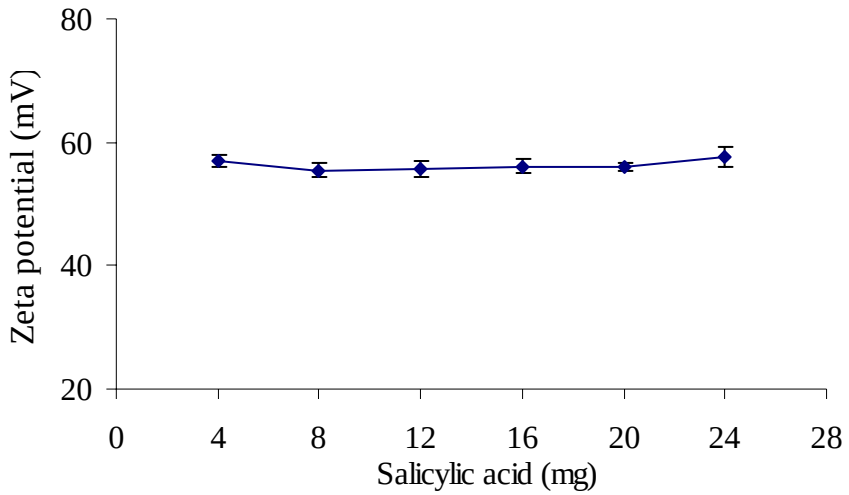

Figure 34. Zeta potential of salicylic acid-chitosan nanoparticles made of pH 3.3 chitosan solution after adding tripolyphosphate with increasing salicylic acid concentration (n = 3)

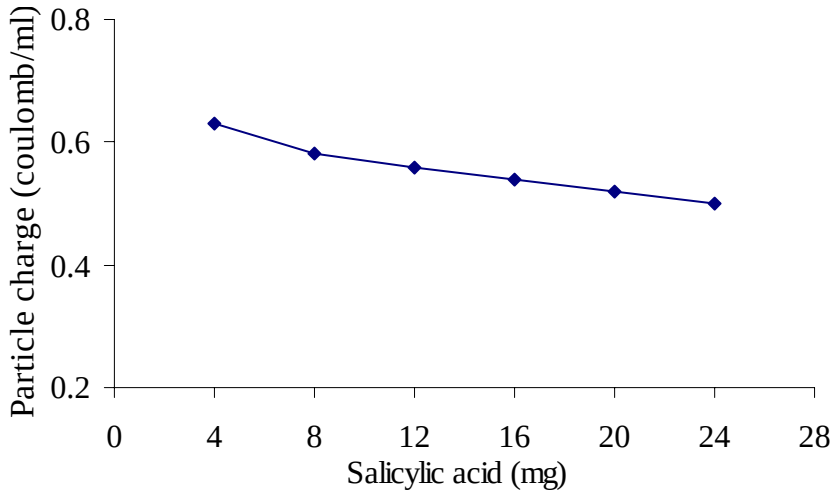

Figure 35. Particle charge of salicylic acid-chitosan nanoparticles made of pH 3.3 chitosan solution after adding tripolyphosphate with increasing salicylic acid concentration (n = 3)

Table 15. Entrapment efficiency of benzoic acid and salicylic acid in chitosan nanoparticles after adding tripolyphosphate with increasing amount of drug in formulations

Amount of drug[a] (mg)	Entrapment efficiency (% ± SD)[b] of	
	Benzoic acid-chitosan nanoparticles	Salicylic acid-chitosan nanoparticles
	After adding TPP	After adding TPP
4	76.7 ± 2.6	71.6 ± 1.7
8	79.5 ± 0.8	77.5 ± 2.8
12	76.9 ± 1.5	70.6 ± 4.5
16	78.7 ± 1.0	76.0 ± 1.7
20	71.4 ± 2.3	67.8 ± 5.3
24	67.9 ± 1.0	65.8 ± 0.5

[a] benzoic acid solution 2 mg/ml
salicylic acid solution 2 mg/ml

[b] mean ± SD (n = 3)

Table 16. Particle size and pH of insulin-chitosan nanoparticle suspension made of pH 3.3 chitosan solution after addition of TPP with increasing amount of insulin

Amount of insulin (mg)	pH of suspension	Particle size (nm)[a]
	After adding TPP	After adding TPP
10	3.6	860.3 ± 17.2
20	3.6	842.3 ± 47.6
30	3.5	847.5 ± 37.8
40	3.5	692.4 ± 14.3
50	3.5	761.2 ± 29.0
60	3.5	605.3 ± 40.0

[a] mean ± SD (n = 3)

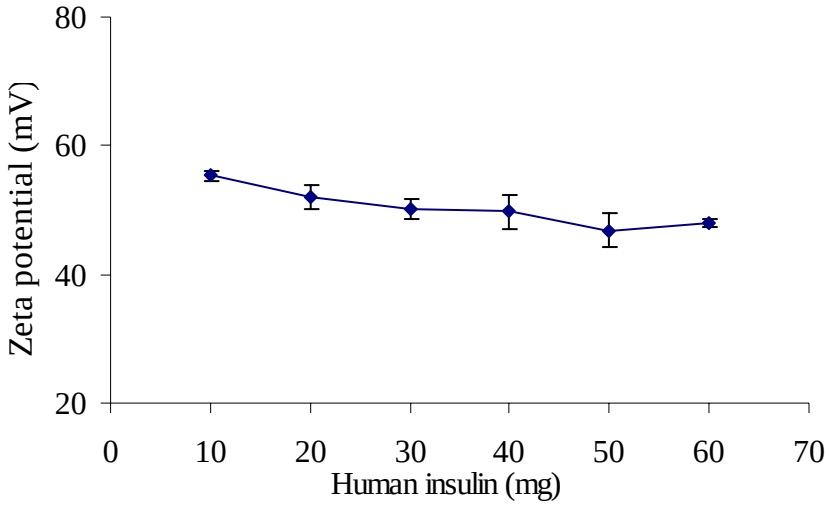

Figure 36. Zeta potential of insulin-chitosan nanoparticles made of pH 3.3 chitosan solution after adding tripolyphosphate with increasing insulin concentration (n = 3)

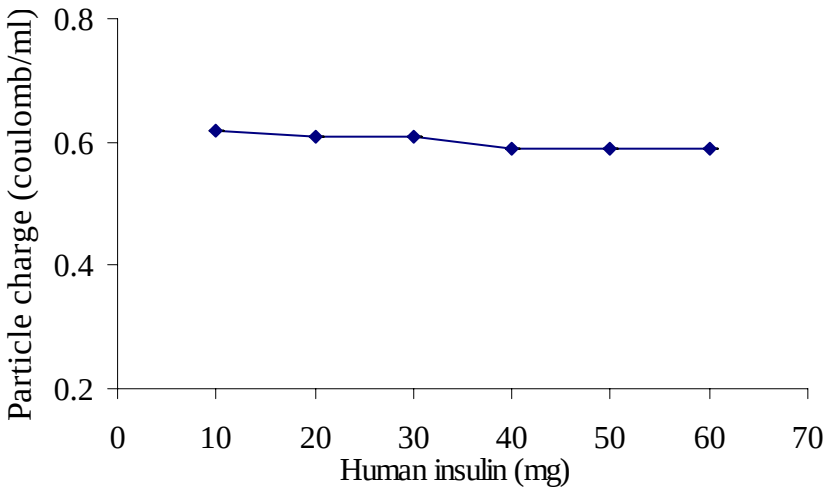

Figure 37. Particle charge of insulin-chitosan nanoparticles made of pH 3.3 chitosan solution after adding tripolyphosphate with increasing insulin concentration (n = 3)

Table 17. The entrapment efficiency of insulin-chitosan nanoparticles made of pH 3.3 chitosan solution after the addition of tripolyphosphate with increasing insulin concentration

Amount of insulin (mg)	Entrapment efficiency (% ± SD)[a] of Insulin-chitosan nanoparticles
	After adding TPP
10	31.0 ± 0.8
20	27.0 ± 2.6
30	23.0 ± 0.6
40	14.2 ± 0.9
50	16.3 ± 1.2
60	13.3 ± 3.5

[a]mean ± SD (n = 3)

the formulation pH was below the insulin isolectric point.

These results (Table 11, 12 and 15) indicate that the entrapment efficiency could be improved by changing the pH of chitosan solution. However, the maximum entrapment efficiency did not occur in the highest ionization range of the model drugs, but were achieved when the pH of formulation solution near the pKa of model drugs. It seems that the ionic interaction between drug and chitosan is not the main mechanism that causes particle formation. The protonated amino groups of chitosan at both pH 3.3 and pH 5 solutions as well as the dissociated functional groups of the model drug were masked by a water layer. The possibility of an electrostatical interaction was therefore low. Because of the preparing conditions (high speed stirring rate and long preparation time) and the reducing of electrostatic repulsion by adding counter ions even when the pH of formulation was near pKa of the model drugs, a flocculation of the colloidal chitosan in solution occurred. Hence, the drug in the microparticles might be partly bound and partly physically entrapped. Due to the fact that at least some amino groups of the chitosan molecule are involved in an electrostatical binding, the addition of tripolyphosphate leads to an increased flocculation; hence the better micro/nanoparticle formation.

2. Immunological activity of human insulin-chitosan microparticles

The immunological response of human insulin in the formulation, especially in the particles was compared with freshly prepared insulin solution. As indicated in Table 18, the amounts of human insulin released from both washed and unwashed insulin-chitosan microparticle suspension were assayed by MEIA test and compared with the amount of insulin obtained by HPLC analysis. The unwashed microparticles contained both entrapped and non-entrapped insulin fraction. The washed microparticle suspension contained the entrapped insulin fraction. It can be concluded that at room temperature (25ºC), insulin-chitosan microparticles prepared by high speed stirrer at a speed of 11,000 rpm, still maintained immune activity of human insulin inside the particles.

Table 18. The amount of insulin released from chitosan microparticles detected by HPLC and MEIA test (mean ± SD, n = 3).

Samples	Release amount (μg) (by HPLC analysis)	Release amount (μg) (by MEIA test)
Unwashed CH6T[a]	51.4 ± 0.2	42.0 ± 4.3
Washed CH6T[a]	17.4 ± 0.2	18.5 ± 0.9
Human insulin solution (5μg/ml)	4.8 ± 0.1[b]	6.3 ± 0.4[b]

[a] the formulation was composed of 6 ml of 5 mg/ml of insulin solution.

[b] n = 2

3. *In vitro* release studies

The drug release studies were carried out in three media, i.e., purified water, pH 7.4 phosphate buffer (PBS) and pH 3 HCl solution. Figure 38 and 39 show the release profiles of unwashed and washed insulin-chitosan microparticles. Most of insulin released within ten minutes from the microparticles in pH 7.4 (PBS) in which the chitosan matrix is not soluble and in the pH 3 HCl solution in which the chitosan should be soluble. Surprisingly, the release profiles were the same and there was no difference between the entrapped drug fractions and the adsorbed drug fractions. One should have expected that the entrapped and bound insulin would show a more sustained release. Insulin showed low release profiles from unwashed and washed particles in purified water due to the low solubility of insulin in water.

In the case of diclofenac-chitosan microparticles, the fast release profiles were achieved for both unwashed and washed particles in pH 7.4 PBS and in purified water (Figures 40-41). Only the release of diclofenac from unwashed particles in acid medium showed the lower release pattern than those in other media which due to its restricted dissociation. However, diclofenac released from washed particles in acid medium showed the burst release profile of a low concentration level. The swelling of gel like particles after washing process may cause the fast release of entrapped diclofenac even in acid.

The burst release of benzoic acid and salicylic acid from unwashed and washed chitosan nanoparticles was observed in three different media (Figures 42-45). It can be seen that after the washing process there was still some amount of benzoic acid or salicylic acid left in the suspension medium (about 20% of total amount). It is possible that most of drugs were physically entrapped into particles and leaked easily during washing process.

A drug release with a strong burst effect which was not followed by a further increase in drug concentrations, especially in pH 7.4 PBS indicates no binding of the drug molecule to the chitosan micro/nanoparticle matrix. In the case of binding it could be expected that at least in the pH 7.4 medium a release profile could be found to follow the square root of time law.

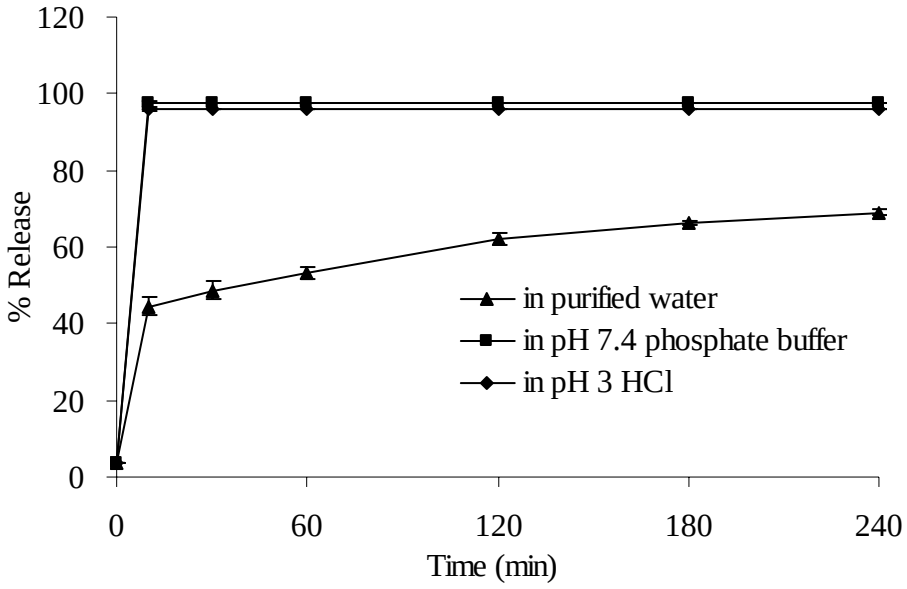

Figure 38. Release profiles of insulin from unwashed insulin-chitosan microparticles in different media (n = 3)

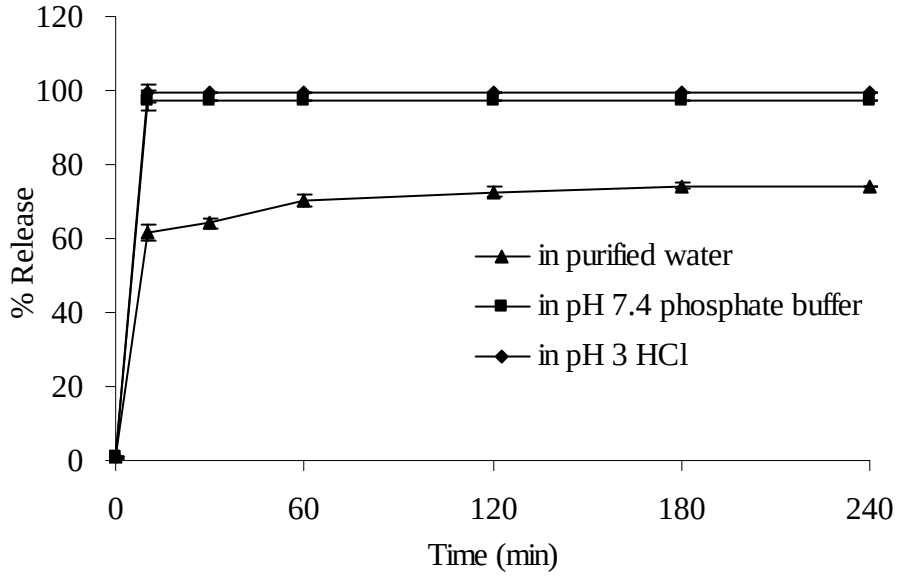

Figure 39. Release profiles of insulin from washed insulin-chitosan microparticles in different media (n = 3)

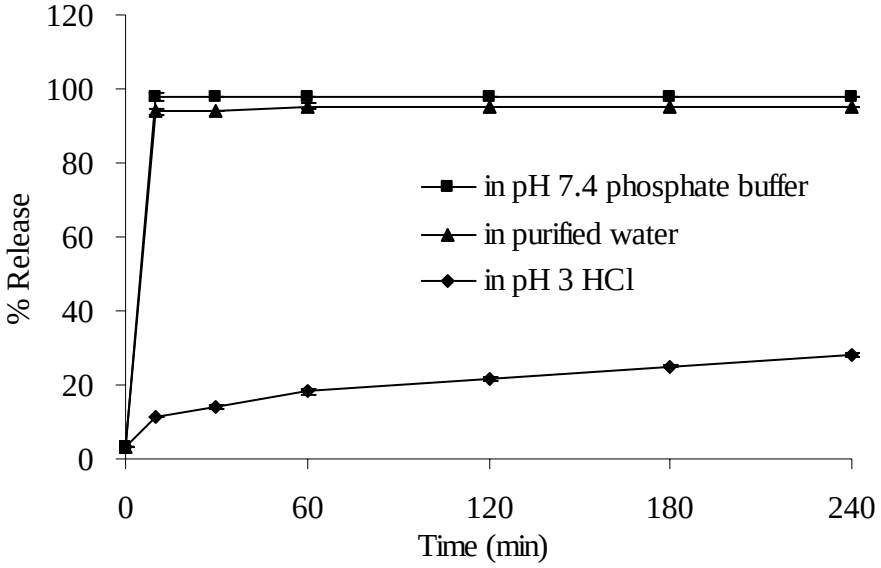

Figure 40. Release profiles of diclofenac from unwashed diclofenac-chitosan microparticles in different media (n = 3)

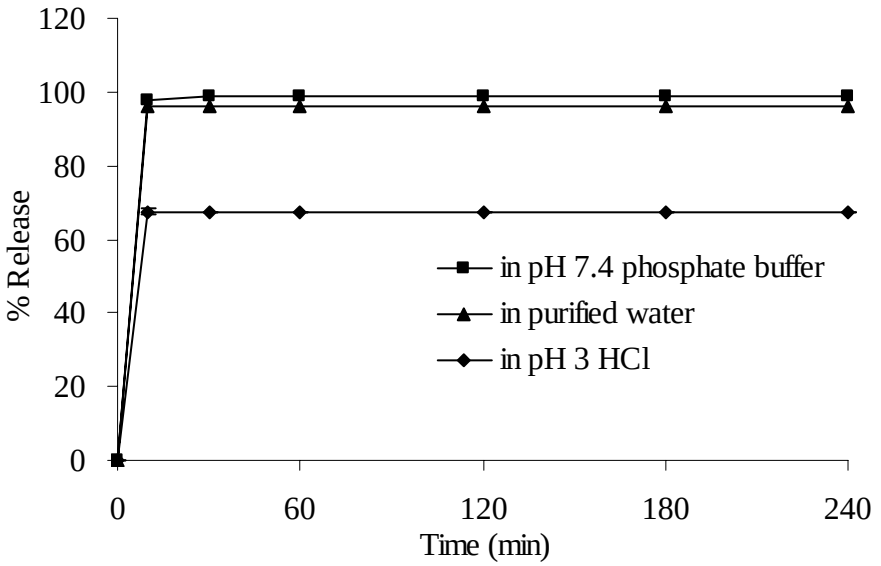

Figure 41. Release profiles of diclofenac from washed diclofenac-chitosan microparticles in different media (n = 3)

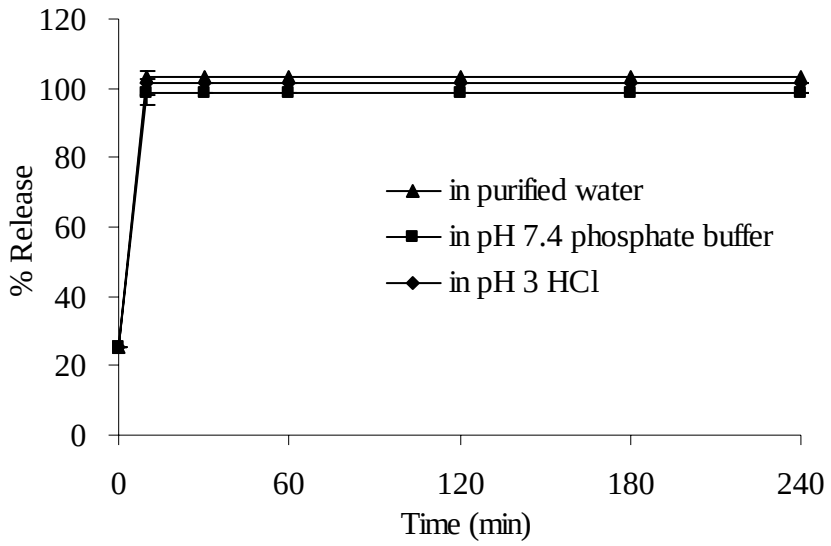

Figure 42. Release profiles of benzoic acid from unwashed benzoic-chitosan nanoparticles in different media (n = 3)

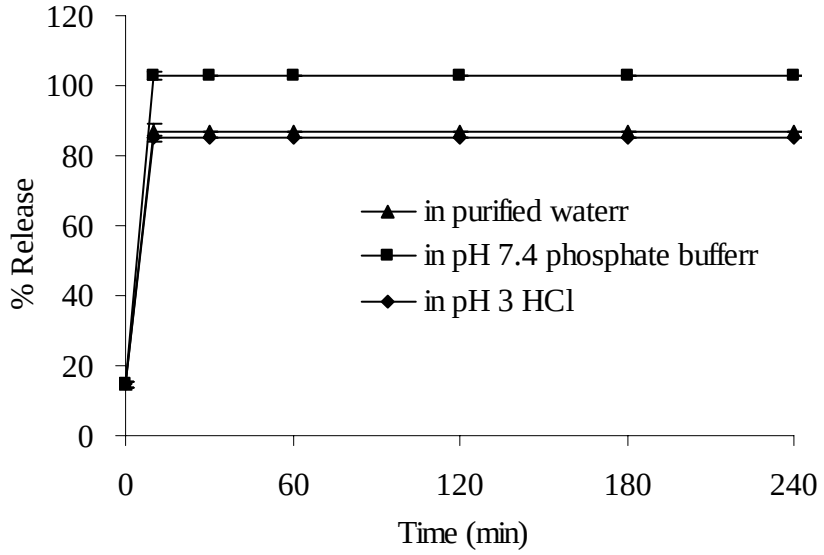

Figure 43. Release profiles of benzoic acid from washed benzoic-chitosan nanoparticles in different media (n = 3)

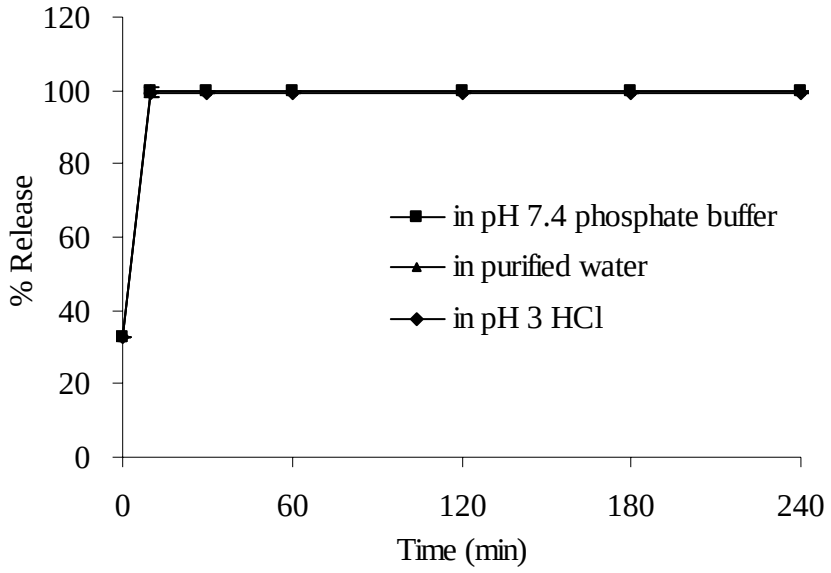

Figure 44. Release profiles of salicylic acid from unwashed salicylic-chitosan nanoparticles in different media (n = 3)

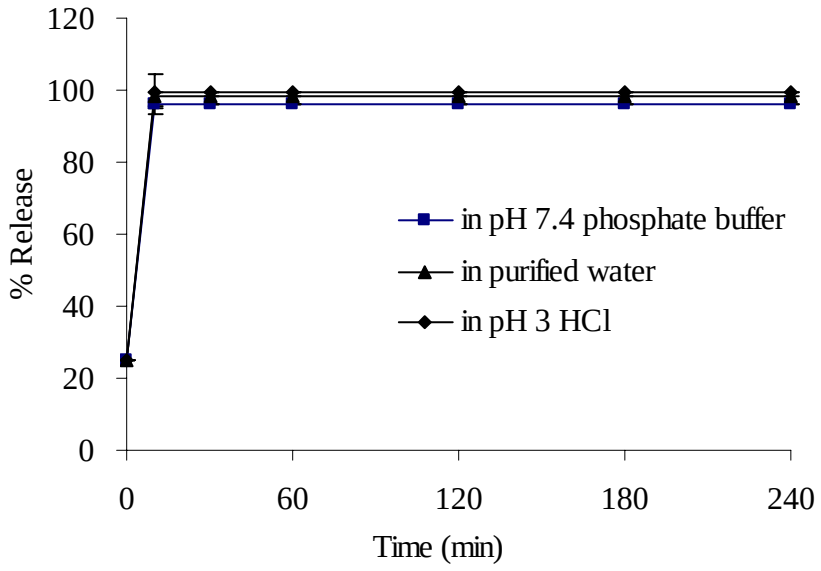

Figure 45. Release profiles of salicylic acid from washed salicylic-chitosan nanoparticles in different media (n = 3)

4. ^{1}H-NMR spectroscopy

Clear solution was obtained when chitosan solution pH 3.3 was mixed with benzoic acid solution (pH 3.0) or salicylic acid solution (pH 4.2). The drug-chitosan nanoparticles were observed after adding the cross-linking agent (tripolyphosphate). The ^{1}H-NMR analysis of these clear mixtures was performed in order to prove the ionic interaction between chitosan and drugs (benzoic acid and salicylic acid). Figure 46 shows the typical ^{1}H-NMR spectra of benzoic acid or salicylic acid. The region of 7.6 to 6.3 ppm represents the aromatic region of salicylic acid or benzoic acid. The region of 6 to 4 represents the huge water signal. The external standard used was DMSO-d_6 with 0.1% tetramethylsilane. The signal at 3.3 ppm indicates traces of water in DMSO-d_6 and the peak at 2.5 ppm is the signal of small amount of DMSO-d_5 in DMSO-d_6. The small peak at 0.0 ppm indicates the peak of tetramethylsilane in external standard.

Figure 47 shows the ^{1}H-NMR spectra of benzoic acid and sodium benzoate solution. The peaks at about 7.5, 7.1 and 7.0 ppm represent ortho-protons, para-proton and meta-protons, respectively. Figure 48 shows the magnificent spectra of salicylic acid in the aromatic region. The peaks at about 7.3, 7.0 and 6.5 indicate ortho, para and meta protons, respectively. Figure 49 and 50 demonstrate the ^{1}H-NMR spectra of benzoic acid, salicylic acid (0.3% to 0.03%) and their sodium salt (0.3%) in purified water. A very small shift of signal of benzoic acid or salicylic acid to the lower direction was observed with decreasing the drug concentrations. The spectra of the sodium salt of drugs in water presented the peaks at lower direction which indicate one hundred percent ionization. The same direction of the chemical shift was observed by proton NMR analysis of various concentrations of drugs and their sodium salt, in 0.2% chitosan solution and 0.2% ammonium acetate solution (see appendix, Figures 81-84). Assuming that the ortho-proton signal was an average signal for benzoic acid and benzoate, Figure 51 is the plot of the chemical shift for the ortho-proton signals of various benzoic acid concentrations in three media mentioned above. It can be interpreted that there is no binding or interaction between benzoic acid and chitosan because the tiny shift of signal in the same direction was detected in several

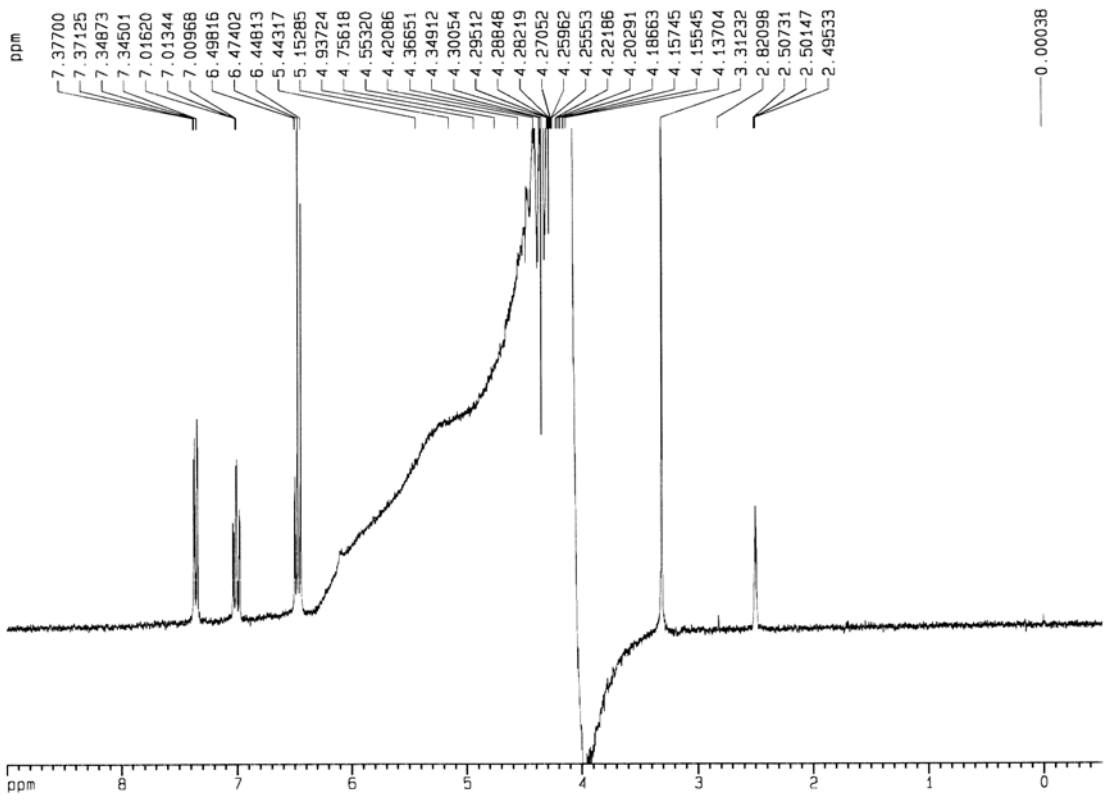

Figure 46. Typical ^{1}H-NMR spectra of benzoic acid or salicylic acid solution

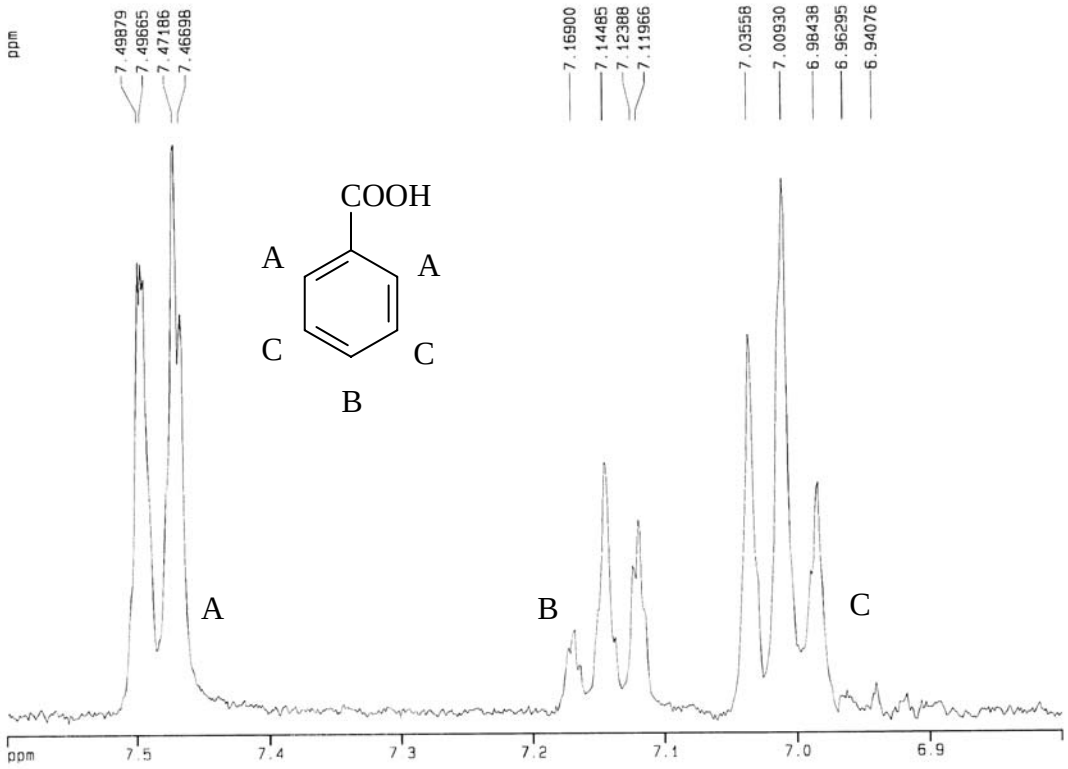

Figure 47. The ^{1}H-NMR spectra presents the peaks at an aromatic region of benzoic acid solution. The peaks indicate ortho protons (A), para proton (B) and meta protons (C).

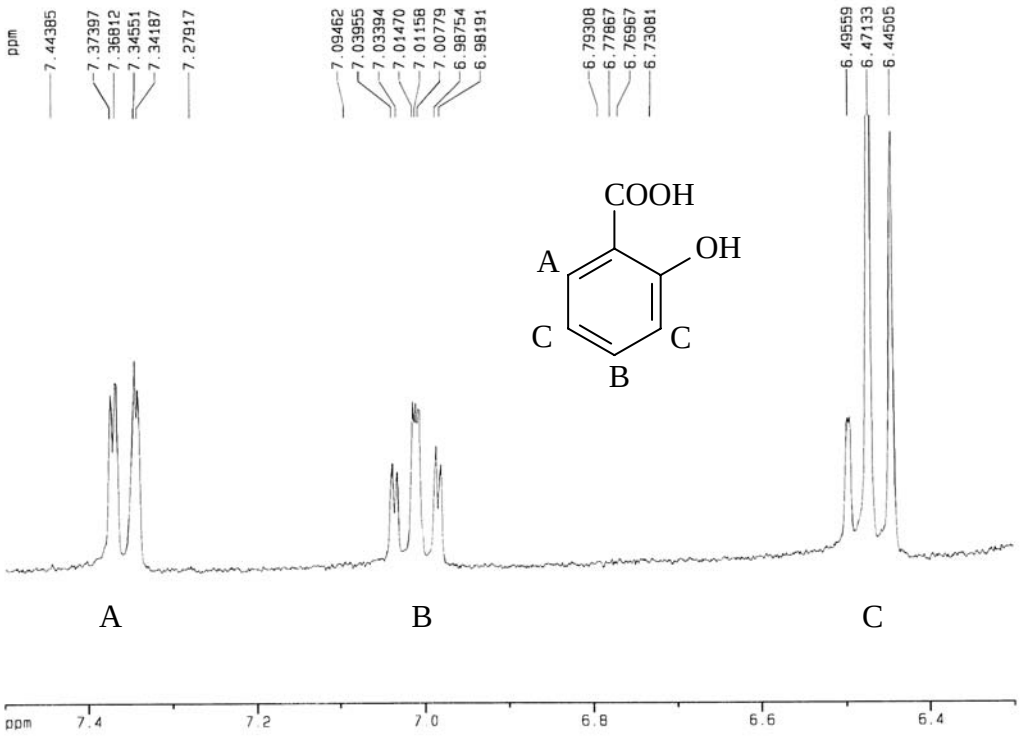

Figure 48. The ^{1}H-NMR spectra presents the peaks at an aromatic region of salicylic acid solution. The peaks indicate ortho protons (A), para proton (B) and meta protons (C).

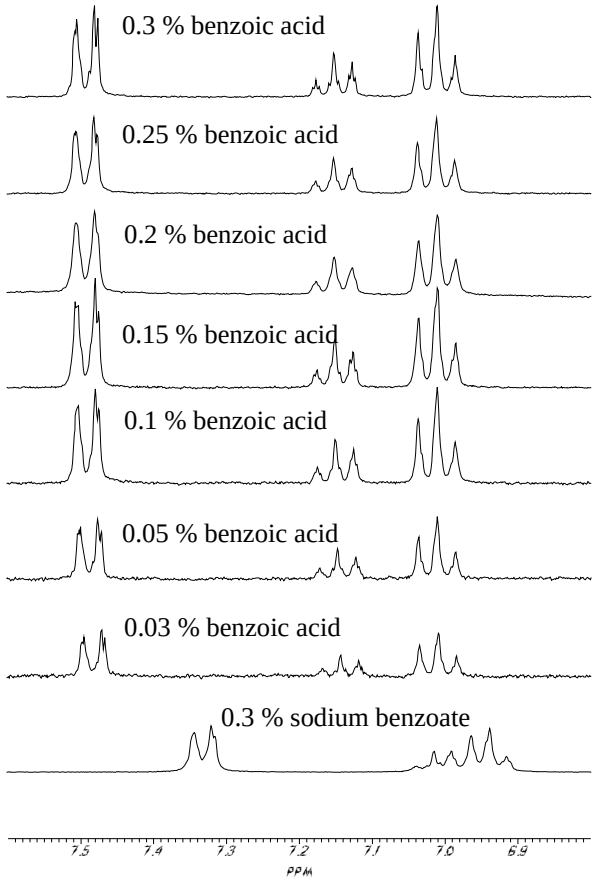

Fig. 49. ^{1}H-NMR spectra of benzoic acid (0.3%-0.03%) and sodium benzoate (0.3%) in purified water

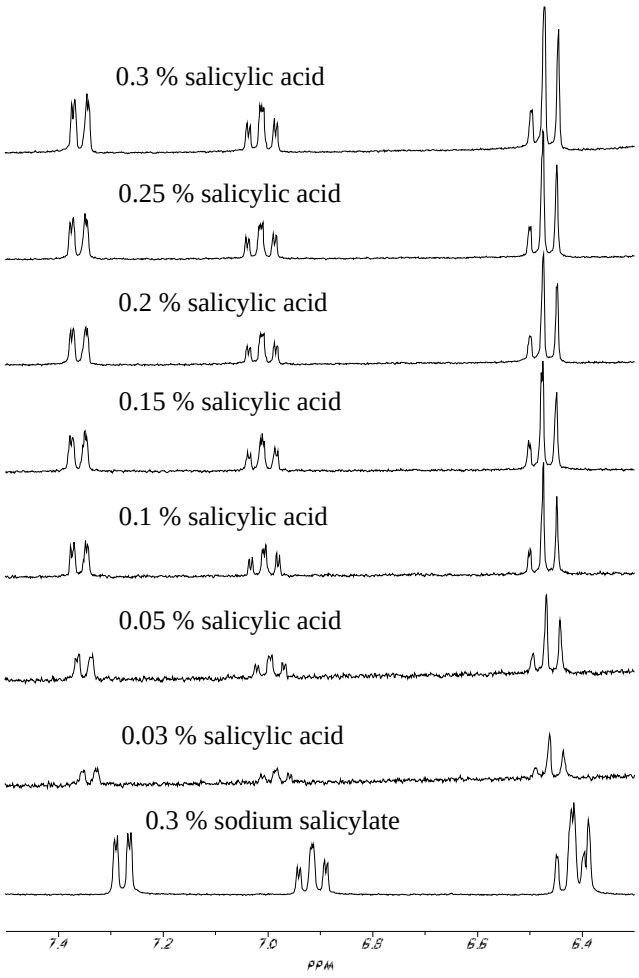

Figure 50. ^{1}H-NMR spectra of salicylic acid (0.3%-0.03%) and sodium salicylate (0.3%) in purified water

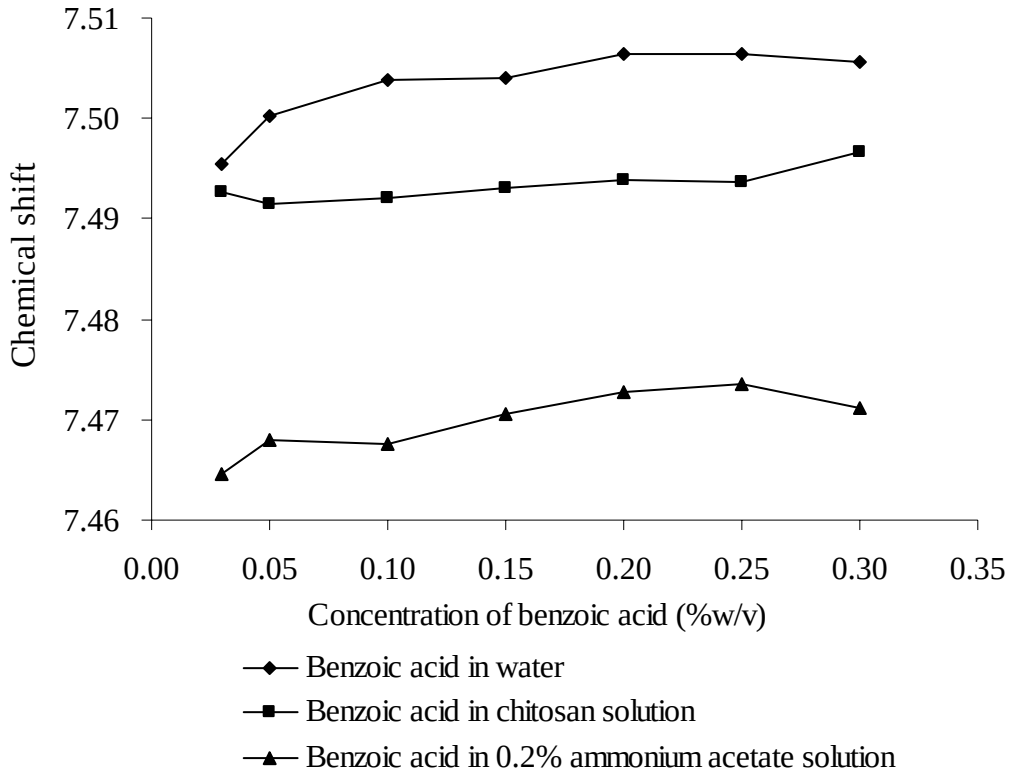

Figure 51. Chemical shift of ortho-proton signal of various concentrations of benzoic acid in different media

mixtures of benzoic acid even in purified water. The dissociation of benzoic acid was increased when the total concentration of benzoic acid in the mixtures was decreased which resulted in increasing the relative amount of benzoate and the shift to the direction of sodium salt shift values. Figure 52 shows the chemical shift of ortho-proton signal of salicylic acid in water, 0.2% chitosan solution and 0.2% ammonium acetate solution. The similar development was observed referring to the same conclusion for salicylic-chitosan mixture.

5. FTIR spectroscopy

FTIR analysis is proposed in many literatures as the possible way to investigate the interaction between the substances (91, 92). In this study, dried drug-chitosan particles were analyzed by FTIR to observe the possible interaction of functional groups between drugs and chitosan. As indicated in Table 3 various concentrations of composition in formulations were used to prepared chitosan micro/nanoparticles. Large molecule model drug and one of small molecule model drug were studied. Chitosan exhibits main characteristic bands of carbonyl groups (C=O-NHR) and amine ($-NH_2$) at 1654 cm^{-1} and 1540 cm^{-1}, respectively (93, 94). The broad band due to the stretching vibration of $-NH_2$ and -OH group can be observed at 3400-3500 cm^{-1}(47, 60). The bands at 1000-1200 cm^{-1} are attributed to the saccharide structure of chitosan (95).

For FTIR spectra of insulin-chitosan microparticles, there was no shift of the bands when the concentrations of tripolyphosphate and chitosan were increased (Figure 53-54). Figure 55 presents the spectra of insulin and insulin-chitosan microparticles with increasing insulin concentration from 1 mg/ml to 6 mg/ml solution. There was no shift of the bands but it seems that some bands of chitosan were overlapped with those of insulin resulted in the wider of the carbonyl bands (1654 cm^{-1}) and amine bands (1540 cm^{-1}) with increasing the concentration of insulin in formulations. In addition, the change of the three small bands at wavenumbers about 1400-1500 cm^{-1} to two bands of insulin was observed. These observations show the possibility of interaction between insulin and chitosan (93, 94).

Figure 56 and 57 represent the spectra of benzoic acid-chitosan nanoparticles with the varying concentration of tripolyphosphate and chitosan, respectively. There was no significant shift of the main bands of chitosan in the spectra. The spectra of benzoic acid and benzoic-chitosan nanoparticles with increasing concentrations of benzoic acid solution in the formulation (from 0.5 mg/ml to 2.5 mg/ml) were shown in Figure 58. There was no noticeable shift of the major bands of chitosan and no bands from benzoic acid could be seen in the spectra of benzoic acid-chitosan nanoparticles. It indicates that there is no interaction between benzoic acid and chitosan (93).

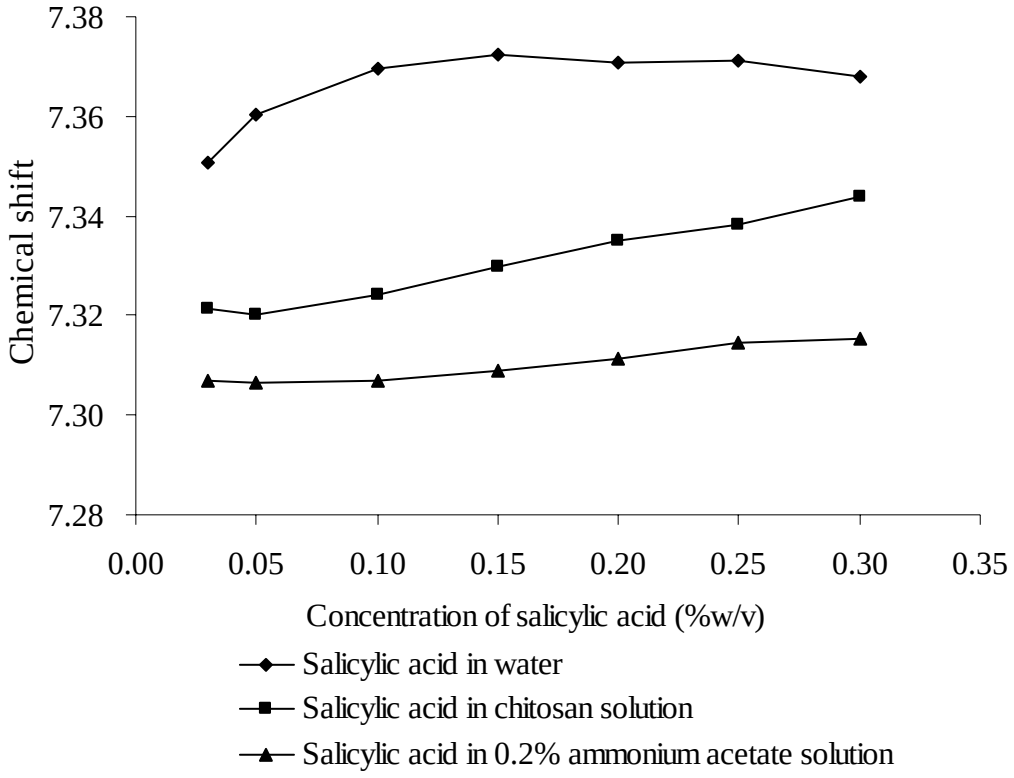

Figure 52. Chemical shift of ortho-proton signal of various concentrations of salicylic acid in different media

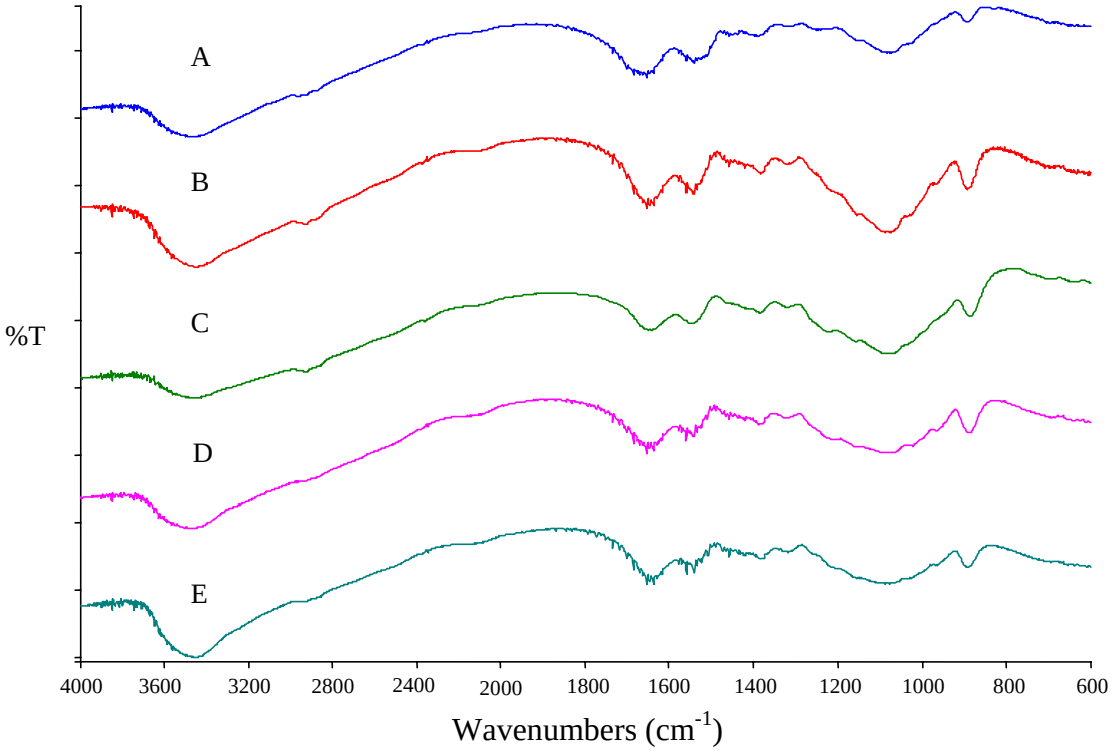

Figure 53. IR spectra of insulin-chitosan microparticles with different concentrations of tripolyphosphate solution used in formulations; 0.1% w/v (A), 0.2% w/v (B), 0.4% w/v (C), 0.8% w/v (D) and 1.6% w/v (E)

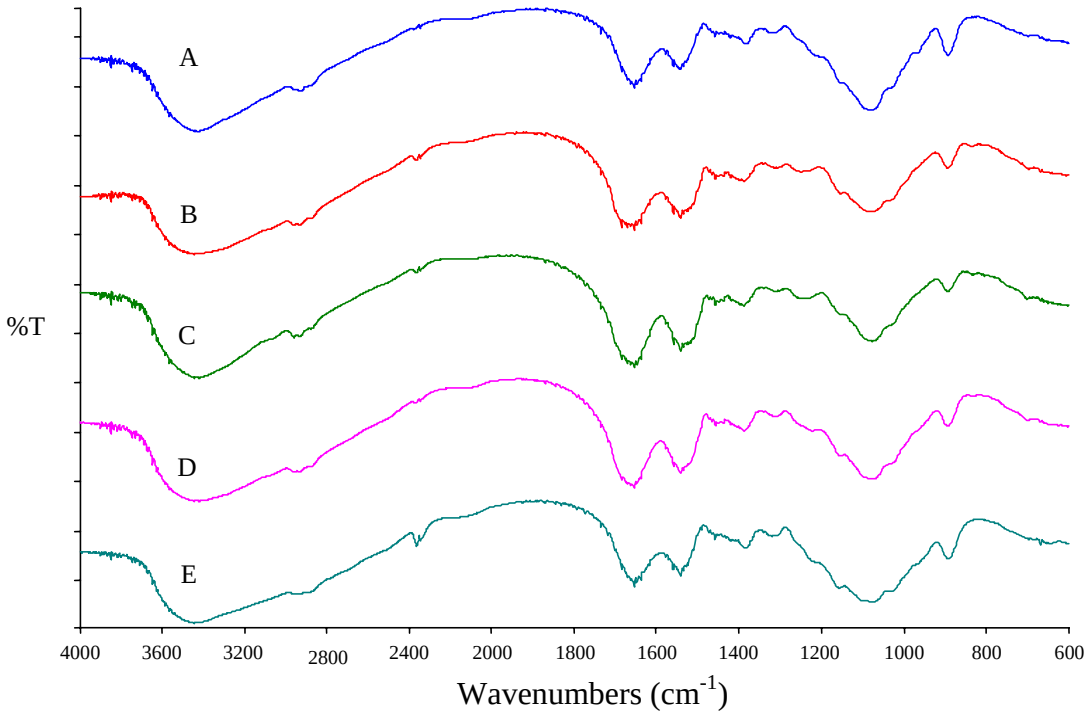

Figure 54. IR spectra of insulin-chitosan microparticles with different concentrations of chitosan solution used in formulations; 0.1% w/v (A), 0.2% w/v (B), 0.3% w/v (C), 0.4% w/v (D) and 0.5% w/v (E)

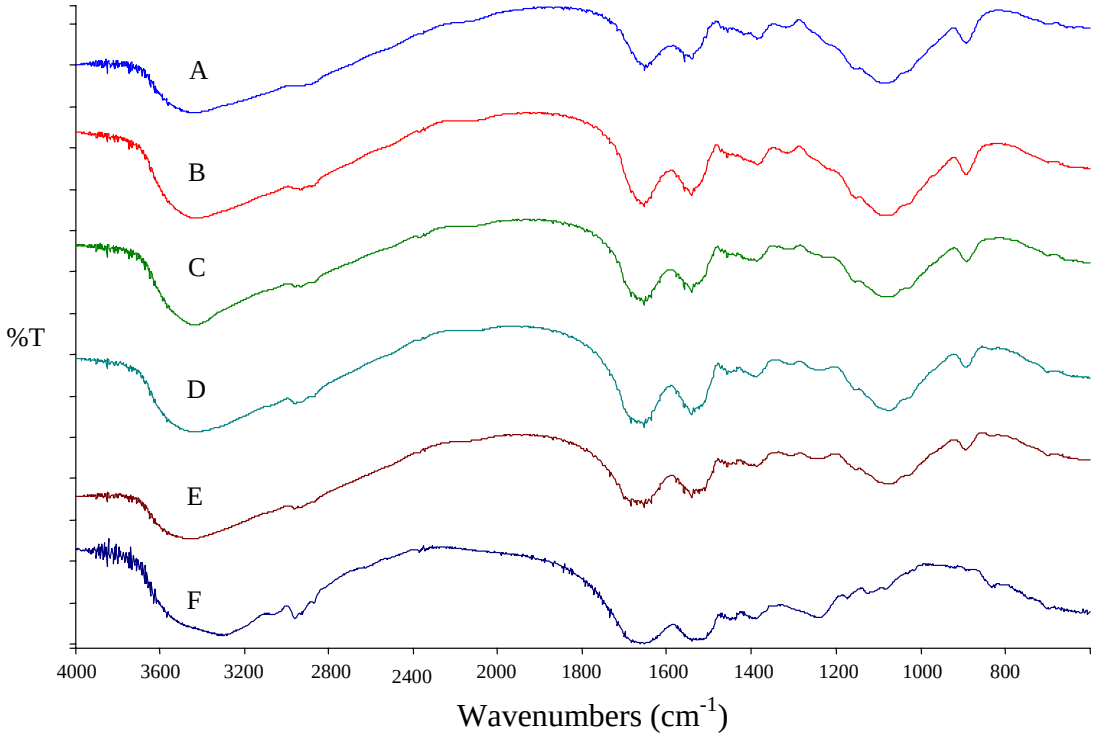

Figure 55. IR spectra of insulin (F) and insulin-chitosan microparticles with different concentrations of insulin solution used in formulations; 1mg/ml (A), 2 mg/ml (B), 3 mg/ml (C), 5 mg/ml (D) and 6 mg/ml (E)

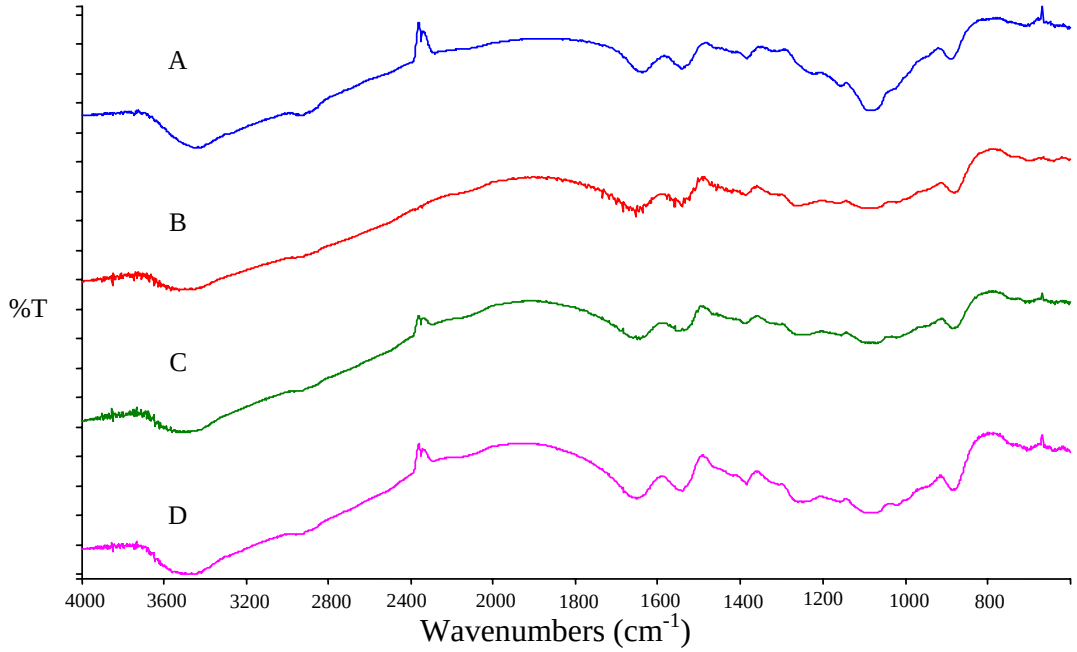

Figure 56. IR spectra of benzoic acid-chitosan nanoparticles with different concentrations of tripolyphosphate solution used in formulations; 0.2% w/v (A), 0.4% w/v (B), 0.8% w/v (C) and 1.6% w/v (D)

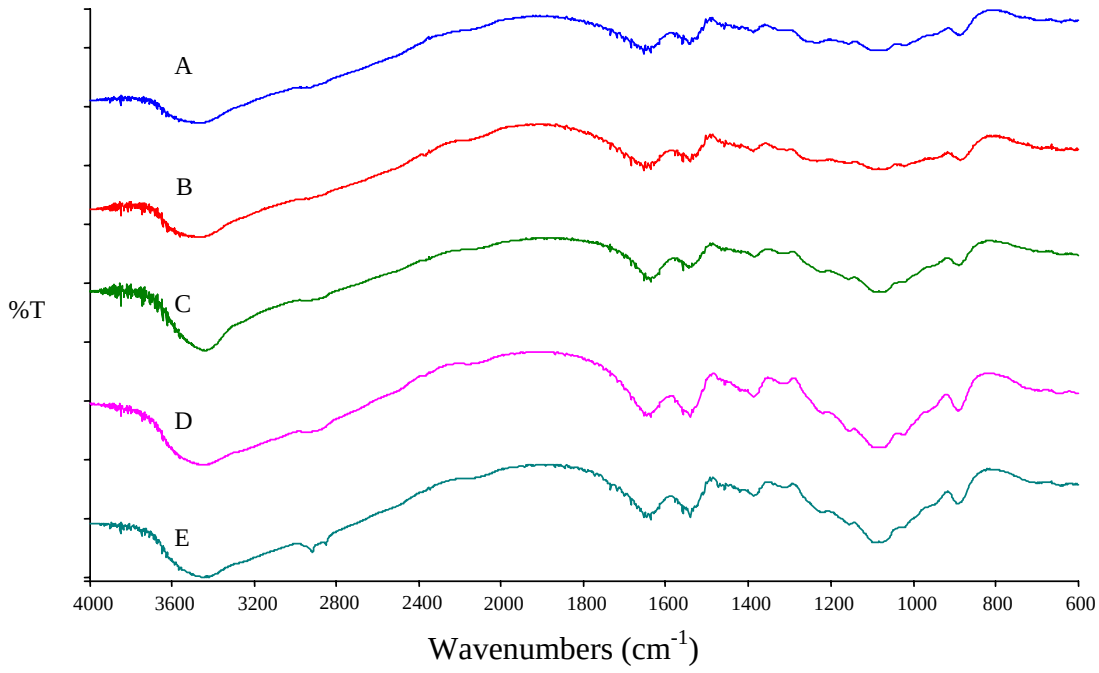

Figure 57. IR spectra of benzoic acid-chitosan nanoparticles with different concentrations of chitosan solution used in formulations; 0.1% w/v (A), 0.2% w/v (B), 0.3% w/v (C), 0.4% w/v (D) and 0.5% w/v (E)

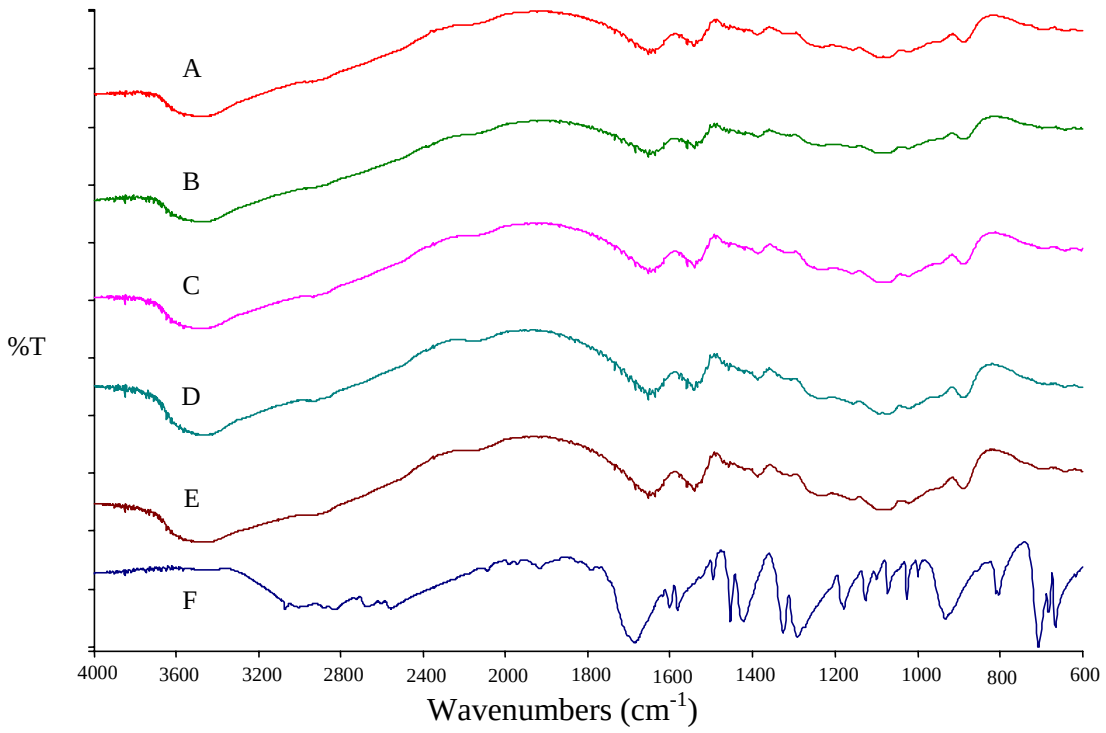

Figure 58. IR spectra of benzoic acid (F) and benzoic acid-chitosan nanoparticles with different concentrations of benzoic acid solution used in formulations; 0.5 mg/ml (A), 1 mg/ml (B), 1.5 mg/ml (C), 2 mg/ml (D) and 2.5 mg/ml (E)

6. Isothermal titration calorimetry

The interaction between opposite charge molecules resulted in the change of enthalpy which can be detected by microcalorimetry. To test the accuracy of a calorimeter, the standard reactions are recommended to perform. Figure 59A and 59B represent the output (heat flow) of the standard reaction between barium chloride and crown ether (18-crown-6). The plot of net heat released as a function of ratio of barium chloride to 18-crown-6 is presented in Figure 60. The enthalpy change (ΔH) of -31.13 kJ/mol and log k of 3.8 were in accordance with several literatures (96, 97).

The interaction between pH 7.2 insulin (5 mg/ml, 860 μM) and pH 5 chitosan (0.2% w/v, 13.3 μM) was followed. Insulin solution in phosphate buffer (0.2 M phosphate buffer with 1N HCl and 1N NaOH) was titrated into titration cell containing 2.5 ml chitosan solution. The raw data for the titration of insulin to chitosan is shown in Figure 61A. The gradual increase of exothermic heat was observed as a function of injection. The heat of dilution was measured by titrating of phosphate buffer to chitosan. The raw calorimetric data is shown in Figure 61B represented exothermic for several injections and finally came to endothermic value. This heat of dilution was then subtracted from the heat of titration between insulin and chitosan (Figure 61A) to obtain the net heat of interaction between them. Figure 62A is the integrated data plotted the enthalpy change (ΔH) per mole of insulin versus the concentration of insulin in titration cell obtained after subtracting the heat of dilution. The interaction between insulin and chitosan is an exothermic reaction. The interaction enthalpy change was not very high (< 500 kcal/mole of insulin) when compared with the binding studies of macromolecules or polymers. For example, the enthalpy change about 1500 kcal/mole of sugar units of chitosan was observed in the reaction of chitosan and β-lactoglobulin (23). The enthalpy change of the interaction between insulin and chitosan is partly due to the ionic interaction between them. However, the big possibilities are caused by the conformational changes, ionization of polar groups and especially, the adsorption phenomena of insulin on to the surfaces (23, 98). The conformational changes are due to the electrostatic interaction,r hydrogen bond between amino acid with charge side chains or hydrophobic interaction of amino acid with nonpolar side chains. The great attention to this study

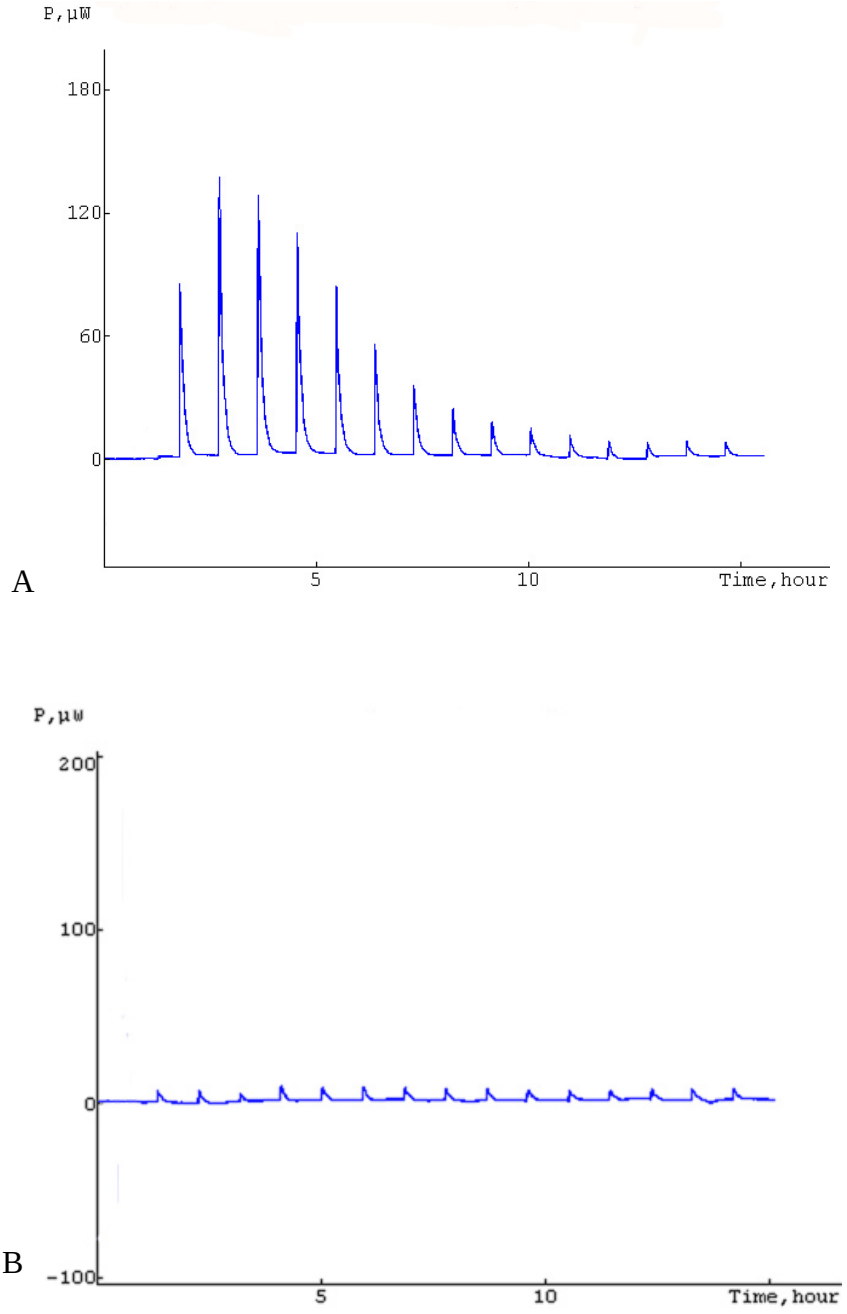

Figure 59. Heat flow versus time profiles for the sequential titrations of barium chloride solution in to crown ether (18-crown-6) (A) and barium chloride solution in to water (B)

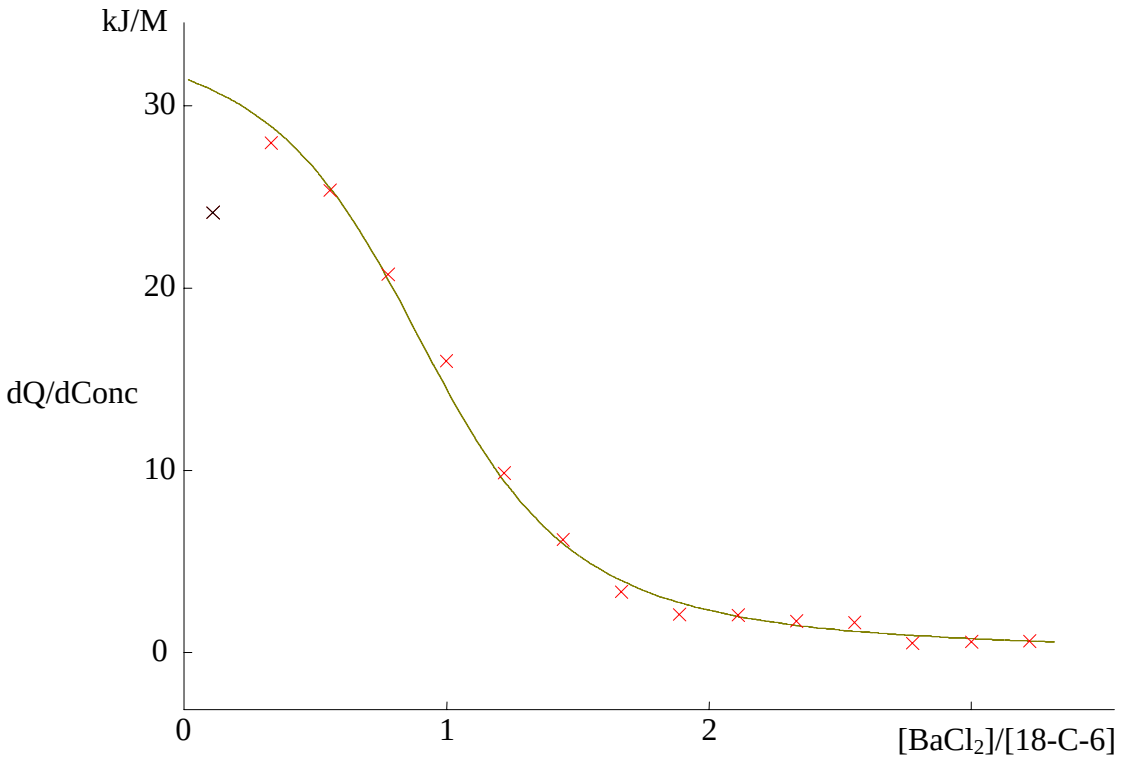

Figure 60. The plot of the interaction enthalpy change per mole of barium chloride as a function of ratio of barium chloride to 18-crown-6

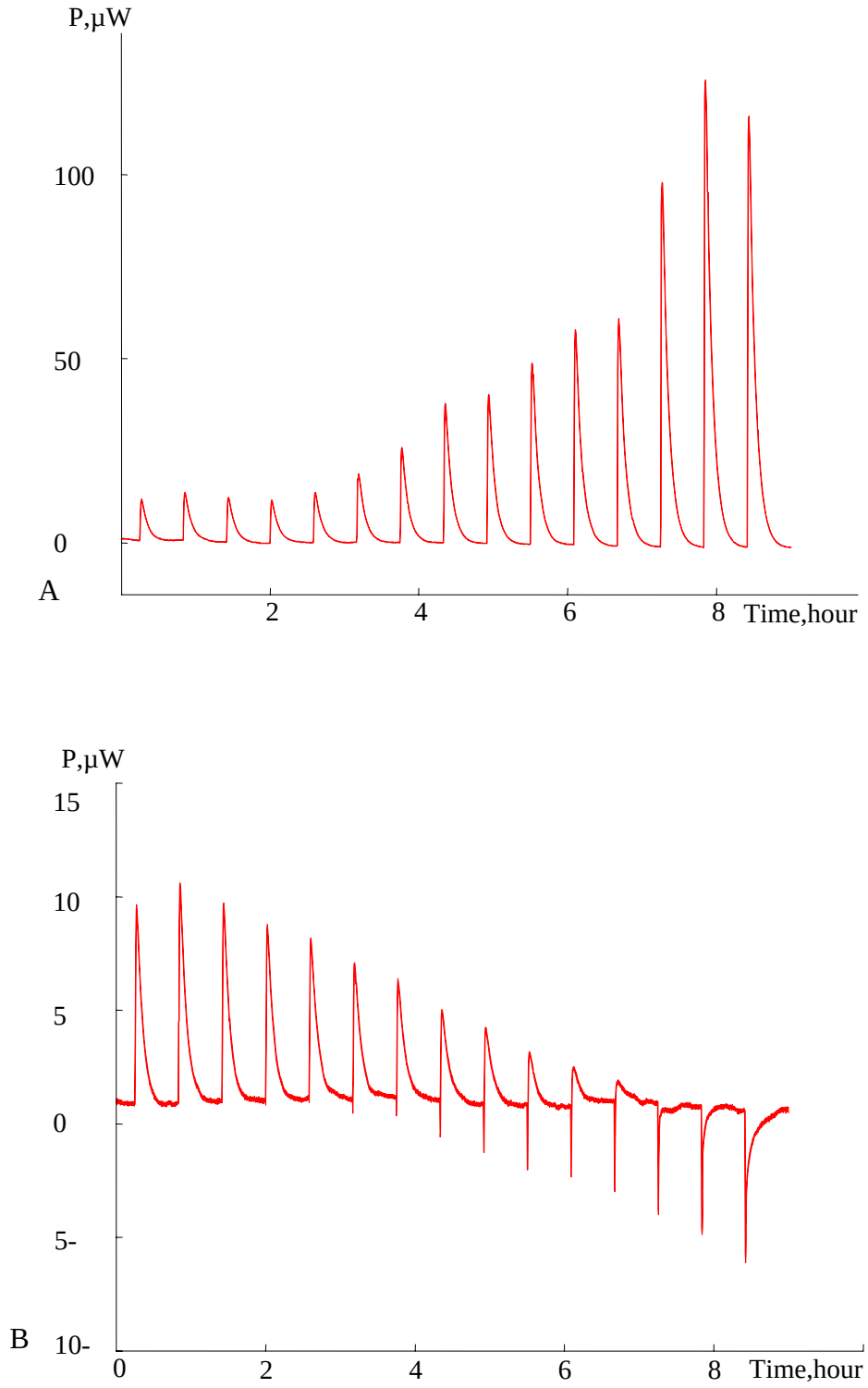

Figure 61. Heat flow versus time profiles for the sequential titrations of insulin solution into chitosan solution (A) and phosphate buffer solution into chtosan solution as a blank experiment (B)

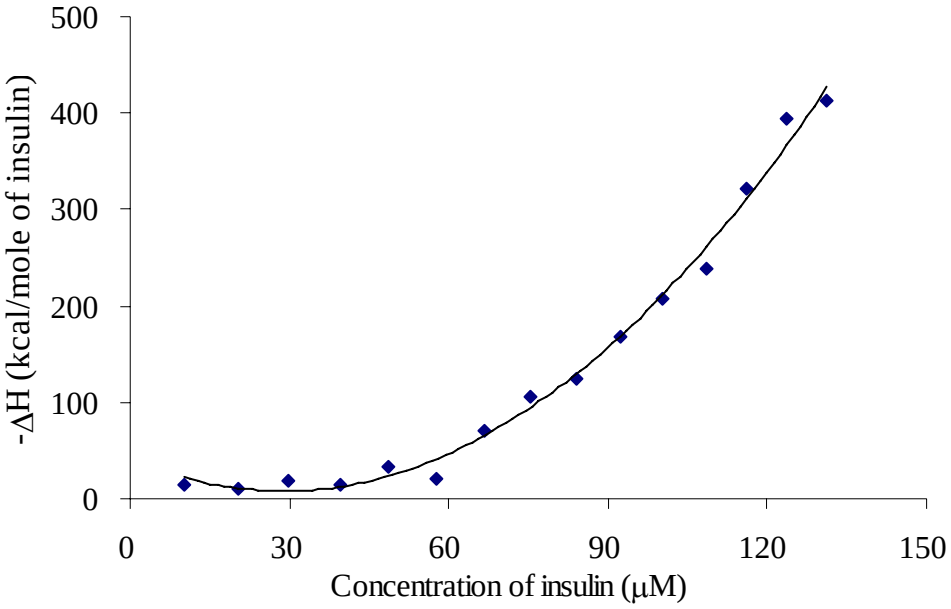

Figure 62. Integrated data obtained from the titration of insulin solution into pH 5 chitosan solution in the reaction cell after subtracting the blank experiment

is the adsorption of insulin on to the surfaces which can be detected by the measurement of the surface charge of the particles. The particle charge of insulin-chitosan microparticles was decreased with increasing insulin in formulation and accompanied by the increase of entrapment efficiency. The unexpected event was the high burst release of insulin with no further release of insulin to dissolution media. These imply that only small amount of negative charge groups of insulin interact with positive charge chitosan. The adsorption of most insulin on the surface of particles seems to be the big reason of high entrapment efficiency, the burst release profile and the change in reaction enthalpy.

The heat flow of the interaction between diclofenac sodium and chitosan is shown in Figure 63A. The blank experiment curve in Figure 63 B indicates quite high constant heat flow. The actual heat of interaction between diclofenac sodium and chitosan is indicated in Figure 64. The titration of diclofenac sodium into chitosan at pH 5 was endothermic at the concentration of diclofenac sodium lower than 1.7 mM. Then, it became exothermic for several injections and finally, the enthalpy change became stable which may due to the saturation of the interaction. In acid condition diclofenac sodium is changed to diclofenac free acid. The –NHR group at the ortho position of diclofenac acid can be protonated and behaves like electron withdrawing group. The $–NH_2R^+$ group can strongly affect the properties of carboxylic acid. For example, it may reduce the pKa of carboxylic acid. The carboxylic group easily then becomes carboxyl group (COO^-). However, the repulsion force between the positive charge of $–NH_2R^+$ group and the positive charge of chitosan prevented the ionic interaction between carboxyl group of diclofenac and amine group of chitosan. The protonation of –NHR group resulted in the change of reaction enthalpy. The enthalpy change was therefore more detectable than those of other small model drugs.

The heat flow versus time profiles for the titration of benzoic acid into pH 3.3 chitosan and pH 3.3 dilute acetic acid (blank experiment) are shown in Figure 65A and 65B, respectively. The almost equal and constant heat flow was observed from both experiments and the heat flow was not drug concentration dependent because no significant decrease with injection number was observed. As depicted in Figure 66, the interaction enthalpy change per mole of benzoic acid (injectant) was very small

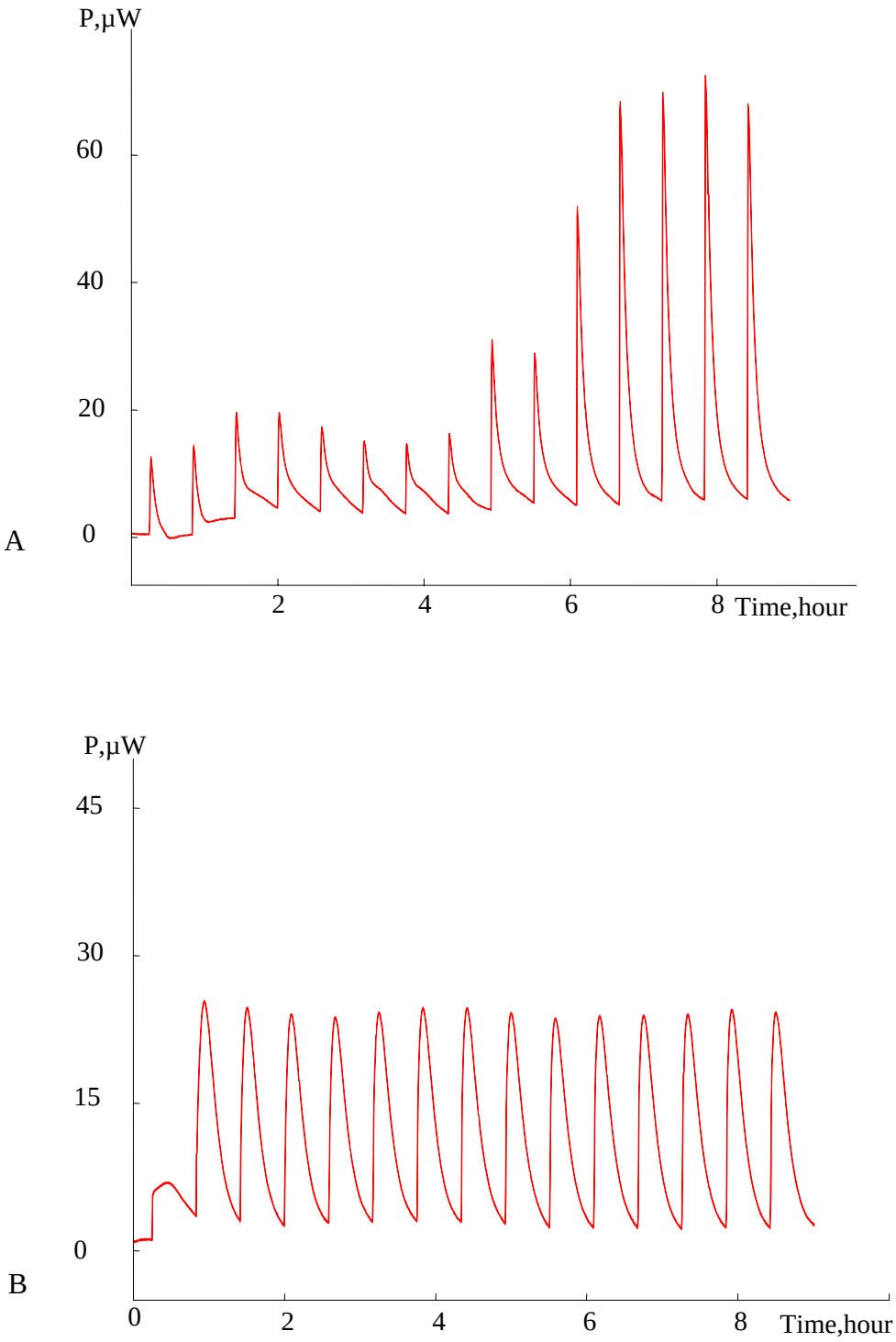

Figure 63. Heat flow versus time profiles for the sequential titrations of diclofenac sodium solution into chitosan solution (A) and diclofenac sodium solution into dilute acetic acid as a blank experiment (B)

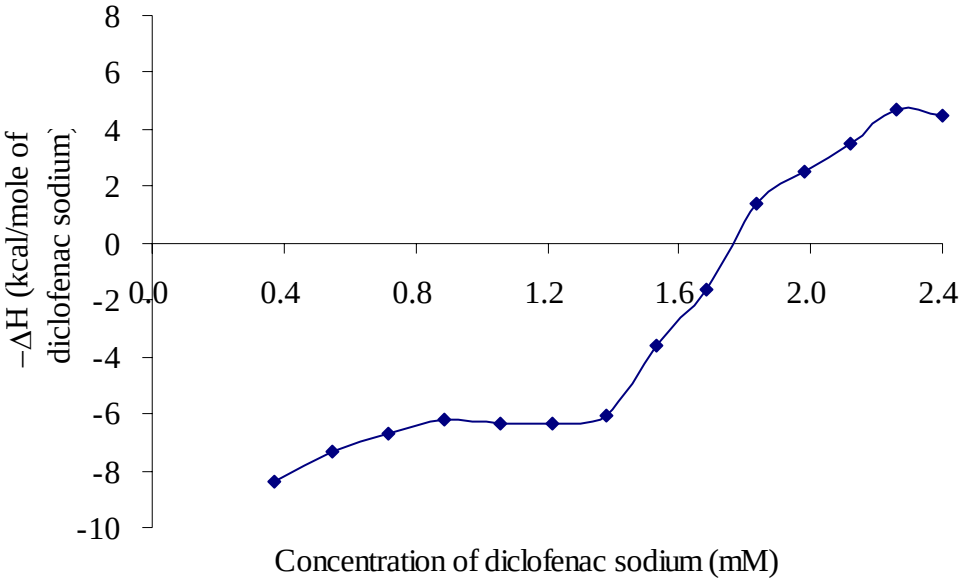

Figure 64. Integrated data obtained from the titration of diclofenac sodium solution into pH 5 chitosan solution in the reaction cell after subtracting the blank experiment

.

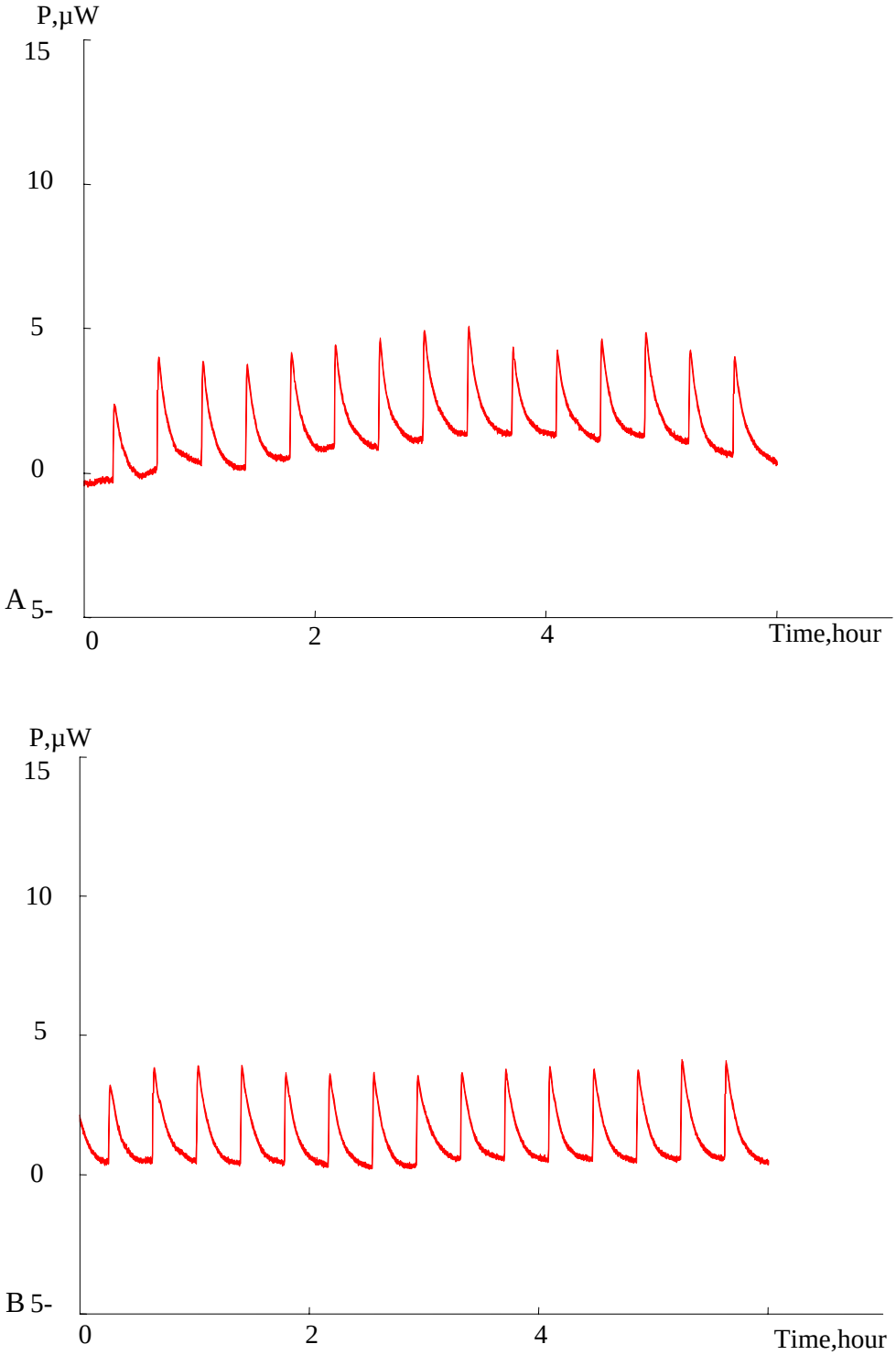

Figure 65. Heat flow versus time profiles for the sequential titrations of benzoic acid solution in to chitosan solution (A) and benzoic acid solution in to dilute acetic acid solution as a blank experiment (B)

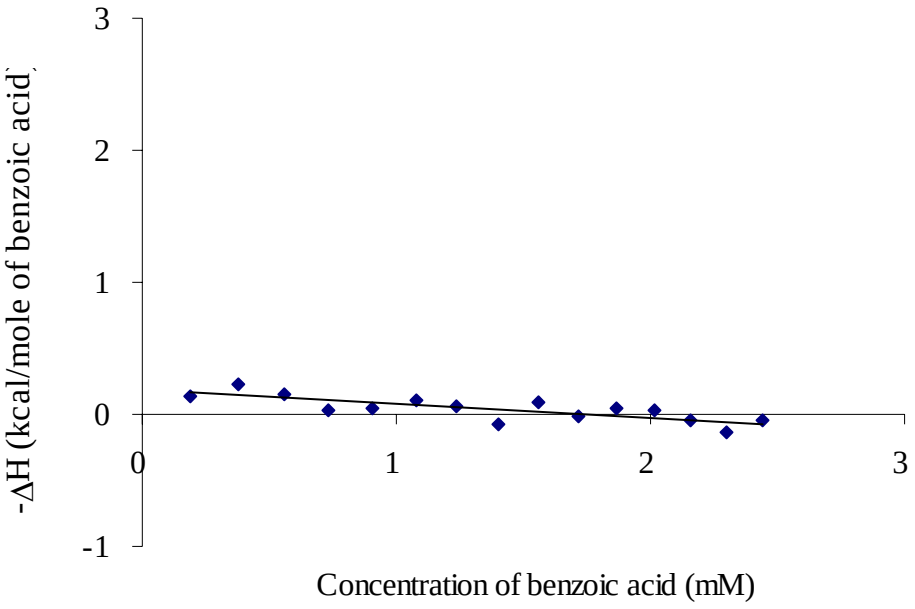

Figure 66. Integrated data obtained from the titration of benzoic acid solution into pH 3.3 chitosan solution in the reaction cell after subtracting the blank experiment

(< 0.3 kcal/mol), which can be implied that there was no significant ionic interaction between benzoic acid and chitoan at pH 3.3 although the high entrapment efficiency was determined. This deduction is coincident with the analysis by ^{1}H-NMR and FTIR.

The similar result could be seen from the sequential titrations to confirm the interaction of salicylic acid and chitosan (Figure 67 and 68). The exothermic interaction enthalpy change (ΔH) was less than 0.5 kcal/mol. Although salicylic acid is stronger acid than benzoic acid, there is no dominantly different binding capacity to chitosan which is a weak base.

The interactions between tripolyphosphate (pH 9.1) and pH 3.3 or pH 5 chitosan were investigated. The heat flow of the titration of tripolyphosphate solution into pH 5 chitosan solution and into pH 5 dilute acetic acid represents exothermic process (Figure 69). The shift of the baselines may be due to the pH compensation signal. From the integrated data (Figure 70), the enthalpy change (ΔH) was fairly small (<8 kcal/mol) which is generally due to the small molecular weight of injectant. However, this may indicated the interaction between them (99, 100). These were also the cases when tripolyphosphate solutions were added to pH 3.3 chitosan solution and pH 3.3 dilute acetic acid solution (Figure 71 and 72). The enthalpy change (ΔH) for the interaction of tripolyphosphate to pH 3.3 chitosan was lower than that to pH 5 chitosan.

Tripolyphosphate is a cross-linking agent used to complete the particle formation. The binding ability of tripolyphosphate to drug-chitosan microparticles or mixtures was evaluated. From the early study, the zeta potential of insulin-chitosan microparticles was decreased about 5-7 mV after addition of tripolyphosphate. By ITC the exothermic enthalpy change was gradually increased with the concentration of tripolyphosphate added and it was not more than 10.5 kcal/mole (Figure 74). For small molecular weight titrant, this indicated the binding of negatively charged tripolyphosphate to the positive charge of chitosan on the surface of microparticles. It can be implied that the prior covering of particle surface by the adsorption of insulin contributed to the only minor change in zeta potential of insulin-chitosan microparticles by adding tripolyphosphate. The curtain amount of positively charged

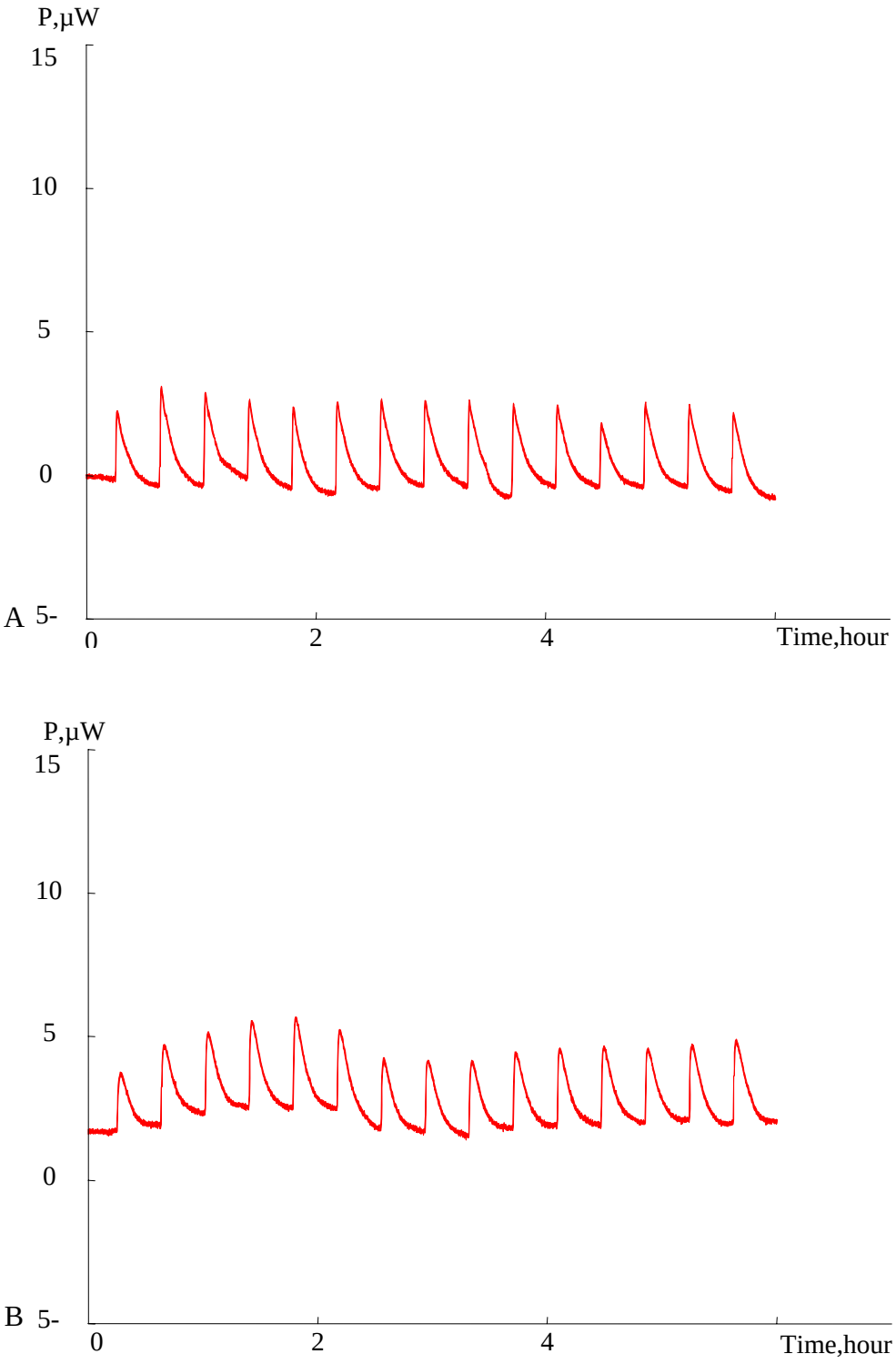

Figure 67. Heat flow versus time profiles for the sequential titrations of salicylic acid solution into chitosan solution (A) and salicylic acid solution into dilute acetic acid solution as a blank experiment (B)

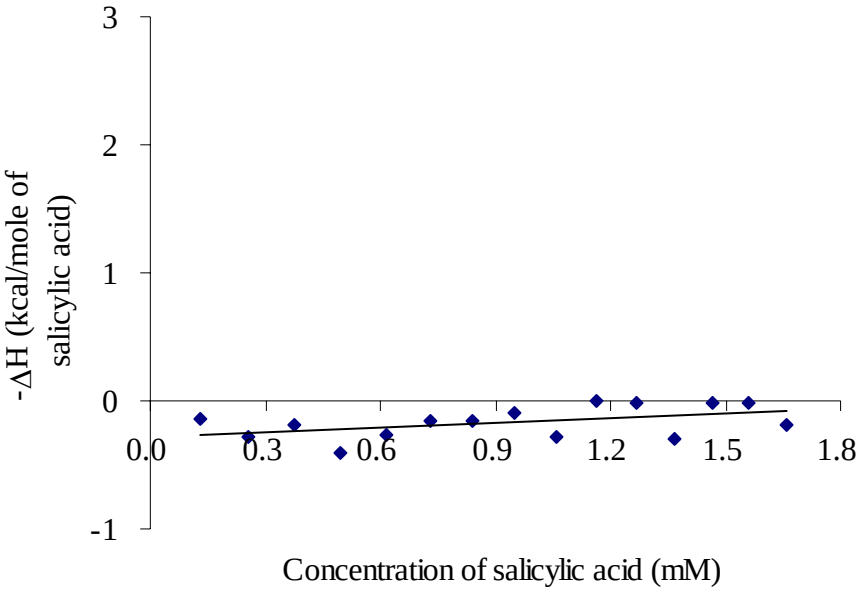

Figure 68. Integrated data obtained from the titration of salicylic acid solution into pH 3.3 chitosan solution in the reaction cell after subtracting the blank experiment

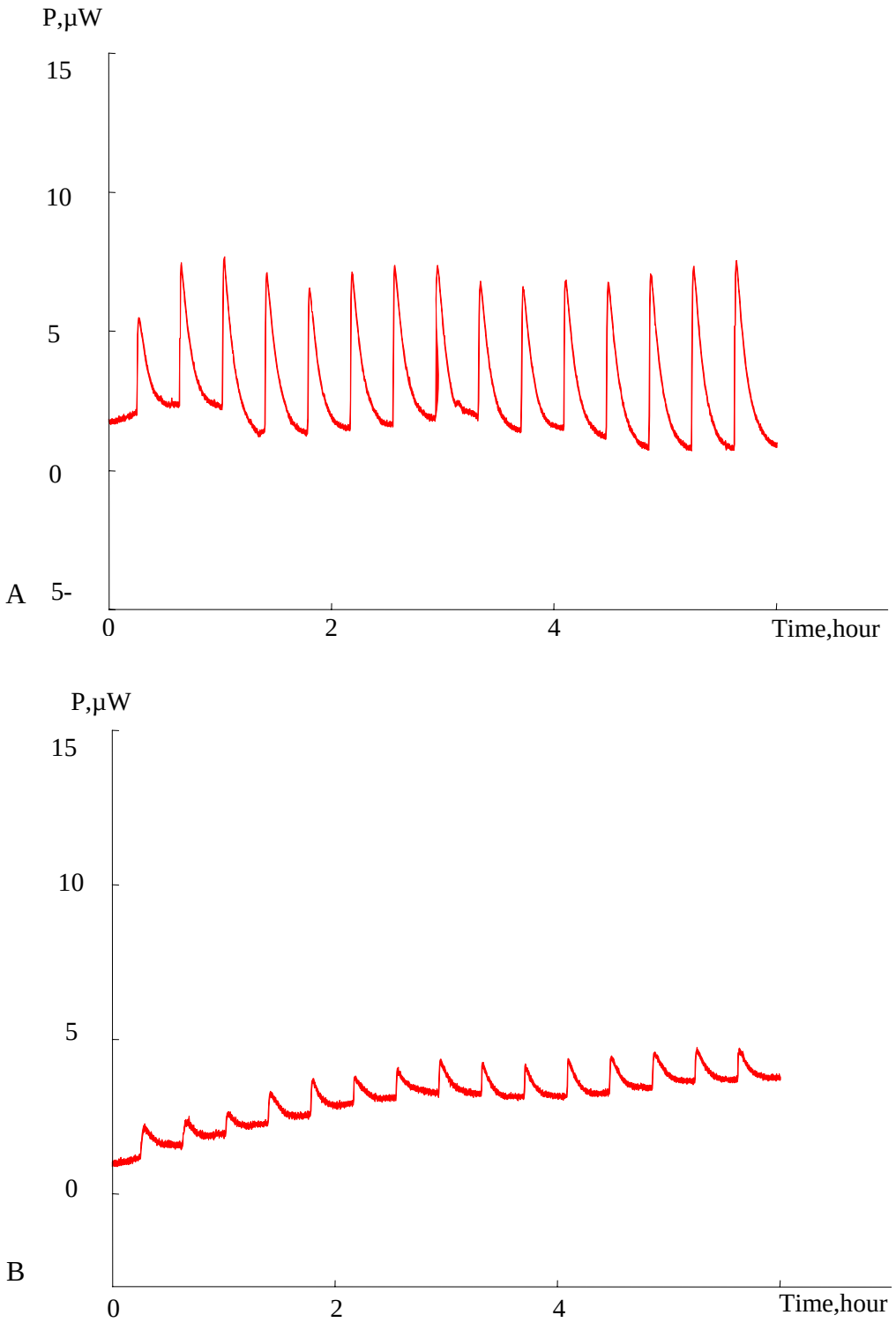

Figure 69. Heat flow versus time profiles for the sequential titrations of tripolyphosphate solution into pH 5 chitosan solution (A) and tripolyphosphate solution into pH 5 dilute acetic acid solution as a blank experiment (B)

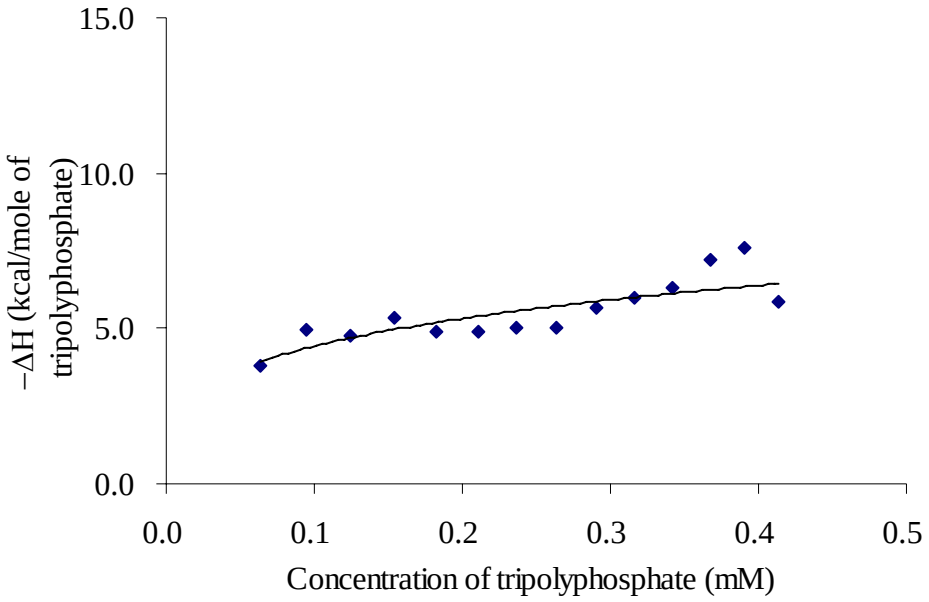

Figure 70. Integrated data obtained from titration of 0.1% w/v tripolyphosphate into 0.2% w/v of pH 5 chitosan solution after substracting the blank experiments

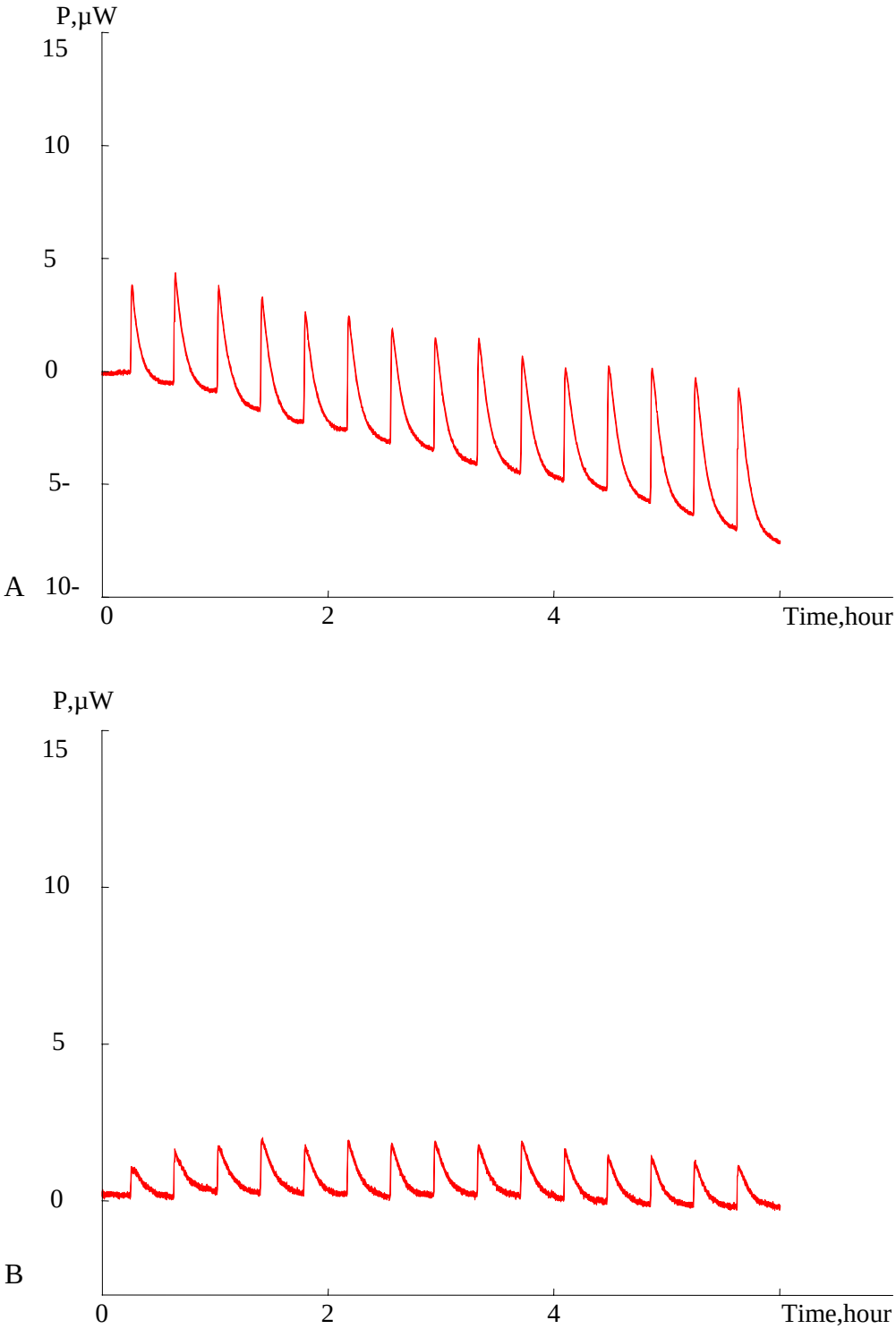

Figure 71. Heat flow versus time profiles for the sequential titrations of tripolyphosphate solution in to pH 3.3 chitosan solution (A) and tripolyphosphate solution in to pH 3.3 dilute acetic acid solution as a blank experiment (B)

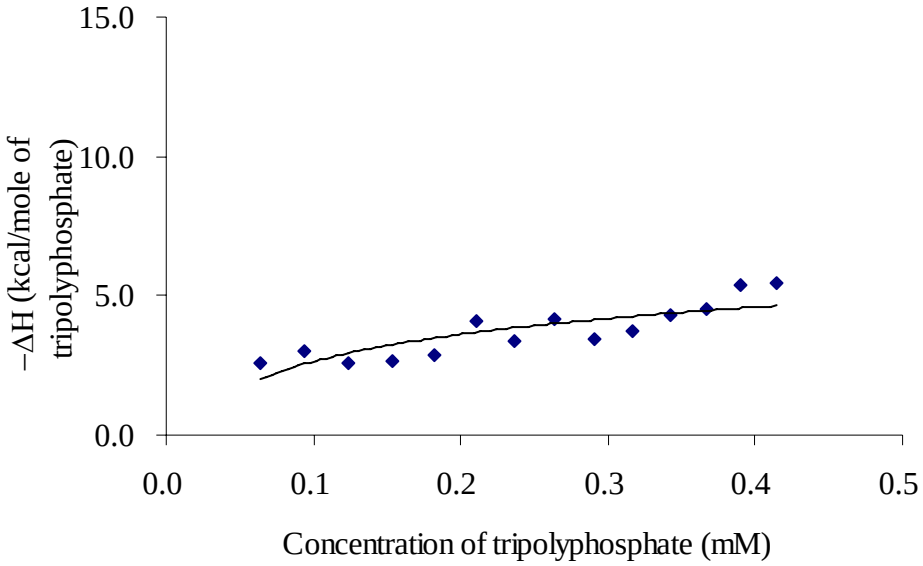

Figure 72. Integrated data obtained from titration of 0.1% w/v tripolyphosphate into 0.2% w/v of pH 3.3 chitosan solution after subtracting the blank experiments

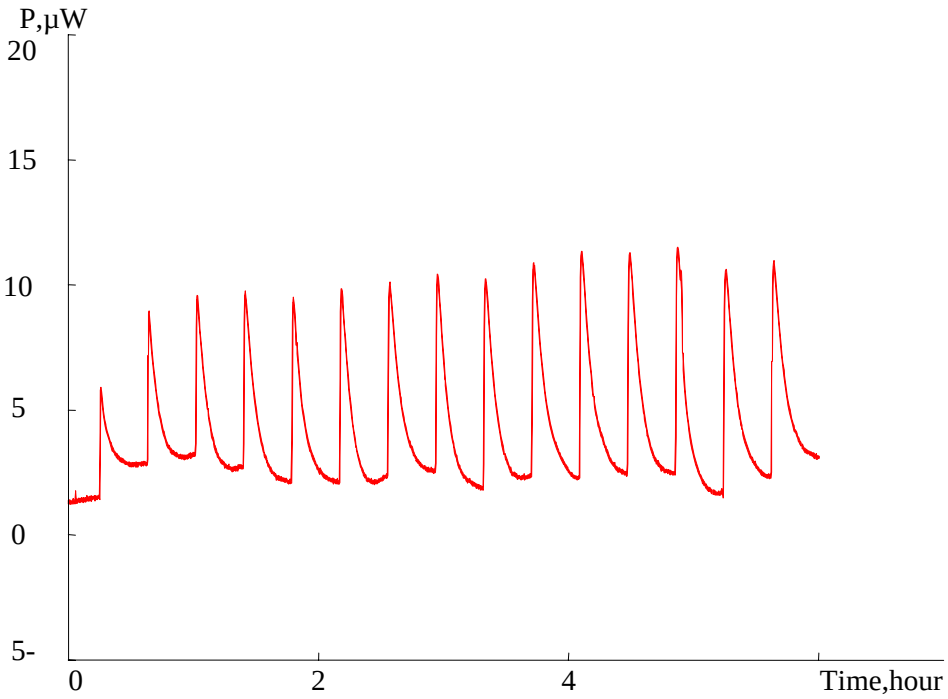

Figure 73. Heat flow versus time profiles for the sequential titrations of tripolyphosphate solution in to insulin-chitosan micropaticles

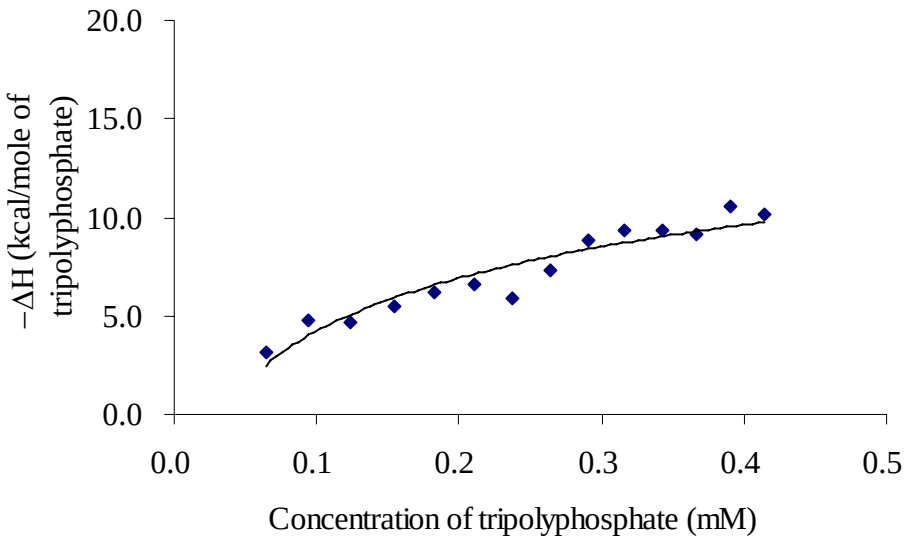

Figure 74. Integrated data obtained from titration of 0.1 % w/v tripolyphosphate into insulin-chitosan microparticles after subtracting the blank experiment

chitosan on the surface of particle could exactly interact to tripolyphosphate and the interaction was detected by ITC.

In the case of the binding of tripolyphosphate to diclofenac-chitosan microparticles (Figures 75-76), almost stable enthalpy changes were obtained with increasing the concentration of tripolyphosphate. It indicates no influence of tripolyphosphate on the diclofenac-chitosan particles, even though there was disagreement with the change in zeta potential and particle charge by addition of tripolyphosphate (Figures 22-23).

For the addition of tripolyphosphate to the mixtures of benzoic acid and chitosan the nanoparticles were formed with the formulation pH about 3.5. The sequential titrations were performed and the blank experiment was the titration of tripolyphosphate solution to dilute pH 3.3 acetic acid solution (Figure 77 and 71B). The interaction enthalpy change (ΔH) was exothermic and quite small (< 2.3 kcal/mole) demonstrating not very strong interaction between tripolyphosphate and chitosan which caused the particle formation (Figure 78). This weak interaction as well as no interaction between benzoic acid and chitosan as illustrated before can be referred to the fast release profiles obtained.

For salicylic acid-chitosan mixture the addition of tripolyphosphate provided the similar exothermic entralpy change (ΔH) as that of salicylic-chitosan mixture (Figure 79 and 80).

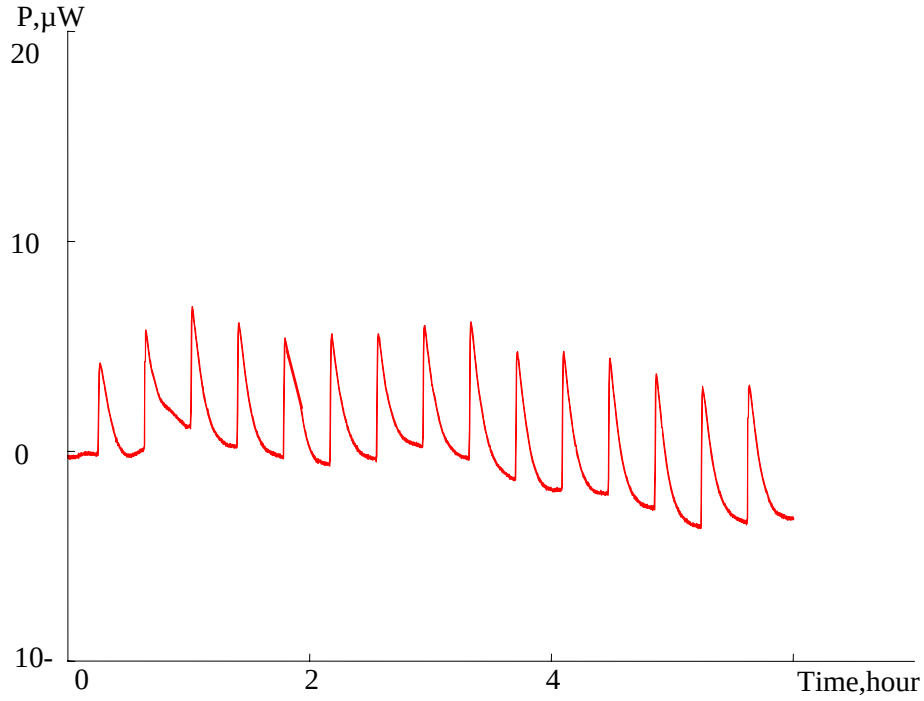

Figure 75. Heat flow versus time profiles for the sequential titrations of tripolyphosphate solution in to diclofenac-chitosan micropaticles

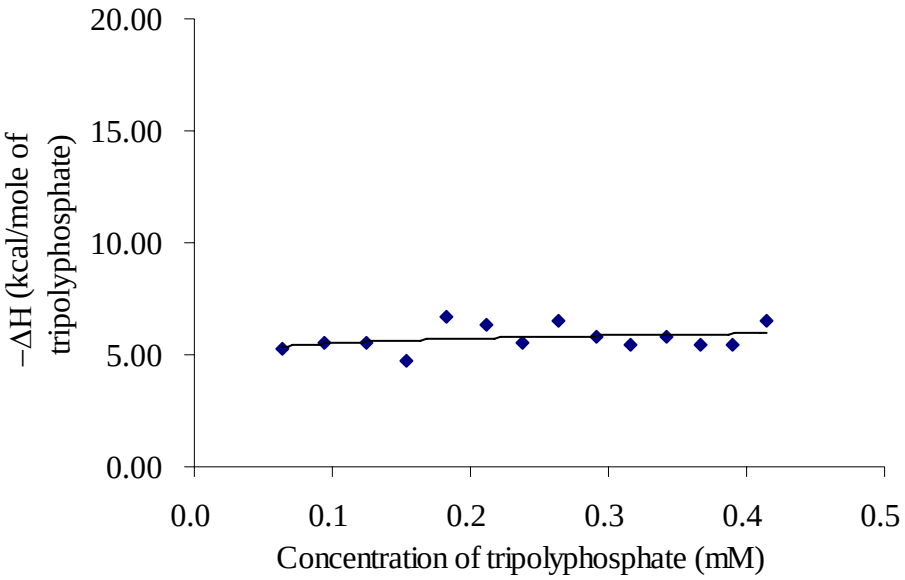

Figure 76. Integrated data obtained from titration of 0.1% w/v tripolyphosphate into diclofenac-chitosan microparticles after subtracting the blank experiment

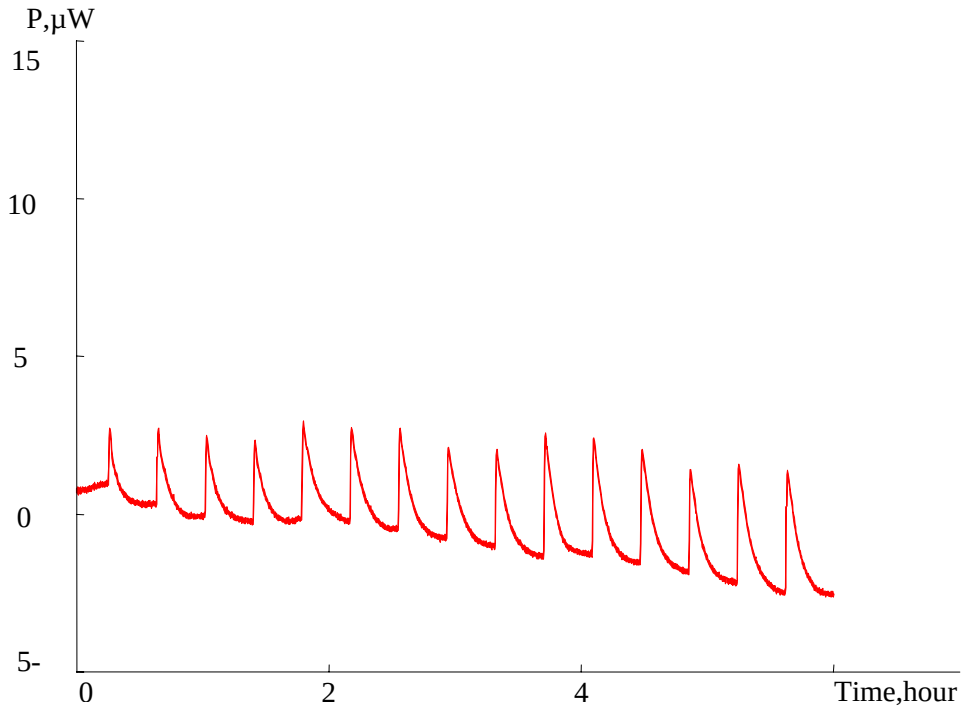

Figure 77. Heat flow versus time profiles for the sequential titrations of tripolyphosphate solution in to benzoic acid-chitosan solution

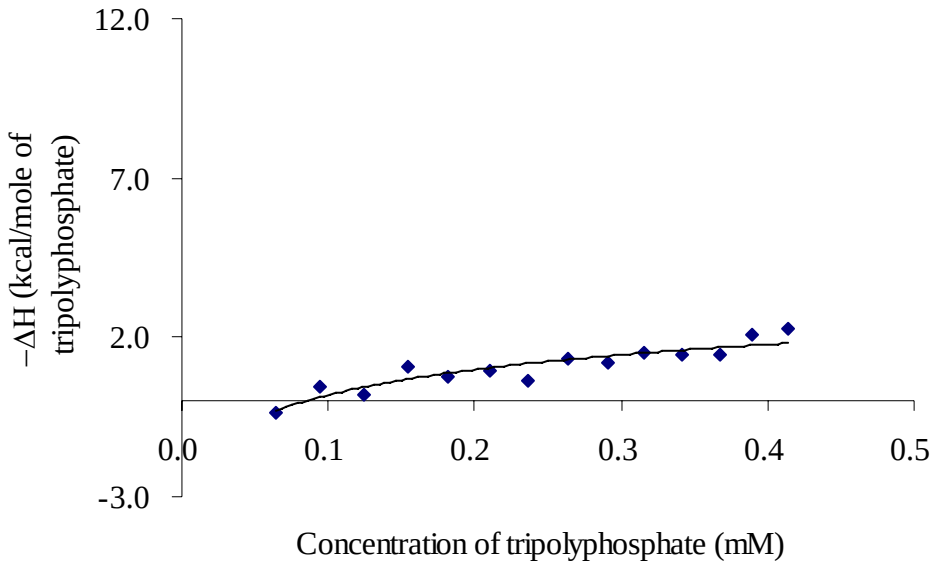

Figure 78. Integrated data obtained from titration of 0.1% w/v tripolyphosphate into benzoic acid-chitosan solution after subtracting the blank experiments

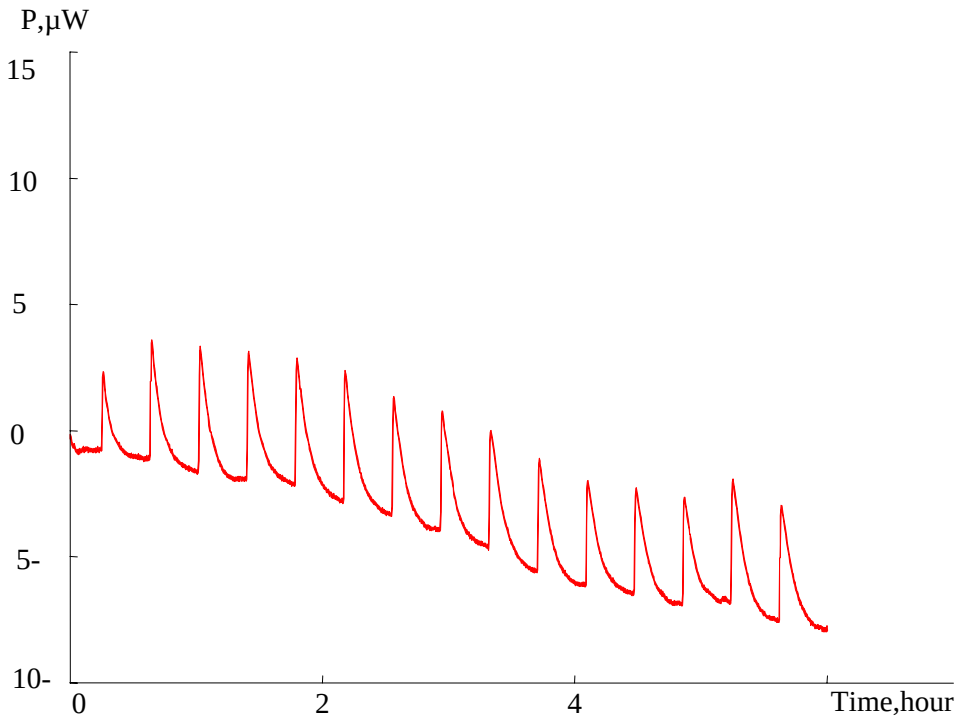

Figure79. Heat flow versus time profiles for the sequential titrations of tripolyphosphate solution in to salicylic acid-chitosan solution

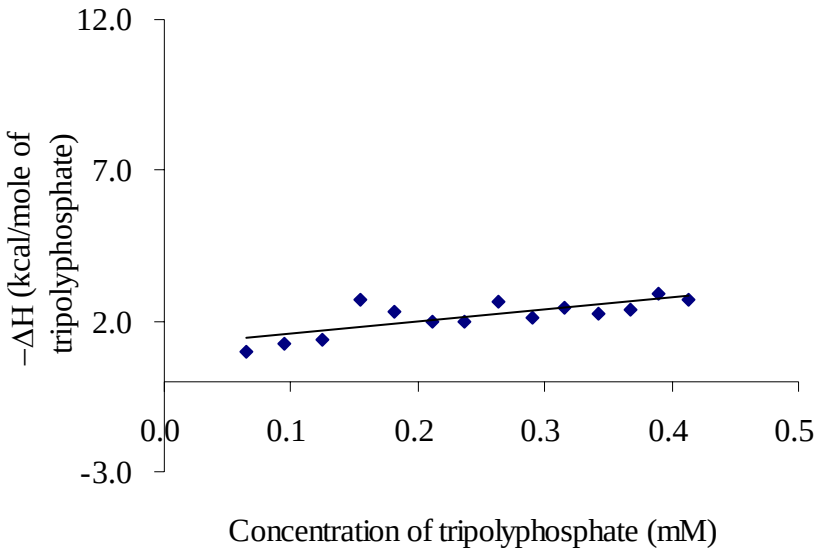

Figure 80. Integrated data obtained from titration of 0.1% w/v tripolyphosphate into salicylic acid-chitosan solution after subtracting the blank experiment

CHAPTER V
CONCLUSION

Chitosan, a natural polymer, has been widely investigated in pharmaceutical field as carrier and drug controlled release polymer. In this study chitosan micro/ nanoparticles based on the interaction between opposite charges of drug and chitosan with out using organic solvents were prepared. Model drugs (human insulin, diclofenac sodium, benzoic acid and salicylic acid) with different pI or pKa were chosen to bind with chitsan. Tripolyphosphate, a cross-linking agent, was incorporated to form particles or to strengthen the particle formation. The role of type and concentration of drugs on physicochemical property and entrapment efficiency of drug-chitosan particles was investigated. *In vitro* release behavior of drug-chitosan particles and binding ability between drugs and chitosan were also studied.

The chitosan particles by ionic interaction show spherical shape and the particle made of large molecule model drug had compacted structure than those of small molecule model drugs. The concentrations of chitosan solution and tripolyphosphate solution affected the size and zeta potential of chitosan particle formed. A 0.1% w/v tripolyphosphate solution and 0.2% w/v chitosan solution were preferred to use in order to get the particle in submicron or early micron range.

Amount of insulin and diclofenac used in formulations showed no correlation with the particle size of drug-chitosan microparticles. But an increase in amount of benzoic acid or salicylic acid related to the decrease in particle size and entrapment efficiency.

The entrapment efficiency influenced the zeta potential and particle charge of drug-chitosan micro/nanoparticles. Nevertheless, no correlation between entrapment efficiency and zeta potential respective particle charge could be found. By changing the formulation pH, the entrapment efficiency of drug-chitosan micro/nanoparticles could be improved. The highest entrapment efficiencies of drugs were achieved at the formulation pH near the pKa of drugs such as pH 5-7 for insulin-chitosan

microparticles, pH 5-6 for diclofenac-chitosan microparticles and pH 3-4 for benzoic acid-chitosan and salicylic acid-chitosan nanoparticles.

By microparticle enzyme immunoassay (MEIA), Human-insulin-chitosan microparticles prepared by high speed stirrer at a speed of 11,000 rpm, at room temperature (25ºC) still maintained the immune activity of human insulin in the particles.

The *in vitro* release behavior of several model drugs from drug-chitosan micro/nanoparticles indicated the fast release profiles. Most of drugs released within 10 minutes from chitosan micro/nanoparticles in pH 7.4 phosphate buffer and purified water at 37ºC. The lower release patterns of insulin and diclofenac in water and in pH 3 HCl solution, respectively were because of their solubility limit. A drug release with strong burst effect especially, in pH 7.4 phosphate buffer referred to the very weak ionic interaction between drug molecules and chitosan molecules.

By ^{1}H-NMR analysis which is limited for the solution samples, the clear mixtures of various concentrations of drugs (benzoic acid and salicylic acid) in several solutions (0.2% chitosan solution, 0.2% ammonium acetate solution and purified water) revealed the similar chemical shift of proton signal indicating the gradually change of ionization of drugs in solutions. It can be concluded that there is no ionic interaction between these two model drugs with chitosan.

By FTIR analysis of insulin-chitosan microparticles (large molecule model drug) and benzoic acid-chitosan nanoparticles (small model drug) no noticeable shift of major bands of chitosan could be seen. However, the wider of carbonyl peaks and amine peaks as well as the change of the three small peaks of chitosan at 1400-1500 cm^{-1} to two small peaks of insulin were found when the concentrations of insulin used to prepare chitosan microparticles were varied from 1 mg/ml to 6 mg/ml. The ionic interaction between insulin and chitosan may be involved in the microparticle formation. But physical entrapment of benzoic acid to chitosan matrix can be implied.

With isothermal titration calorimetric study more information about the interaction between drugs and chitosan was obtained. The weak interaction of insulin and diclofenac to chitosan could be detected. For the titration of insulin to chitosan,

the enthalpy change (ΔH) observed due to the conformation change and especially, adsorption phenomena of insulin on the surfaces of particles. The early investigations of this study e.g. *in vitro* release and FTIR study supported this conclusion. The enthalpy change (ΔH) for the titration of diclofenac sodium to chitosan was caused by the protonation of amine group at the ortho position of diclofenac acid. Benzoic acid and salicylic acid revealed no ionic interaction with chitosan by ITC study. Moreover, all the former investigations (e.g. the physicochemical property measurement, *in vitro* release, ^{1}H-NMR and FTIR analysis) of benzoic acid-chitosan and salicylic acid-chitosan nanoparticles always brought to the same conclusion. Tripolyphosphate showed larger enthalpy change for the binding to pH 5 chitosan than pH 3.3 chitosan.

Conclusively, these results indicate that the binding ability of insulin and diclofenac molecule to chitosan is very weak by ionic interaction and there is no ionic interaction between benzoic acid and salicylic acid to chitosan. However, the high entrapment efficiency of drug-chitosan micro/nanoparticles could be prepared by carefully control formulation pH. Due to physical entrapment of drug to chitosan network, the fast release of drug was observed. Although drug-chitosan micro/ nanoparticles prepared by ionic gelation method in submicron or early micron range present too weak ionic interaction to control drug release, the combination of this system with site specific carriers can improve the absorption of drugs.

REFERENCES

1. Upadrashta SM, Katikaneni PR, Nuessle NO. Chitosan as a tablet binder. Drug Dev Ind Pharm 1992;18:1701-8.
2. Nigalaye AG, Adusumilli P, Bolton S. Investigation of prolonged drug release from matrix formations of chitosan. Drug Dev Ind Pharm 1990;16:449-67.
3. Chandy T, Sharma CP. Chitosan matrix for oral sustained delivery of ampicillin. Biomaterials 1993;14:939-44.
4. Goskonda S, Upadrashta SM. Avicel RC-591/chitosan beads by extrusion spheronization technology. Drug Dev Ind Pharm 1993;19(8):915-27.
5. Mitra S, Gaur U, Ghosh PC, Maitra AN. Tumor targeted delivery of encapsulated dextran-doxorubicin conjugate using chitosan nanoparticles as carrier. J Controlled Release 2001;74:317-23.
6. Tokumitsu H, Ichikawa H, Fukumori Y. Chitosan-godopentetic acid complex nanoparticles for godolinium neutron capture therapy of cancer: preparation by novel emulsion-droplet coalescence technique and characterization. Pharm Res 1999;16:1830-5.
7. Vila A, Sanchez A, Janes K, Behrens I, Kissel T, Vila Jato JL, et al. Low molecular weight chitosan nanoparticles as new carriers for nasal vaccine delivery in mice. Eur J Pharm Biopharm 2004;57:123-31.
8. Leong YS, Candau F. Inverse microemulsion polymerization. J Phys Chem 1982;86(13):2269-71.
9. Thanoo BC, Sunny M, Jayakrishnan A. Cross-linked chitosan microsphere: preparation and evaluation as a matrix for the controlled release pharmaceuticals. J Pharm Pharmacol 1992;44:283-6.
10. Jameela SR, Kumary TV, Lal AV, Jayakrishnan A. Progesterone-loaded chitosan microspheres: a long acting biodegradable controlled delivery system. J Controlled Release 1998;52(1-2):17-24.

11. Ganza-Gonzalez A, Anguiano-Igea S, Otero-Espinar F, Mendez JB. Chitosan and chondroitin microspheres for oral-admisnistration controlled release of metoclopramide. Eur J Pharm Biopharm 1999;48:149-55.
12. Vasiliu S, Popa M, Rinaudo M. Polyelectrolyte capsules made of two biocompatible natural polymers. European Polymer Journal2005;41: 923-32.
13. Polk A, Amsden B, Yao KD, Peng T, A GMF. Controlled release of albumin from chitosan-alginate microcapsules. J Pharm Sci 1994;83:178-85.
14. Bodmeier R, Oh K-H, Pramar Y. Preparation and evaluation of drug-containing chitosan beads. Drug Dev Ind Pharm 1989;15(9):1475-94.
15. Mi FL, Shyu SS, Kuan CY, Lee SL, Lu KT, Jang SF. Chitosan-polyelectrolyte complexation for the preparation of gel beads and controlled release of anticancer drug. II. Effect of pH-dependent ionic crosslinking or interpolymer complex using tripolyphosphate or polyphosphate as reagent. J Appl Polym Sci 1999;74:1093-107.
16. Ma Z, Yeoh HH, Lim LY. Formulation pH modulates the interaction of insulin with chitosan nanoparticles. J Pharm Sci 2002;91(6):1396-404.
17. Calvo P, Remunan-Lopez C, Vila-Jato JL, Alonso MJ. Chitosan and chitosan/ ethylene oxide-propylene oxide block copolymer nanoparticles as novel carriers for proteins and vaccines. Pharm Res 1997;14(10):1431-6.
18. Fernandez-Urrusuno R, Calvo P, Remunan-Lopez C, Vila-Jato JL, Alonso MJ. Enhancement of nasal absorption of insulin using chitosan nanoparticles. Pharm Res 1999;16(10):1576-81.
19. Calvo P, Remunan -Ropez C, Vila-Jato JL, Alonso MJ. Novel hydrophilic chitosan-polyethylene oxide nanoparticles as protein carriers. J Appl Polym Sci 1997;63:125-32.
20. Mi FL, Shyu SS, Kuan CY, Lee SL, Lu KT, Jang SF. Chitosan-polyelectrolyte complexation for the preparation of gel beads and controlled release of anticancer drug. I. Effect of phosphorous polyelectrolyte complex and enzymatic hydrolysis of polymer. J Appl Polym Sci 1999;74:1868-79.

21. Meshali MM, Gahr KE. Effect of interpolymer complex formation of chitosan with pectin or acacia on the release behaviour of chlorpromazine HCl. Int J Pharm 1993;89:177-81.
22. Mueller H, Grelier S, Pardon P, Coma V. Antimicrobial and physicochemical properties of chitosan-HPMC-based films. J Agric Food Chem 2004;52:6585-91.
23. Guzey D, MaClements DJ. Characterzation of β–lactoglobulin-chitosan interaction in aqueous solutions: a calorimetry, light scattering, electrophoretic mobility and solubility study. Food Hydrocolloids 2006;20:124-31.
24. Singla AK, Chawla M. Chitosan : some pharmaceutcal and biological aspects-an update. J Pharm Pharmacol 2001;53:1047-67.
25. Domb AJ, Sashiwa H, Muzzarelli C, Muzzarelli RAA, Kumar RMNV. Chitosan chemistry and pharmaceutical perspectives. Chem Rev 2004;104:6017-84.
26. Illum L. Chitosan and its use as a pharmaceutical excipient. Pharm Res 1998;15 (9):1326-31.
27. Urrusuno RF, Calvo P, Lopez CR, Vila Jato JL, Alonso MJ. Enhancement of nasal absorption of insulin using chitosan nanoparticles. Pharmaceutical research 1999;16(10):1576-81.
28. Kas HS. Chitosan: properties, preparations and application to microparticulate systems. J Microencap 1997;14(6):689-711.
29. Sawayanagi Y, Nambu N, Nagai T. Directly compressed tablets containing chitin or chitosan in addition to lactose or potato starch. Chem Pharm Bull 1982;30:2935-40.
30. Yao T, Yamada A, Yamahara H, Yoshida M. Tableting of coated particles. I. Small particle size chitosan as an agent protecting coating membrane from mechanical damage of compression force. Chem Pharm Bull 1997;45(9):1510-14.

31. Luessen HL, de Leeuw BJ, Langemeyer MW, de Boer AB, Verhoef JC, Junginger HE. Mucoadhesive polymers in peroral peptide drug delivery. VI. Carbomer and chitosan improve the intestinal absorption of the peptide drug buserelin in vivo. Pharm Res 1996;13(11):1668-72.
32. He P, Davis SS, Illum L. In vitro evaluation of mucoadhesive properties of chitosan microsphere. Int J Pharm 1998;166:75-88.
33. Takeuchi H, Yamamoto SS, Illum L. Enteral absorption of insulin in rats from mucoadhesive chitosan-coated liposomes. Pharm Res 1996;13:896-901.
34. Anderberg EK, Nystrom C, Artursson P. Epithelial transport of drugs in cell culture. VII. Effects of pharmaceutical surfactant excipients and bile acids on transepithelial permeability in monalayers of human intesternal epithelial (Caco-2 cells. J Pharm Sci 1992;8(9):879-87.
35. Schipper NGM, Varum KM, Artursson P. Chitosans as absorption enhancers for poorly absorbable drugs. 1: influence of molecular weight and degree of acetylation on drug transport across human intestinal epithelial (Caco-2)cells. Pharm Res 1996;13(11):1686-92.
36. Dodane V, Khan M, Merwin JR. Effect of chitosan on epithelial permeability and structure. Int J Pharm 1999;182:21-32.
37. Gotoh T, Matsushima K, Kikuchi SI. Preparation of alginate-chitosan hybrid gel beads and adsorption of divalent metal ions. Chemosphere 2004;55:135-40.
38. Bernkop-Schnuerch A. Polymer-inhibitor conjugates: a promising strategy to overcome the enzymatic barrier to perorally administered (poly) peptide drugs. STP Pharm Sci 1999;9:78-87.
39. Kojima K, Okamoto Y, Kojima J, Miyatake K, Fujise H, Shigemasa Y, et al. Effects of chitin and chitosan on collagen synthesis in wound healing. Journal of Veternary Medicine Science 2004;66(12):1595-8.
40. Kanauchi O, Deuchi K, Imasato Y, Shizukuishi M, Kobayashi E. Mechanism for the inhibition of fat digestion by chitosan and for the synergistic effect of ascorbate. Biosci Biotech Biochem 1995;59(5):786-90.
41. Gades MD, Stern JS. Chitosan supplementation and fat absorption in men and women. J Am Diet Assoc 2005;105:72-7.

42. Sugano M, Watanabe S, Kishi A, Izume M, Ohtakara A. Hypocholesterolemic action of chitosans with different viscosity in rats. Lipids 1988;23:187-91.
43. Kweon D-K, Song S-B, Park Y-Y. Preparation of water-soluble chitosan/heparin complex and its application as wound healing acceleration. Biomaterials 2003;24:1595-601.
44. Okamoto Y, Shibazaki K, Minami S, Matsuhashi A, Tanioka S, Shigemasa Y. Evaluation of chitin and chitosan in open wound healing in dogs. J Vet Med Sci 1995;57:851-7.
45. Ueno H, Nakamura F, Murakami M, Okumura M, Kadosawa T, Turu F. Evaluation effects of chitosan for the extracellular matrix production by fibroblasts and the growth factors production by macrophages. Biomaterials 2001;22:2125-30.
46. Suzuki Y, Okamoto Y, Morimoto M, Sashiwa H, Saimoto H, Tanioka S-i, et al. Influence of physico-chemical properties of chitin and chitosan on complement activation. Carbohy Polym 2000;42:307-10.
47. Wang X, Du Y, Liu H. Preparation, characterization and antibacterial activity of chitosan-Zn complex. Carbohy Polym 2004;56:21-6.
48. Liu H, Du Y, Wang X, Hu Y, Kennedy JF. Interaction between chitosan and alkyl β-D-glucopyranoside. Carbohy Polym 2004;56:243-50.
49. Qi L, Xu Z, Jiang X, Hu C, Zou X. Preparation and antibacterial activity of chitosan nanoparticles. Carbohy Res 2004;339:2693-700.
50. Zheng LY, Zhu JF. Study on antimicrobial activity of chitosan with different molecular weights. Carbohy Polym 2003;54:527-30.
51. Calsteren VM-R, Begin A. Antimicrobial films produced from chitosan. Int J Bio Macro 1999;26:63-7.
52. Jumaa M, Furkert FH, Mueller BW. A new lipid emulsion formulation with high antimicrobial effacacy using chitosan. European Journal of Pharmaceutical Sciences 2002;53:115-23.
53. Banerjee T, Mitra S, Kumar Singh A, Kumar Sharma R, Maitra A. Preparation, characterization and biodistribution of ultrafine chitosan nanoparticles. Int J Pharm 2002;243(1-2):93-105.

54. Jameela SR, Latha P, Subramoniam A, Jayakrishnan A. Antitumour activity of mitoxantrone-loaded chitosan microspheres against ehrlich ascites carcinoma. J Pharm Pharmacol 1996;48:685-8.
55. Agnihotri SA, Mallikarjuna NN, Aminabhavi TM. Recent advances on chitosan-based micro-and nanoparticles in drug delivery. J Controlled Release 2004;100:5-28.
56. Bayomi M, Al-Suwayeh S, El-Helw A, Mesnad A. Preparation of casein-chitosan microspheres containing diltiazem hydrochloride by an aqueous coacervation technique. Pharma Acta Helv 1998;73:187-92.
57. Grenha A, Seijo B, Remunan-Lopez C. Microencapsulated chitosan nanoparticles for lung protein delivery. Eur J Pharm Sci 2005;25:427-37.
58. Shu XZ, Zhu KJ. A novel approach to prepare tripolyphosphate/chitosan complex beads for controlled release drug delivery. Int J Pharm 2000;201(1):51-8.
59. Ko JA, Park HJ, Hwang SJ, Park JB, Lee JS. Preparation and characterization of chitosan microparticles intended for controlled drug delivery. Int J Pharm 2002;249(1-2):165-74.
60. Xu Y, Du Y. Effect of molecular structure of chitosan on protein delivery properties of chitosan nanoparticles. Int J Pharm 2003;250:215-26.
61. Shiraishi S, Imai T, Otagiri M. Controlled release of indomethacin by chitosan-polyelectrolyte complex: optimization and in vivo/in vitro evaluation. J Controlled Release 1993;25:217-25.
62. Aydin Z, Akbuga J. Chitosan beads for the delivery of salmon calcitonin: preparation and release characteristics. Int J Pharm 1996;131:101-3.
63. Hormones and growth factors used therapeutically. In: Walsh G, editor. Proteins Biochemistry and Biotechnology. West Sussex: John Wiley & Sons, Ltd.; 2002. p. 282-315.
64. Reynolds JEF. Martindale. 29 ed. London: Pharmaceutical press; 1989.
65. Fernando R, Fernando G. (1990). Insulin. In IPCSINTOX betabank; [Online]. Available:http//www.tox.org/databank/documents/pharm/insulin/insulin.htm [2005, September 15].
66. Milthorpe BK, Nichol LW, Jeffrey PD. The polymerization pattern of zinc(II)-insulin at pH 7.0. Biochem Biophys Acta 1977;495(2):195-202.

67. IV IP, Philipson LH, Steiner DF. (2004) Insulin biosynthesis, secretion, structure and structure-activity releationships. In Endotext; [Online]. Available: http//www.endotext.com/diabetes/diabetes3_new/diabetesfram3.htm [2005, May 20].
68. Proteins. In: Stoker HS, editor. General, Organic, and Biological Chemistry. New York: Houghton Mifflin Company; 1998. p. 570-602.
69. Jeffrey PD, Milthorpe BK, Nichol LW. Polymerization pattern of insulin at pH 7.0. Biochemistry 1976;15(21):4660-5.
70. Brange J, Langkjaer L, Havelund S, Volund A. Chemical stability of insulin. 1. Hydrolytic degradation during storage of pharmaceutical preparations. Pharm Res 1992;9(6):715-126.
71. Geiger T, Clarke S. Deamidation, isomerization and recimization at asparaginyl and aspartyl residues in peptides. Succinimide-linked reactions that contribute to protein degradation. J Biol Chem. 1987;262(2):785-94.
72. Pikal MJ, Rigsbee DR. The stability of insulin in crystalline and amorphous solids: observation of greater stability for the amorphous form. Pharm Res 1997;14(10):1379-87.
73. Slobin LI, Carpenter FH. The labile amide in insulin: preparation of desalamine-desamido-insulin. Biochemistry 1963;2(1):22-8.
74. Caliceti P, Veronese FM, Lora S. Polyphosphazene microspheres for insulin delivery. Int J Pharm 2000;211:57-65.
75. Fisher BV, Porter PB. Stability of bovine insulin. J Pharm Pharmacol 1981;33:203-6.
76. Adeyeye MC, Li P-K. Diclofenac sodium. In: Florey K, editor. Analytical Profiles of Drug Substances. California, USA: Academic Press, INC; 1990. p. 123-44.
77. Kai L, Mueller BW. W/O/W multiple emulsions with diclofenac sodium. Eur J Pharm Biopharm 2004;58:621-7.
78. Biju SS, Saisivam S, Maria Gerald Rajan NS, Mishra PR. Dual coated erodible microcapsules for modified release of diclofenac sodium. Eur J Pharm Biopharm 2004;58:61-7.

79. Ughini F, Andreazza IF, Ganter JLMS, Bresolin TMB. Evaluation of xanthan and highly substituted galactomannan from *M. Scabrella* as a sustained release matrix. Int J Pharm 2004;271:197-205.
80. Manning MC, Patel K, Borchardt RT. Stability of protein pharmaceuticals. Pharm Res 1989;6(11):903-17.
81. Gupta KC, Ravi Kumar MNV. Drug release behavior of beads and microgranules of chitosan. Biomaterials 2000;21:1115-9.
82. Benzoic acid. In: Arthur HK, editor. Handbook of Pharmaceutical Excipients. 3ed. Washington: American Pharmaceutical Association and Pharmaceutical Press; 2000. p. 38-40.
83. Indrayanto G, Mugihardjo AS, Soeharjono AR, Tanudjojo W, Susanti S, Yuwono M, et al. Benzoic acid. In: Harry GB, editor. Analytical Profiles of Drug Substances and Excipients. California: Academic Press; 1999. p. 1-46.
84. Byrne RS, Deasy PB. Use of commercial porous ceramic particles for sustained drug delivery. Int J Pharm 2002;246:61-73.
85. Abounassif MA, Mian MS, Mian NAA. Salicylic acid. In: Harry GB, editor. Analytical Profiles of Drug Substances and Excipients. Calofornia: Academic Press; 1994. p. 421-70.
86. O'Neil MJ, Smith A, Heckelman PE, Obenchain JR, Gallipeau JAR, D'Arecca MA. The Merck Index. 13 ed. New Jersey: Merck Research Laboratories; 2001.
87. Frenning G, Fichtner F, Alderborn G. A new method for characterizating the release of drugs from single agglomerates. Chem Eng Sci 2005;60:3909-18.
88. Lara MG, Bentley MVLB, Collett JH. In vitro drug release mechanism and drug loading studies of cubic phase gels. Int J Pharm 2005;293:241-50.
89. Trenktrog T, Mueller BW. Preparation and characterization of a peptide containing w/o emulsion. Int J Pharm 1995;123:199-207.
90. Charistensen JJ, Ruckman J, Eatough DJ, Izatt RM. Determination of equilibrium constants by titration calorimetry. Thermochim Acta 1972;3:203-18.

91. Otagiri M, Saito H, Shiraishi S, Imai T. Interaction of indomethacin with low molecular weight chitosan and improvements of some pharmaceutical properties of indomethacin by low molecular weight chitosans. Int J Pharm 1991;67:11-20.

92. Liu W, Sun S, Cao Z, Zhang X, Yao K, Lu WW, et al. An investigation on the physicochemical properties of chitosan/DNA polyelectrolyte complexes. Biomaterials 2005;26:2705-11.

93. Arof AK, Osman Z. FTIR studies of chitosan acetate based polymer electrolytes. Electrochimica Acta 2003;48:993-9.

94. Salokhe VM, Rakshit SK, Pranoto Y. Enhancing antimicrobial activity of chitosan films by incorporating garlic oil, potassium sorbate and nisin. Lebensm-Wiss und Technol Article in press 2005;38(8):859-65.

95. Mincheva R, Manolova N, Sabov R, Kjurkchiev G, Rashkov l. Hydrogels from chitosan crosslinked with poly(ethyleneglycol) diacid as bone regeneration materials. e-Polymers 2004;058:1-11.

96. Buschmann HJ, Schollmeyer E. A test reaction from macrocyclic chemistry for calorimetric titrations. Thermochim Acta 1999;333:49-53.

97. Buschmann HJ, Schollmeyer E, Mutihac L. The formation of amino acid and dipeptide complexes with α-cyclodextrin and cucurbit[6]uril in aqueous solutions studied by titration calorimetry. Thermochim Acta 2003;399:203-8.

98. Girard M, Turgeon SL, Gauthier SF. Thermodynamic parameter of β–lactoglobulin-pectin complexes assessed by isothermal titration calorimetry. J Agric Food Chem 2003;51:4450-5.

99. Kissel T, Simon M, Wittmar M, Bakowsky U. Self-assembling nanocomplexes from insulin and water-soluble branched polyesters, poly[(vinyl-3-(diethylamino)-propylcarbamate-co-(vinyl acetate)-co-(vinyl alcohol)]-graft-poly(L-lactic acid): a novel carrier for transmucosal delivery of peptides. Bioconjugate Chem 2004;15:841-9.

100. Joshi H, Shirude PS, Bansal V, Ganesh KN, Sastry M. Isothermal titration calorimetry studies on the binding of amino acid to gold nanoparticles. Journal of Physical Chemistry 2004;108:11535-40.

APPENDIX

APPENDIX
EXPERIMENTAL DATA

Effect of various concentrations of chitosan and tripolyphosphate on the particle size and zeta potential of chitosan micro/nanoparticles

Table 19. Influence of tripolyphosphate (TPP) concentration on particle size and zeta potential of insulin-chitosan suspension (the concentration of insulin and chitosan in the suspension was 0.07% and 0.12% w/v, respectively)

TPP (% w/v)	Particle size (μm)[a]	Zeta potential (mV)[a]
0.1	3.3 ± 0.2	30.0 ± 1.0
0.2	5.3 ± 0.4	16.3 ± 0.4
0.4	9.4 ± 0.5	3.7 ± 0.4
0.8	8.5 ± 0.6	-0.2 ± 0.4
1.6	11.5 ± 0.4	-1.4 ± 0.6

[a] mean ± SD (n = 3)

Table 20. Influence of tripolyphosphate (TPP) concentration on particle size and zeta potential of benzoic acid-chitosan suspension (the concentration of benzoic acid and chitosan in the suspension were 0.03% w/v and 0.12% w/v, respectively)

TPP (% w/v)	Particle size (µm)[a]	Zeta potential (mV)[a]
0.1	0.4 ± 0.0	57.0 ± 3.4
0.2	0.2 ± 0.0	51.1 ± 1.0
0.4	1.5 ± 0.2	17.5 ± 1.1
0.8	3.4 ± 0.4	7.5 ± 0.7
1.6	4.5 ± 0.4	5.6 ± 0.3

[a] mean ± SD (n = 3)

Table 21. Influence of chitosan concentration on particle size and zeta potential of insulin-chitosan suspension (the concentration of insulin and tripolyphosphate in the suspension was 0.07% w/v and 0.02% w/v, respectively)

Chitosan solution (% w/v)	Particle size (μm)[a]	Zeta potential (mV)[a]
0.10	7.5 ± 0.3	5.5 ± 0.4
0.2	3.3 ± 0.2	26.5 ± 0.5
0.3	2.3 ± 0.1	40.5 ± 0.5
0.4	5.5 ± 0.6	45.2 ± 0.6
0.5	11.5 ± 0.7	45.3 ± 0.9

[a] mean ± SD (n = 3)

Table 22. Influence of chitosan concentration on particle size and zeta potential of benzoic-chitosan suspension (the concentration of benzoic acid and tripolyphosphate in the suspension was 0.03 % w/v and 0.02% w/v, respectively).

Chitosan solution (% w/v)	Particle size (μm)[a]	Zeta potential (mV)[a]
0.1	10.0 ± 2.4	9.7 ± 1.6
0.2	0.6 ± 0.1	25.3 ± 0.4
0.3	15.0 ± 4.9	44.3 ± 2.0
0.4	15.7 ± 2.7	53.4 ± 0.1
0.5	26.3 ± 1.3	61.9 ± 1.1

[a] mean ± SD (n = 3)

Effect of amount of drugs on physicochemical properties of chitosan micro/ nanoparticles

Table 23. Zeta potential and particle charge of insulin-chitosan microparticles before and after adding tripolyphosphate with increasing insulin concentration

Amount of insulin (mg)	Zeta potential (mV)[a]		Particle charge (coulomb/ml)[a]	
	Before adding TPP	After adding TPP	Before adding TPP	After adding TPP
10	49.8 ± 0.3	42.0 ± 1.4	1.01 ± 0.00	0.44 ± 0.00
20	41.5 ± 2.4	33.2 ± 0.9	0.92 ± 0.01	0.38 ± 0.01
30	39.5 ± 2.2	29.7 ± 0.9	0.81 ± 0.00	0.32 ± 0.00
40	33.4 ± 0.8	27.2 ± 1.1	0.73 ± 0.00	0.23 ± 0.00
50	30.3 ± 1.1	22.3 ± 1.0	0.64 ± 0.00	0.18 ± 0.00
60	26.7 ± 1.8	19.5 ± 1.9	0.55 ± 0.01	0.15 ± 0.00
70	23.9 ± 1.4	17.3 ± 0.1	0.49 ± 0.01	0.14 ± 0.00
80	19.5 ± 1.9	17.0 ± 0.2	0.45 ± 0.00	0.11 ± 0.00
90	18.9 ± 2.4	17.0 ± 0.2	0.40 ± 0.00	0.12 ± 0.01
100	20.7 ± 2.8	16.7 ± 0.2	0.35 ± 0.00	0.11 ± 0.00
110	18.6 ± 2.0	15.5 ± 0.8	0.32 ± 0.00	0.12 ± 0.00
120	21.4 ± 1.2	13.6 ± 0.5	0.30 ± 0.00	0.10 ± 0.00
130	18.9 ± 2.9	12.5 ± 0.7	0.28 ± 0.00	0.10 ± 0.00
140	17.9 ± 1.1	12.5 ± 0.8	0.26 ± 0.00	0.09 ± 0.01

[a] mean ± SD (n = 3)

Table 24. Zeta potential and particle charge of diclofenac-chitosan microparticles before and after adding tripolyphosphate with increasing diclofenac sodium concentration

Amount of diclofenac sodium (mg)	Zeta potential (mV)[a]		Particle charge (coulomb/ml)[a]	
	Before adding TPP	After adding TPP	Before adding TPP	After adding TPP
10	44.2 ± 2.5	38.3 ± 0.8	0.93 ± 0.01	0.42 ± 0.01
20	42.4 ± 0.3	37.5 ± 1.6	0.86 ± 0.00	0.36 ± 0.00
30	40.5 ± 1.4	33.3 ± 1.9	0.77 ± 0.01	0.27 ± 0.00
40	39.2 ± 0.5	35.1 ± 1.6	0.66 ± 0.01	0.22 ± 0.00
50	39.3 ± 1.1	32.4 ± 0.4	0.59 ± 0.00	0.13 ± 0.00
60	40.3 ± 0.5	31.4 ± 0.4	0.51 ± 0.00	0.10 ± 0.00
70	39.1 ± 1.4	30.3 ± 1.0	0.45 ± 0.00	0.06 ± 0.00
80	39.9 ± 1.1	28.8 ± 0.6	0.43 ± 0.01	0.04 ± 0.00
90	39.0 ± 0.8	25.4 ± 1.1	0.40 ± 0.00	0.03 ± 0.00
100	38.2 ± 0.9	24.5 ± 2.8	0.26 ± 0.00	0.01 ± 0.00
110	37.4 ± 0.3	22.4 ± 1.8	0.15 ± 0.00	0.00 ± 0.00
120	44.2 ± 2.5	38.3 ± 0.8	0.93 ± 0.01	0.42 ± 0.01
130	42.4 ± 0.3	37.5 ± 1.6	0.86 ± 0.00	0.36 ± 0.00
140	40.5 ± 1.4	33.3 ± 1.9	0.77 ± 0.01	0.27 ± 0.00

[a] mean ± SD (n = 3)

Table 25. Zeta potential and particle charge of benzoic acid-chitosan microparticles made of pH 5 chitosan solution after adding tripolyphosphate with increasing benzoic acid concentration

Amount of benzoic acid (mg)	Zeta potential (mV)[a]	Particle charge (coulomb/ml) [a]
	After adding TPP	After adding TPP
4	50.7 ± 2.4	0.47 ± 0.00
8	47.0 ± 3.6	0.45 ± 0.00
12	49.6 ± 2.7	0.45 ± 0.00
16	45.2 ± 1.5	0.42 ± 0.00
20	48.4 ± 1.2	0.41 ± 0.00
24	43.3 ± 1.1	0.39 ± 0.00

[a] mean ± SD (n = 3)

Table 26. Zeta potential and particle charge of salicylic acid-chitosan nanoparticles made of pH 5 chitosan solutions after adding tripolyphosphate with increasing salicylic acid concentration

Amount of salicylic acid (mg)	Zeta potential (mV)[a]	Particle charge (coulomb/ml)[a]
	After adding TPP	After adding TPP
6	51.9 ± 3.2	0.47 ± 0.00
12	49.6 ± 0.3	0.45 ± 0.00
18	49.6 ± 2.0	0.43 ± 0.00
24	50.8 ± 1.5	0.42 ± 0.00
30	49.6 ± 1.2	0.40 ± 0.00
36	49.5 ± 0.9	0.37 ± 0.00

[a] mean ± SD (n = 3)

Table 27. Zeta potential and particle charge of benzoic acid-chitosan nanoparticles made of pH 3.3 chitosan solutions after adding tripolyphosphate with increasing benzoic acid concentration

Amount of benzoic acid (mg)	Zeta potential (mV)[a]	Particle charge (coulomb/ml) [a]
	After adding TPP	After adding TPP
4	56.0 ± 0,7	0.61 ± 0.01
8	56.4 ± 1.8	0.57 ± 0.00
12	56.1 ± 0.1	0.55 ± 0.00
16	55.8 ± 0.5	0.54 ± 0.00
20	56.1 ± 1.4	0.52 ± 0.00
24	55.4 ± 0.2	0.50 ± 0.00

[a] mean ± SD (n = 3)

Table 28. Zeta potential and particle charge of salicylic acid-chitosan nanoparticles made of pH 3.3 chitosan solutions after adding tripolyphosphate with increasing salicylic acid concentration

Amount of salicylic acid (mg)	Zeta potential (mV)[a]	Particle charge (coulomb/ml) [a]
	After adding TPP	After adding TPP
4	57.0 ± 0.9	0.63 ± 0.01
8	55.5 ± 1.2	0.58 ± 0.00
12	55.7 ± 1,3	0.56 ± 0.00
16	56.1 ± 1.1	0.54 ± 0.00
20	55.9 ± 0.7	0.52 ± 0.00
24	57.6 ± 1.5	0.50 ± 0.00

[a] mean ± SD (n = 3)

Table 29. Zeta potential and particle charge of insulin-chitosan nanoparticles made of pH 3.3 chitosan solutions after adding tripolyphosphate with increasing insulin concentration

Amount of insulin (mg)	Zeta potential (mV)[a]	Particle charge (coulomb/ml) [a]
	After adding TPP	After adding TPP
10	55.4 ± 0.8	0.62 ± 0.00
20	52.1 ± 1.8	0.61 ± 0.00
30	50.2 ± 1.6	0.61 ± 0.00
40	49.7 ± 2.6	0.59 ± 0.00
50	46.8 ± 2.7	0.59 ± 0.00
60	48.1 ± 0.6	0.59 ± 0.00

[a] mean ± SD (n = 3)

In vitro release studies

Table 30. Release data of insulin from unwashed insulin-chitosan microparticles in different media

Time (min)	% Release[a]		
	Release media		
	Purified water	pH7.4 PBS	pH 3 HCl
0	3.79 ± 0.05	3.79 ± 0.05	3.79 ± 0.05
10	44.52 ± 2.45	97.37 ± 0.64	95.79 ± 0.21
30	48.72 ± 2.19	97.37 ± 0.00	95.79 ± 0.00
60	53.27 ± 1.48	97.37 ± 0.00	95.79 ± 0.00
120	62.11 ± 1.4	97.37 ± 0.00	95.79 ± 0.00
180	66.27 ± 0.76	97.37 ± 0.00	95.79 ± 0.00
240	69.00 ± 0.91	97.37 ± 0.00	95.79 ± 0.00

[a] mean ± SD (n = 3)

Table 31. Release data of insulin from washed insulin-chitosan microparticles in different media

Time (min)	% Release[a]		
	Release media		
	Purified water	pH7.4 PBS	pH 3 HCl
0	1.02 ± 0.05	1.02 ± 0.25	1.02 ± 0.25
10	61.57 ± 2.11	97.32 ± 2.71	99.25 ±2.34
30	64.13 ± 1.18	97.32 ± 0.00	99.25 ± 0.00
60	70.30 ± 1.44	97.32 ± 0.00	99.25 ± 0.00
120	72.68 ± 1.49	97.32 ± 0.00	99.25 ± 0.00
180	74.25 ± 0.99	97.32 ± 0.00	99.25 ± 0.00
240	74.25 ± 0.00	97.32 ± 0.00	99.25 ± 0.00

[a] mean ± SD (n = 3)

Table 32. Release data of diclofenac from unwashed diclofenac-chitosan microparticles in different media

Time (min)	% Release[a]		
	Release media		
	Purified water	pH7.4 PBS	pH 3 HCl
0	3.15 ± 0.00	3.15 ± 0.00	3.15 ± 0.00
10	93.79 ± 0.60	97.76 ± 1.25	11.35 ± 0.24
30	93.79 ± 0.00	97.76 ± 0.00	14.06 ± 0.51
60	95.37 ± 0.82	97.76 ± 0.00	18.22 ± 0.71
120	95.37 ± 0.00	97.76 ± 0.00	21.63 ± 0.30
180	95.37 ± 0.00	97.76 ± 0.00	24.94 ± 0.34
240	95.37 ± 0.00	97.76 ± 0.00	28.03 ± 0.38

[a] mean ± SD (n = 3)

Table 33. Release data of diclofenac from washed diclofenac-chitosan microparticles in different media

Time (min)	% Release[a]		
	Release media		
	Purified water	pH7.4 PBS	pH 3 HCl
0	0.00	0.00	0.00
10	96.04 ± 0.67	97.63 ± 1.05	67.55 ± 0.81
30	96.04 ± 0.00	98.68 ± 0.95	67.55 ± 0.00
60	96.04 ± 0.00	98.68 ± 0.00	67.55 ± 0.00
120	96.04 ± 0.00	98.68 ± 0.00	67.55 ± 0.00
180	96.04 ± 0.00	98.68 ± 0.00	67.55 ± 0.00
240	96.04 ± 0.00	98.68 ± 0.00	67.55 ± 0.00

[a] mean ± SD (n = 3)

Table 34. Release data of benzoic acid from unwashed benzoic acid-chitosan nanoparticles in different media

Time (min)	% Release[a]		
	Release media		
	Purified water	pH7.4 PBS	pH 3 HCl
0	25.43 ± 0.24	25.43 ± 0.24	25.43 ± 0.24
10	103.36 ± 0.65	98.80 ± 3.87	101.38 ± 3.57
30	103.36 ± 0.00	98.80 ± 0.00	101.38 ± 0.00
60	103.36 ± 0.00	98.80 ± 0.00	101.38 ± 0.00
120	103.36 ± 0.00	98.80 ± 0.00	101.38 ± 0.00
180	103.36 ± 0.00	98.80 ± 0.00	101.38 ± 0.00
240	103.36 ± 0.00	98.80 ± 0.00	101.38 ± 0.00

[a] mean ± SD (n = 3)

Table 35. Release data of benzoic acid from washed benzoic acid-chitosan nanoparticles in different media

Time (min)	% Release[a]		
	Release media		
	Purified water	pH 7.4 PBS	pH 3 HCl
0	14.73 ± 0.95	14.73 ± 0.95	14.73 ± 0.95
10	87.07 ± 1.80	102.95 ± 0.95	84.94 ± 0.95
30	87.07 ± 0.00	102.95 ± 0.00	84.94 ± 0.00
60	87.07 ± 0.00	102.95 ± 0.00	84.94 ± 0.00
120	87.07 ± 0.00	102.95 ± 0.00	84.94 ± 0.00
180	87.07 ± 0.00	102.95 ± 0.00	84.94 ± 0.00
240	87.07 ± 0.00	102.95 ± 0.00	84.94 ± 0.00

[a] mean ± SD (n = 3)

Table 36. Release data of salicylic acid from unwashed salicylic acid-chitosan nanoparticles in different media

Time (min)	% Release[a]		
	Release media		
	Purified water	pH 7.4 PBS	pH 3 HCl
0	32.83 ± 0.00	32.83 ± 0.00	32.83 ± 0.00
10	99.93 ± 0.90	100.00 ± 1.52	99.49 ± 1.41
30	99.93 ± 0.00	100.00 ± 0.00	99.49 ± 0.00
60	99.93 ± 0.00	100.00 ± 0.00	99.49 ± 0.00
120	99.93 ± 0.00	100.00 ± 0.00	99.49 ± 0.00
180	99.93 ± 0.00	100.00 ± 0.00	99.49 ± 0.00
240	99.93 ± 0.00	100.00 ± 0.00	99.49 ± 0.00

[a] mean ± SD (n = 3)

Table 37. Release data of salicylic acid from washed salicylic acid-chitosan nanoparticles in different media

Time (min)	% Release[a]		
	Release media		
	Purified water	pH 7.4 PBS	pH 3 HCl
0	25.26 ± 0.00	25.26 ± 0.00	25.26 ± 0.00
10	98.36 ± 3.19	96.30 ± 2.94	99.59 ± 4.86
30	98.36 ± 0.00	96.30 ± 0.00	99.59 ± 0.00
60	98.36 ± 0.00	96.30 ± 0.00	99.59 ± 0.00
120	98.36 ± 0.00	96.30 ± 0.00	99.59 ± 0.00
180	98.36 ± 0.00	96.30 ± 0.00	99.59 ± 0.00
240	98.36 ± 0.00	96.30 ± 0.00	99.59 ± 0.00

[a] mean ± SD (n = 3)

^{1}H-NMR spectroscopy

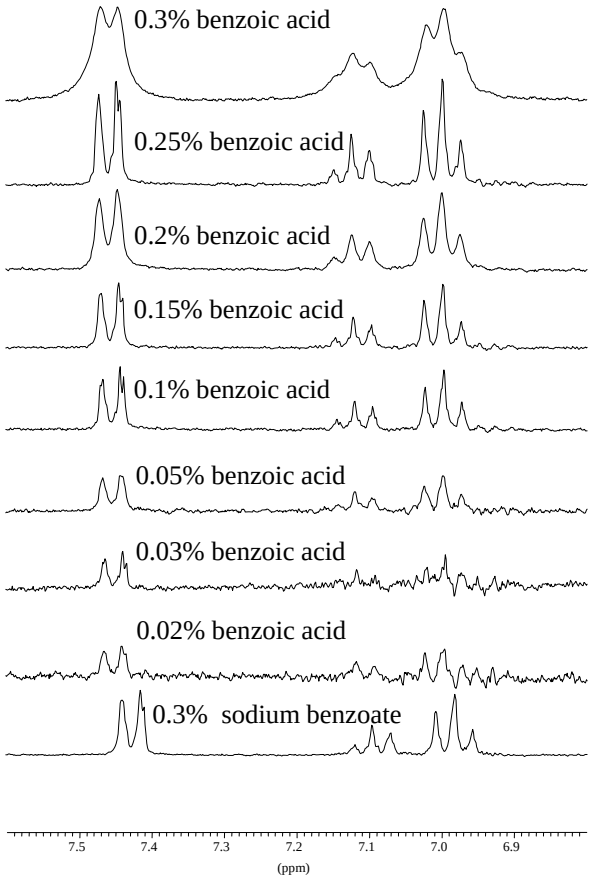

Figure 81. ^{1}H-NMR spectra of benzoic acid (0.3%-0.02%) and sodium benzoate (0.3%) in 0.2% ammonium acetate solution

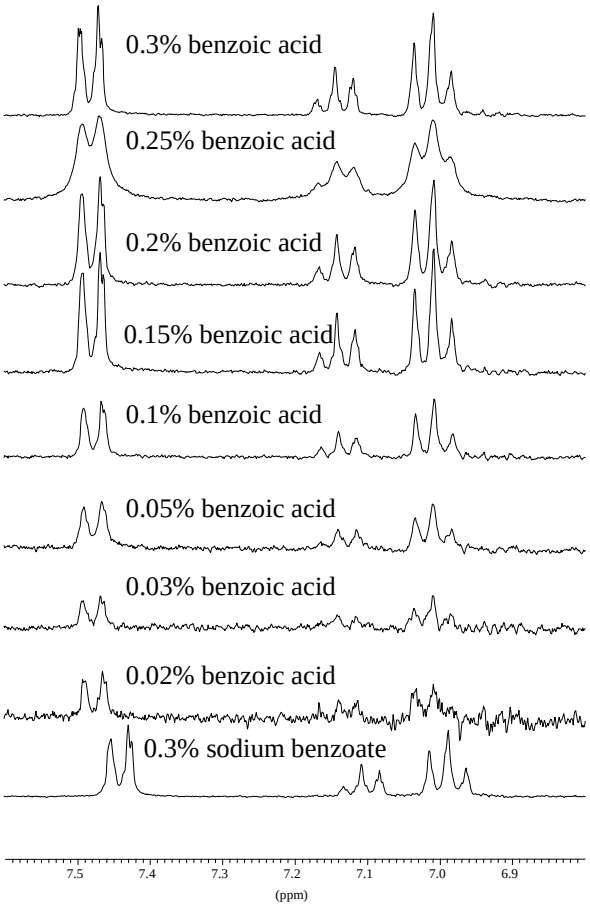

Figure 82. ^{1}H-NMR spectra of benzoic acid (0.3%-0.02%) and sodium benzoate (0.3%) in 0.2% chitosan solution

Table 38. Chemical shift data of ortho-proton signal of various concentration of benzoic acid in different media

Salicylic acid concentration (%w/v)	Chemical shift (ppm)		
	Purified water	Chitosan (0.2% w/v)	Amonium acetate (0.2%w/v)
0.03	7.49553	7.49261	7.46464
0.05	7.50022	7.49142	7.46800
0.1	7.50381	7.49202	7.46764
0.15	7.50393	7.49308	7.47058
0.2	7.50632	7.49386	7.47268
0.25	7.50643	7.49361	7.47354
0.3	7.50559	7.49665	7.47114

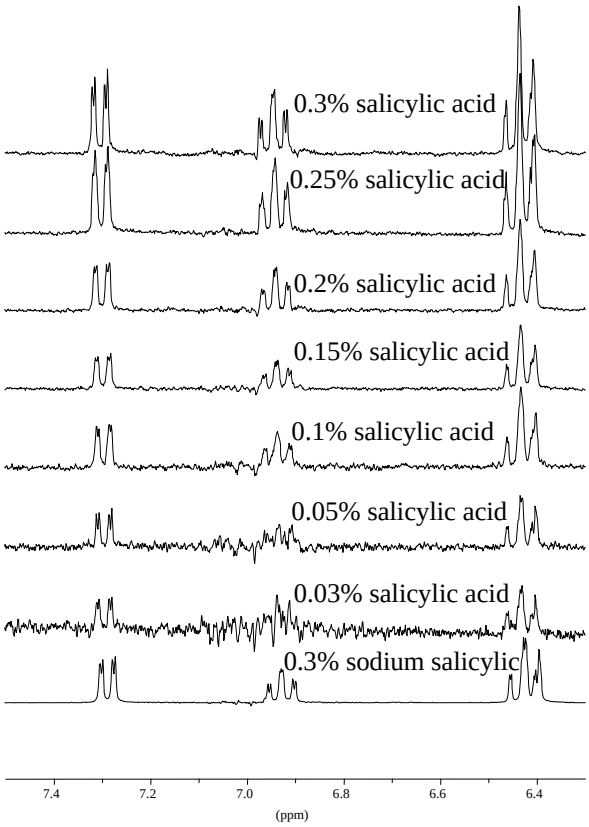

Figure 83. ^{1}H-NMR spectra of salicylic acid (0.3%-0.03%) and sodium salicylate (0.3%) in 0.2% ammonium acetate solution

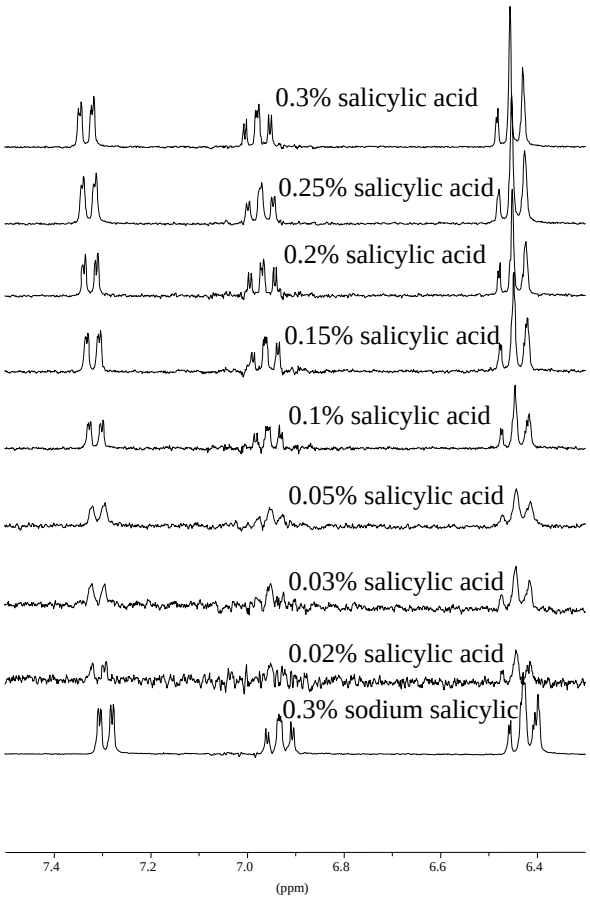

Figure 84. ^{1}H-NMR spectra of salicylic acid (0.3%-0.02%) and sodium salicylate (0.3%) in 0.2% chitosan solution

Table 39. Chemical shift data of ortho-proton signal of various concentration of salicylic acid in different media

Salicylic acid concentration (%w/v)	Chemical shift (ppm)		
	Purified water	Chitosan (0.2% w/v)	Amonium acetate (0.2%w/v)
0.03	7.35064	7.32137	7.30673
0.05	7.36047	7.32020	7.30643
0.1	7.36965	7.32404	7.30679
0.15	7.37245	7.32964	7.30891
0.2	7.37096	7.33502	7.31114
0.25	7.37125	7.33842	7.31456
0.3	7.36812	7.34376	7.31530

Isothermal titration Calorimetry

Table 40. The data for the sequential titrations of insulin solution into chitosan solution and the titration of PBS into chitosan solution (blank experiment)

Injections[a]	Concentration[b] of insulin in cell (µM)	Heat flow for the titration of insulin to chitosan (µW)	Heat flow for the tiration of PBS to chitosan (µW)	−ΔH/mole of insulin injected (kcal/mole)
1	10.210	4.439	2.802	15.147
2	20.180	4.702	3.659	9.628
3	29.920	4.786	2.785	18.485
4	39.437	4.691	3.026	15.369
5	48.738	4.674	2.363	33.266
6	57.830	5.850	2.246	21.360
7	66.722	9.350	1.757	70.071
8	75.419	12.778	1.364	105.333
9	83.927	14.441	0.963	124.388
10	92.253	18.690	0.467	168.183
11	100.403	22.564	0.135	206.983
12	108.381	25.645	-0.137	237.923
13	116.194	33.982	-0.817	321.142
14	123.847	41.563	-1.139	394.047
15	131.344	42.646	-2.161	413.500

[a] n = 2

[b] 30 µl of 5 mg/ml insulin solution was injected sequentially.

Table 41. The data for the sequential titrations of diclofenac sodium solution into chitosan solution and into dilute acetic acid solution (blank experiment)

Injections[a]	Concentration[b] of diclofenac sodium in cell (mM)	Heat flow for the titration of diclofenac sodium to chitosan (µW)	Heat flow for the tiration of diclofenac sodium to dilute acetic acid (µW)	−ΔH/mole of diclofenac sodium injected (kcal/mole)
1	0.186	1.962	12.654	-5.38
2	0.368	3.250	19.828	-8.37
3	0.546	5.298	19.795	-7.32
4	0.720	6.137	19.422	-6.71
5	0.890	6.814	19.080	-6.19
6	1.056	6.239	18.785	-6.34
7	1.218	6.744	19.303	-6.34
8	1.377	6.891	18.890	-6.06
9	1.532	11.706	18.893	-3.63
10	1.684	16.240	19.543	-1.67
11	1.833	22.516	19.790	1.38
12	1.978	24.809	19.820	2.53
13	2.121	26.866	19.978	3.48
14	2.261	29.231	19.958	4.70
15	2.397	28.666	19.812	4.47

[a] n = 2

[b] 30 µl of 5 mg/ml diclofenac sodium solution was injected sequentially.

Table 42. The data for the sequential titrations of benzoic acid solution into chitosan solution and the titration of benzoic acid into dilute acetic acid solution (blank experiment)

Injections[a]	Concentration[b] of benzoic acid in cell (mM)	Heat flow for the titration of benzoic acid to chitosan (μW)	Heat flow for the tiration of benzoic acid to dilute acetic acid (μW)	–ΔH/mole of benzoic acid injected (kcal/mole)
1	0.189	1.088	0.798	0.143
2	0.375	1.510	1.041	0.232
3	0.556	1.320	1.020	0.149
4	0.732	1.247	1.184	0.032
5	0.906	1.275	1.187	0.043
6	1.075	1.203	0.990	0.106
7	1.239	1.262	1.126	0.067
8	1.401	1.268	1.409	-0.070
9	1.559	1.394	1.204	0.094
10	1.714	1.204	1.240	-0.018
11	1.865	1.308	1.215	0.046
12	2.013	1.309	1.244	0.032
13	2.159	1.246	1.346	-0.050
14	2.301	1.127	1.414	-0.142
15	2.441	1.192	1.294	-0.051

[a] n = 2

[b]30 μl of 1.96 mg/ml benzoic acid solution was injected sequentially.

Table 43. The data for the sequential titrations of salicylic acid solution into chitosan solution and the titration of salicylic acid into pH 5 dilute acetic acid solution (blank experiment)

Injections[a]	Concentration[b] of salicylic acid in cell (mM)	Heat flow for the titration of salicylic acid to chitosan (µW)	Heat flow for the tiration of salicylic acid to dilute acetic acid (µW)	–ΔH/mole of salicylic acid injected (kcal/mole)
1	0.129	0.416	0.387	-0.141
2	0.255	0.870	0.528	-0.280
3	0.377	0.900	0.479	-0.195
4	0.497	1.014	0.548	-0.412
5	0.615	1.347	0.424	-0.269
6	0.729	1.318	0.520	-0.153
7	0.842	1.160	0.491	-0.160
8	0.951	1.247	0.566	-0.095
9	1.059	1.429	0.518	-0.288
10	1.164	1.308	0.589	-0.006
11	1.266	1.259	0.416	-0.011
12	1.367	1.295	0.533	-0.296
13	1.466	1.303	0.491	-0.015
14	1.562	1.465	0.474	-0.021
15	1.657	1.391	0.460	-0.180

[a] n = 2

[b]30 µl of 1.50 mg/ml salicylic acid solution was injected sequentially.

Table 44. The data for the sequential titrations of tripolyphosphate (TPP) solution into pH 3.3 chitosan solution and the titration of tripolyphosphate into pH 3.3 dilute acetic acid solution (blank experiment)

Injections[a]	Concentration[b] of TPP in cell (mM)	Heat flow for the titration of TPP to chitosan (μW)	Heat flow for the tiration of TPP to dilute acetic acid (μW)	–ΔH/mole of TPP injected (kcal/mole)
1	0.032	0.678	0.387	0.849
2	0.064	1.404	0.528	2.557
3	0.094	1.510	0.479	3.012
4	0.124	1.444	0.548	2.616
5	0.154	1.330	0.424	2.660
6	0.182	1.511	0.520	2.895
7	0.211	1.894	0.491	4.098
8	0.237	1.701	0.535	3.404
9	0.264	1.953	0.518	4.191
10	0.291	1.764	0.589	3.430
11	0.316	1.699	0.416	3.749
12	0.342	2.001	0.533	4.285
13	0.367	2.038	0.491	4.517
14	0.390	2.311	0.474	5.364
15	0.414	2.312	0.460	5.425

[a] n = 2

[b]30 μl of 0.1 mg/ml tripolyphosphate solution was injected sequentially.

Table 45. The data for the sequential titrations of tripolyphosphate (TPP) solution into insulin-chitosan microparticles and the titration of tripolyphosphate into pH 5 dilute acetic acid solution (blank experiment)

Injections[a]	Concentration[b] of TPP in cell (mM)	Heat flow for the titration of TPP to insulin-chitosan particles (µW)	Heat flow for the tiration of TPP to dilute acetic acid (µW)	–ΔH/mole of TPP injected (kcal/mole)
1	0.032	1.531	0.425	3.231
2	0.064	1.464	0.390	3.138
3	0.094	2.004	0.357	4.811
4	0.124	2.002	0.413	4.642
5	0.154	2.216	0.344	5.468
6	0.182	2.374	0.323	6.182
7	0.211	2.610	0.360	6.574
8	0.237	2.346	0.335	5.879
9	0.264	2.809	0.325	7.265
10	0.291	3.370	0.332	8.875
11	0.316	3.520	0.319	9.352
12	0.342	3.583	0.382	9.351
13	0.367	3.510	0.366	9.182
14	0.390	3.951	0.337	10.558
15	0.414	3.821	0.353	10.131

[a] n = 2

[b]30 µl of 0.1 mg/ml tripolyphosphate solution was injected sequentially.

Table 46. The data for the sequential titrations of tripolyphosphate (TPP) solution into diclofenac-chitosan microparticles and the titration of tripolyphosphate into pH 5 dilute acetic acid solution (blank experiment)

Injections[a]	Concentration[b] of TPP in cell (mM)	Heat flow for the titration of TPP to insulin-chitosan particles (µW)	Heat flow for the tiration of TPP to dilute acetic acid (µW)	–ΔH/mole of TPP injected (kcal/mole)
1	0.032	1.904	0.425	4.325
2	0.064	2.185	0.390	5.248
3	0.094	2.259	0.357	5.558
4	0.124	2.300	0.413	5.516
5	0.154	1.952	0.344	4.699
6	0.182	2.628	0.323	6.735
7	0.211	2.513	0.360	6.298
8	0.237	2.216	0.335	5.495
9	0.264	2.566	0.325	6.552
10	0.291	2.324	0.332	5.819
11	0.316	2.180	0.319	5.438
12	0.342	2.253	0.382	5.819
13	0.367	2.588	0.366	5.438
14	0.390	2.961	0.337	5.467
15	0.414	2.816	0.353	6.495

[a] n = 2

[b]30 µl of 0.1 mg/ml tripolyphosphate solution was injected sequentially.

Table 47. The data for the sequential titrations of tripolyphosphate (TPP) solution into benzoic acid-chitosan microparticles and the titration of tripolyphosphate into pH 3.3 dilute acetic acid solution (blank experiment)

Injections[a]	Concentration[b] of TPP in cell (mM)	Heat flow for the titration of TPP to benzoic acid-chitosan particles (µW)	Heat flow for the tiration of TPP to dilute acetic acid (µW)	–ΔH/mole of TPP injected (kcal/mole)
1	0.032	-0.107	0.387	-1.777
2	0.064	0.408	0.528	-0.349
3	0.094	0.642	0.479	0.477
4	0.124	0.626	0.548	0.230
5	0.154	0.781	0.424	1.049
6	0.182	0.787	0.520	0.782
7	0.211	0.809	0.491	0.930
8	0.237	0.794	0.566	0.669
9	0.264	0.975	0.518	1.338
10	0.291	0.996	0.589	1.190
11	0.316	0.933	0.416	1.511
12	0.342	1.038	0.533	1.476
13	0.367	0.995	0.491	1.473
14	0.390	1.195	0.474	2.107
15	0.414	1.239	0.460	2.277

[a] n = 2

[b] 30 µl of 0.1 mg/ml tripolyphosphate solution was injected sequentially.

Table 48. The data for the sequential titrations of tripolyphosphate (TPP) solution into salicylic acid-chitosan microparticles and the titration of tripolyphosphate into pH 3.3 dilute acetic acid solution (blank experiment)

Injections[a]	Concentration[b] of TPP in cell (mM)	Heat flow for the titration of TPP to benzoic acid-chitosan particles (µW)	Heat flow for the tiration of TPP to dilute acetic acid (µW)	−ΔH/mole of TPP injected (kcal/mole)
1	0.032	0.416	0.387	0.092
2	0.064	0.870	0.528	1.005
3	0.094	0.900	0.479	1.230
4	0.124	1.014	0.548	1.363
5	0.154	1.347	0.424	2.698
6	0.182	1.318	0.520	2.333
7	0.211	1.160	0.491	1.957
8	0.237	1.247	0.566	1.992
9	0.264	1.429	0.518	2.663
10	0.291	1.308	0.589	2.101
11	0.316	1.259	0.416	2.463
12	0.342	1.295	0.533	2.227
13	0.367	1.303	0.491	2.375
14	0.390	1.465	0.474	2.895
15	0.414	1.391	0.460	2.723

[a] n = 2

[b]30 µl of 0.1 mg/ml tripolyphosphate solution was injected sequentially.

BIOGRAPHY

NAME	Ms. Yaowalak Boonsongrit
DATE OF BIRTH	August 25, 1973
PLACE OF BIRTH	Yala, Thailand
INSTITUTIONS ATTENDED	Mahidol University, 1993-1998: Bachelor of Science in Pharmacy (First class honors) Mahidol University, 2000-2006: Doctor of Philosophy (Pharmaceutics)
POSITION & OFFICE	1998-2000: Nakonnayok Hospital, Thailand Position: Pharmacist
HOME ADDRESS	19/6 Moo 6 Soi Watcharaphon Ramintra Road, Bangkhen District, Bangkok 10220 Thailand Tel. +66-2-948-1176 E-mail: ywl457@yahoo.com
GRADUATION GRANT	Thailand Research Fund through the Royal Golden Jubilee Ph.D. Program (Grant No. PHD/0169/2542) The German Academic Exchange Service (Deutscher Akademischer Austauschdienst, DAAD) scholarship